

Gaussian Filtering in Broadband Quantum Teleportation

Joseph Richard Nelson



The University of Auckland
October 2009

Contents

Acknowledgements	v
1 Introduction	1
1.1 Quantum optics and teleportation: a brief history	1
1.2 What is Quantum Teleportation?	2
1.3 Outline of dissertation	3
2 Early Teleportation Protocols	5
2.1 Discrete Teleportation Protocols	5
2.2 Entanglement	8
2.2.1 Introduction	8
2.2.2 Formal description of two-particle states	8
2.2.3 The Schmidt Decomposition and entanglement defined	10
2.2.4 Maximal entanglement	11
2.3 Continuous-variable Teleportation Protocols	12
3 Quantum Optics Aspects	14
3.1 Introduction: Quantisation of the electromagnetic field	14
3.2 Squeezed Light	16
3.3 Quantum optics description of a beamsplitter	20
3.4 Balanced Homodyne Detection	22
3.5 Correlation Functions and the Classification of Light	24
4 Correlation Functions	29
4.1 For squeezed vacuum fields	29
4.2 For resonance fluorescence	31
5 The optical protocol of Furusawa <i>et al.</i>	37
5.1 Description	37
5.2 First-Order Correlation Functions for the output field	39
5.2.1 Gaussian Filtering in the absence of filtering by Alice	39
5.2.2 Lorentzian Filtering in the absence of filtering by Alice	42
5.2.3 Spectrum of the teleported vacuum	42
5.2.4 Spectrum of the teleported resonance fluorescence field	46
5.2.5 Analytical work with the first-order correlation function	53
5.3 Second-Order Correlation Functions for the output field	55
5.3.1 Vacuum terms in the second order correlation function	56
5.3.2 The non-vacuum term in the second order correlation function	57
5.4 Other filtering possibilities	64

6 Conclusions and future directions	65
Appendices	67
Appendix A	67
Appendix B	69
Appendix C	73
Appendix D	74
References	75

Acknowledgements

I would like to acknowledge my supervisors, Prof. Howard Carmichael and A-Prof. Matthew Collett, for their invaluable input and support throughout the year as I was writing this dissertation.

Thanks must also go to Changsuk Noh, whose doctoral thesis [7] provided a sound basis for the much of the calculative work in this report.

Chapter 1

Introduction

1.1 Quantum optics and teleportation: a brief history

‘Quantum optics’ is a phrase that is used broadly to describe theories that give a quantum description of light and light-matter interactions. We give a brief historical overview of this large and diverse field. See for example, [10] and [13].

The realisation that ‘something’ in light-matter interactions was quantised began with work by M. Planck in 1901 with the spectrum of blackbody radiation. The hypothesis was formulated that blackbody radiation is emitted in discrete energy packets, although at the time it wasn’t immediately obvious that this was due to the quantum nature of light itself. This hypothesis arose once more in 1905, with the description of the photoelectric effect by A. Einstein. An early experiment performed by G.I. Taylor in 1909 attempted to detect quantum effects in light by using very low intensity light sources in a Young’s double-slit experiment, but the resulting interference pattern was ultimately unchanged by the low source intensity.

Quantisation of light emerged as a formal theory in the 1920’s, with the word ‘photon’ coined by American chemist G.N. Lewis in 1926, to describe the energy quanta associated with light fields. Perhaps the first experiments done in quantum optics were the now famous ones performed in 1956 by R. Hanbury-Brown and R. Q. Twiss. These experiments arose in the course of their work in developing a light intensity interferometer for stellar observation purposes. From a quantum point of view, Hanbury-Brown and Twiss observed a phenomenon known as *photon bunching* in a thermal light source. Although their results were explainable in classical theory, these experiments were surely among the first to measure light intensity fluctuations on short time scales.

Four years later followed the invention of the laser. Though an excellent source of coherent light (one with little variation in phase and amplitude), the properties of laser light (in particular, its *photon statistics*) were not drastically different from conventional light sources of the time. Laser light didn’t have any uniquely *quantum* properties. It would not be until 1963, with theoretical work done by R.J. Glauber, that states of light having a true quantum signature were uncovered. In 1977, H.J. Kimble, M. Dagenais and L. Mandel demonstrated experimentally the concept of *photon antibunching*, sources of light where detection of a photon corresponds to a reduced probability for detecting a subsequent photon. This is a unique property of certain states of light and is only explainable in a quantum picture. Later, in 1985, R. E. Slusher experimentally demonstrated *squeezed light*. As we shall see further on, squeezed light sources are among the necessary quantum-optical tools needed in modern quantum teleportation protocols.

The focus of this dissertation is *quantum teleportation*. Quantum teleportation is a notion of recent vintage, and it wasn't born in the quantum optics realm. It was first proposed by C.H. Bennett *et al.* [1] in 1993, with the authors using a spin-1/2 quantum system to demonstrate the fundamental ideas. The connection to quantum optics was never far off, however, for the two level spin-1/2 system has plenty of analogies with the two level system formed by considering orthogonal polarisations of photons. Quantum teleportation was extended not long after this in 1994 by Lev Vaidman [6] to include teleportation of continuous variables (such as position and momentum). Only three years would pass before quantum teleportation was experimentally demonstrated, in 1997, by D. Bouwmeester *et al.* Their demonstration essentially followed the Bennett protocol, but used polarisation-entangled photon pairs. Sources of such photon pairs were already well established, and had proved useful in the pioneering work of A. Aspect *et al.*, commencing around 1981, demonstrating violations of Bell's Inequality. In 1998, S.L. Braunstein and H.J. Kimble proposed a new quantum teleportation protocol [3] that made use of squeezed states of light. This differed from the 1997 experimental work of D. Bouwmeester in that the proposal was capable of teleporting continuous variables. That same year, their proposal was experimentally realised by A. Furusawa *et al.* [2]. This protocol, with some modifications, is the one that shall be considered for calculative purposes in this report.

1.2 What is Quantum Teleportation?

At this point it is worth reviewing what we mean by the phrase *quantum teleportation*.

Firstly, without the 'quantum' prefix, the perception one has of the word 'teleportation' is probably best summed up by its dictionary definition. We follow the lead of Vaidman [4] and quote from the Oxford English Dictionary:

Teleportation. *Psychics and Science Fiction.* The conveyance of persons (esp. of oneself) or things by psychic power; also in futuristic description, apparently instantaneous transportation of persons, etc., across space by advanced technological means.

In prefixing 'quantum' to the above however, the situation is quite different. What quantum teleportation refers to is the teleportation of *quantum states*. By this, we in fact do *not* refer to the instantaneous teleportation of 'persons, etc.' – i.e. *matter* – through a quantum teleporter.

At first, this doesn't quite appear to fit into an everyday perception of teleportation. A quantum teleporter is capable of transporting the quantum state of a given system over some distance, but the 'matter' comprising the system originally possessing this quantum state is effectively left behind at the teleporter input. Have we really teleported anything at all then?

It turns out that leaving the constituents of the original system behind is not a difficulty in a quantum mechanical framework. This is because in the quantum realm, *elementary* particles comprising the given system are completely indistinguishable from the same particles elsewhere in the universe. Lev Vaidman, whose continuous variable teleportation protocol we mentioned earlier (of which we shall have more to say later) discusses [4]:

“According to quantum theory, all elementary particles of the same kind are identical. There is no difference between the electrons in my body and the electrons in a rock on the moon.”

Hence, the distinguishing characteristic of a particular system is its quantum state, not the elementary particles comprising it. In light of this, we see that teleporting quantum states only is perfectly sufficient; all we need to do is 'imprint' this quantum state on the same elementary particles at the teleporter output. Movement of matter between the teleporter input and output is not needed – teleportation of the *state* is enough to consider a given system to be 'teleported'. To quote Lev Vaidman again on the matter [4]:

“If I want to move to the moon, I need not move my electrons, protons, etc. to the moon. It is enough to reconstruct the quantum state of the same particles there.”

The section “What is actually teleported?” of [4] provides an in-depth discussion on the above points. All the teleportation protocols discussed in this report are of the quantum variety, and so are in the business of teleporting quantum states. Two points are in order here:

- Although matter comprising the original system input into a quantum teleporter is left behind, its original quantum state is *not*. We shall see that the measurement processes required to do quantum teleportation are destructive and do not preserve the original state at the teleporter input.
- We shall also see that teleportation is possible for *unknown* quantum states, where determination of the state by measurement alone would be impossible. This is a distinguishing mark of quantum teleportation, as opposed to ‘classical’ teleportation, where a system state is first fully determined by measurement and then reconstructed at the teleporter output.

1.3 Outline of dissertation

In [2], Furusawa *et al.* discuss an optical quantum teleportation protocol using squeezed light which was subsequently implemented by the authors, with experimental results also discussed. Part of a recent doctoral thesis at the University of Auckland [7] looked at modifying this quantum teleportation protocol to include additional noise filtering at the output, with the aim of increasing the fidelity (quality) of the teleportation. Some results of this consideration are outlined by Noh *et al.* in [5]. For this noise filtering, Lorentzian shaped filters were considered.

In [5] however, it is also noted that Lorentzian filters are “far from ideal for suppressing background noise”, where background noise arises from the squeezed light used in this particular teleportation protocol. The aim of this dissertation is to look at possibility of using filters of other shapes at the output. Specifically, filters utilising a Gaussian shape are explored, and compared with Lorentzian filtering to gauge success.

We investigate the effect that these types of filtering have on the squeezed vacuum, as well as their effect on the teleported field of resonance fluorescence, through the use of correlation functions and relevant spectra.

This report is structured as follows.

Section 1

Introduction, outline and preliminaries.

Section 2

Here we introduce and discuss the original BBCJPW protocol [1], a discrete teleportation protocol. The aforementioned continuous variable protocol of Lev Vaidman [6] is also discussed. These early protocols highlight many of the fundamental ideas behind quantum teleportation. Additionally, we select the topic of *quantum entanglement* and formally define this as well, for it is of great significance in quantum teleportation.

Section 3

This section begins our venture into the quantum optics arena. Relevant theory and background needed to understand the protocol of Furusawa *et al.* [2] and its modifications, which form the basis of the calculative work in this report, is presented.

Section 4

As mentioned earlier, the effectiveness of filtering procedures introduced into the teleportation protocol are to be tested by consideration of input/output correlation functions and spectra. This section presents the necessary correlation functions for squeezed vacuum states and for the resonance fluorescence field.

Section 5

In this section the Furusawa protocol [2] is set forth, and correlation functions for the teleporter output (which involve filtering) are derived from those in Section 4. Various plots are produced for comparative purposes, and analytical expressions for these correlation functions and spectra are given. Aside from numerical work, these analytical expressions give us insights as to what happens when certain limits are taken for the parameters controlling the teleportation.

Chapter 2

Early Teleportation Protocols

2.1 Discrete Teleportation Protocols

One of the first quantum teleportation protocols described in the literature is that of Bennett *et al.* [1], also known as the BBCJPW protocol (to give the letters of all the authors). We present this now.

We begin by considering a particle (labelled *Particle 1*) which is in some spin state

$$|\phi_1\rangle = a|+_1\rangle + b|-_1\rangle \quad (2.01)$$

Here $|+\rangle$ is the state of spin-up, and $|-\rangle$ that of spin down, as usual. However, generally speaking, what we are about to describe does apply equally well to two-state systems other than spin. The polarisation states of photons was an example given earlier.

To perform teleportation, we have also at hand two further particles 2 and 3 in the spin-singlet state¹

$$|\Psi_{23}^-\rangle = \frac{1}{\sqrt{2}}(|+_2\rangle|-_3\rangle - |-_2\rangle|+_3\rangle) \quad (2.02)$$

which involves two correlated spins.

Alice receives particles 1 and 2. To describe their collective state, it is convenient to introduce the *Bell operator basis*, given by

$$|\Psi_{12}^{(\pm)}\rangle = \frac{1}{\sqrt{2}}(|+_1\rangle|-_2\rangle \pm |-_1\rangle|+_2\rangle) \quad (2.03)$$

$$|\Phi_{12}^{(\pm)}\rangle = \frac{1}{\sqrt{2}}(|+_1\rangle|+_2\rangle \pm |-_1\rangle|-_2\rangle) \quad (2.04)$$

Equivalently,

$$|\pm_1\rangle|\mp_2\rangle = \frac{1}{\sqrt{2}}(|\Psi_{12}^+\rangle \pm |\Psi_{12}^-\rangle) \quad (2.05)$$

$$|\pm_1\rangle|\pm_2\rangle = \frac{1}{\sqrt{2}}(|\Phi_{12}^+\rangle \pm |\Phi_{12}^-\rangle) \quad (2.06)$$

¹ The *spin-singlet state* is also referred to as the *EPR-Bohm State* due to its use by Bohm in discussions relating to the famous EPR Paradox. It is also known as the *completely anticorrelated state* due to the anticorrelated nature of its entanglement.

The Bell operator basis is complete and orthonormal; this will be made clearer in Section 2.2. Then, prior to any measurement, the total system consisting of Particles 1,2 and 3 is in a pure product state

$$\begin{aligned}
 |\Psi_{123}\rangle &= |\phi_1\rangle|\Psi_{23}^-\rangle \\
 &= \frac{a}{\sqrt{2}}|+1\rangle|+2\rangle|-3\rangle - \frac{a}{\sqrt{2}}|+1\rangle|-2\rangle|+3\rangle + \frac{b}{\sqrt{2}}|-1\rangle|+2\rangle|-3\rangle - \frac{b}{\sqrt{2}}|-1\rangle|-2\rangle|+3\rangle
 \end{aligned}
 \tag{2.07}$$

We now expand this state in the Bell operator basis using the equations above:

$$\begin{aligned}
 |\Psi_{123}\rangle &= \frac{1}{2}|\Psi_{12}^+\rangle(-a|+3\rangle + b|-3\rangle) + \frac{1}{2}|\Psi_{12}^-\rangle(-a|+3\rangle - b|-3\rangle) \\
 &\quad + \frac{1}{2}|\Phi_{12}^+\rangle(a|-3\rangle - b|+3\rangle) + \frac{1}{2}|\Phi_{12}^-\rangle(a|-3\rangle + b|+3\rangle)
 \end{aligned}
 \tag{2.08}$$

At this point, the particle in state $|\phi_1\rangle$ and the EPR pair are not entangled in any way. In order to couple the two, Alice makes a measurement in the Bell basis.

We don't specify precisely the nature of Alice's measurement; all that we require of such a measurement is that it projects the state $|\Psi_{123}\rangle$ onto exactly one of the states $|\Psi_{12}^+\rangle$, $|\Psi_{12}^-\rangle$, $|\Phi_{12}^+\rangle$, or $|\Phi_{12}^-\rangle$, and further, that Alice is able to tell as a result of her measurement which one of these states is projected onto. In practice, there may exist an observable and operator pair whose eigenfunctions are precisely these 4 states, having a 1-1 correspondence between eigenvalues and eigenfunctions, which happens to be experimentally realisable, but we don't consider such difficulties or the exact nature of this operator here.

The state describing Particles 1 and 2 (which are with Alice) then collapse into one of the 4 states $|\Psi_{12}^{(\pm)}\rangle$ or $|\Phi_{12}^{(\pm)}\rangle$ with equal probabilities each. Bob's particle 3 is then put into the corresponding 'coefficient state' from $|\Psi_{123}\rangle$ in Eq. (2.08).

It remains only for Bob to apply a unitary operator to his particle 3 to recover the original state $|\phi_1\rangle$ at his measuring station. Which unitary operator he needs to apply depends on Alice's measurement result (which she sends to Bob), as seen in the following table.

Alice's measurement result	State of Particle 3 as a 2-component spinor	Unitary operator that Bob applies	Final State of Particle 3
$ \Psi_{12}^+\rangle$	$\begin{pmatrix} -a \\ b \end{pmatrix}$	$\begin{pmatrix} -1 & 0 \\ 0 & 1 \end{pmatrix}$	$\begin{pmatrix} a \\ b \end{pmatrix}$
$ \Psi_{12}^-\rangle$	$\begin{pmatrix} -a \\ -b \end{pmatrix}$	$\begin{pmatrix} 1 & 0 \\ 0 & 1 \end{pmatrix}$	$\begin{pmatrix} -a \\ -b \end{pmatrix}$
$ \Phi_{12}^+\rangle$	$\begin{pmatrix} -b \\ a \end{pmatrix}$	$\begin{pmatrix} 0 & -1 \\ 1 & 0 \end{pmatrix}$	$\begin{pmatrix} -a \\ -b \end{pmatrix}$
$ \Phi_{12}^-\rangle$	$\begin{pmatrix} b \\ a \end{pmatrix}$	$\begin{pmatrix} 0 & 1 \\ 1 & 0 \end{pmatrix}$	$\begin{pmatrix} a \\ b \end{pmatrix}$

In all cases, the final state of Particle 3 is identical to that of the input Particle 1, up to a phase factor ($\exp(i\pi) = -1$ in the middle two cases). Other unitary operators having different phases could be used, though we have adhered to the convention set out in [1].

As an aside, the 2x2 matrix representation of rotation is given by Eq. 3.2.45 of [15]:

$$D(\hat{\mathbf{n}}, \phi) = \begin{bmatrix} \cos\left(\frac{\phi}{2}\right) - in_z \sin\left(\frac{\phi}{2}\right) & (-in_x - n_y) \sin\left(\frac{\phi}{2}\right) \\ (-in_x + n_y) \sin\left(\frac{\phi}{2}\right) & \cos\left(\frac{\phi}{2}\right) + in_z \sin\left(\frac{\phi}{2}\right) \end{bmatrix} \quad (2.09)$$

Here, we speak of a rotation by angle ϕ about an axis specified by the normal vector $\hat{\mathbf{n}} = [n_x \ n_y \ n_z]^T$, where for positive ϕ the rotation is counter-clockwise about that axis. Rotations of π radians about the z, y, and x axes thus involve the matrices

$$\begin{pmatrix} -i & 0 \\ 0 & i \end{pmatrix}, \quad \begin{pmatrix} 0 & -1 \\ 1 & 0 \end{pmatrix}, \quad \text{and} \quad \begin{pmatrix} 0 & -i \\ -i & 0 \end{pmatrix} \quad (2.10)$$

respectively. Up to a phase, these are precisely the unitary operators that Bob applies in the case of measurement results $|\Psi_{12}^+\rangle$, $|\Phi_{12}^+\rangle$ and $|\Phi_{12}^-\rangle$, so that Bob's unitary operators have a physical interpretation as rotations of the 2-level system of Particle 3. With the measurement result $|\Psi_{12}^-\rangle$, no unitary operator needs to be applied as indicated in the above table.

As for the fate of Particles 1 and 2 at Alice's measurement station, they end up in precisely the state given under 'Alice's measurement result' in the table above. As we mentioned in the Introduction, the original state is *not* preserved at the teleporter input. In fact, this is a consequence of a quite general result in quantum physics, which we state now. We quote Theorem 20.1 of [12]:

The Quantum No-Cloning Theorem

There is no quantum operation that can perfectly duplicate an unknown quantum state. This holds under the assumption that every physically permitted operation is described by a *unitary* transformation.

So we see that our teleporter must necessarily destroy its input state, in order to not violate this No-Cloning Theorem.

Now, the BBCJPW protocol is not restricted to states of the form seen in Eq. (2.01). An interesting phenomenon is found if we input a Particle 1 that is itself entangled with an external *Particle 0*. Let the state be a singlet one:

$$|\Psi_{01}^-\rangle = \frac{1}{\sqrt{2}} (|+_0\rangle|-_1\rangle - |-_0\rangle|+_1\rangle) \quad (2.11)$$

As before, prior to any measurement, the system (now consisting of 4 particles) is in a product state

$$\begin{aligned} |\Psi_{0123}\rangle &= |\Psi_{01}^-\rangle|\Psi_{23}^-\rangle \\ &= \frac{1}{2} |+_0\rangle|-_1\rangle|+_2\rangle|-_3\rangle + \frac{1}{2} |-_0\rangle|+_1\rangle|-_2\rangle|+_3\rangle - \frac{1}{2} |-_0\rangle|+_1\rangle|+_2\rangle|-_3\rangle - \frac{1}{2} |+_0\rangle|-_1\rangle|-_2\rangle|+_3\rangle \end{aligned} \quad (2.12)$$

In the Bell Basis, this is:

$$\begin{aligned} |\Psi_{0123}\rangle &= \frac{1}{2} |\Psi_{12}^+\rangle \left(\frac{1}{\sqrt{2}} |+_0\rangle|-_3\rangle + \frac{1}{\sqrt{2}} |-_0\rangle|+_3\rangle \right) + \frac{1}{2} |\Psi_{12}^-\rangle \left(\frac{-1}{\sqrt{2}} |+_0\rangle|-_3\rangle + \frac{1}{\sqrt{2}} |-_0\rangle|+_3\rangle \right) \\ &\quad + \frac{1}{2} |\Phi_{12}^+\rangle \left(\frac{-1}{\sqrt{2}} |+_0\rangle|+_3\rangle - \frac{1}{\sqrt{2}} |-_0\rangle|-_3\rangle \right) + \frac{1}{2} |\Phi_{12}^-\rangle \left(\frac{1}{\sqrt{2}} |+_0\rangle|+_3\rangle - \frac{1}{\sqrt{2}} |-_0\rangle|-_3\rangle \right) \end{aligned} \quad (2.13)$$

Alice makes her measurements in the Bell basis as before; the ‘coefficients’ above show the measurement results. Bob’s application of the unitary operators listed in the above table (which act only on Particle 3, note) give the final collective state of Particles 0 and 3 as $|\Psi_{03}^-\rangle$, i.e. the teleportation scheme ‘swaps’ the original entanglement of Particles 0 and 1 to Particles 0 and 3, a phenomenon known as *entanglement swapping*.

2.2 Entanglement

2.2.1 Introduction

An important feature of the BBCJPW protocol was the sharing between two observers of a state that is non-locally correlated. In the case of the aforementioned protocol, this was the spin-singlet state of two spin-1/2 particles. This *non-local resource* is an essential feature of quantum teleportation protocols. In this section, we give a systematic discussion of *entangled states*, which possess precisely the sort of non-local correlations desired in teleportation. The origin of the phrase ‘entangled states’, and their description, is attributed to Erwin Schrodinger, who in 1935 brought them to light in discussing the infamous EPR paradox. Chapter 6 of Garrison and Chiao [12] gives a sizable discussion on many aspects of entanglement and provided much of the background for what follows.

2.2.2 Formal description of two-particle states

We begin with the mathematical description of two-particle states. In fact, we have already used these in our description of the BBCJPW protocol, so here we backtrack a little to define things formally. A two-particle system of *distinguishable* particles is described by treating each particle as living in a Hilbert space of appropriate dimension – call these H_A and H_B . Our designation of the overall two-particle system then, is as a state in the tensor product space denoted by $H_C = H_A \otimes H_B$.

A *product state* of H_C is a state of the form $|\Lambda\rangle = |\psi\rangle|\theta\rangle$, where $|\psi\rangle$ is a state in H_A , and $|\theta\rangle$ one in H_B . The overall space H_C then refers to all linear combinations of all such possible product states. In H_C , the inner product of two of these product states is defined by

$$\langle \Lambda' | \Lambda \rangle = \langle \psi' | \psi \rangle \langle \theta' | \theta \rangle \quad (2.14)$$

where $|\Lambda'\rangle = |\psi'\rangle|\theta'\rangle$.

Let the sets $\{|\phi_A\rangle\}$ and $\{|\eta_B\rangle\}$ be orthonormal basis sets for H_A and H_B respectively. The set of product states given by

$$\{|\phi_A\rangle|\eta_B\rangle: |\phi_A\rangle \in H_A, |\eta_B\rangle \in H_B\} \quad (2.15)$$

is capable of providing a basis of the product space H_C . This basis is also orthonormal. To see this, write $|\chi_{\alpha,\beta}\rangle = |\phi_\alpha\rangle|\eta_\beta\rangle$, then observe that

$$\langle \chi_{\alpha',\beta'} | \chi_{\alpha,\beta} \rangle = \langle \phi_{\alpha'} | \phi_\alpha \rangle \langle \eta_{\beta'} | \eta_\beta \rangle = \delta_{\alpha'\alpha} \delta_{\beta'\beta} \quad (2.16)$$

using Eq. (2.14) to perform the inner product. A general state $|\Psi\rangle$ in H_C can then be expanded over this basis as

$$|\Psi\rangle = \sum_{\alpha,\beta} \Psi_{\alpha\beta} |\chi_{\alpha\beta}\rangle \quad (2.17)$$

where $\Psi_{\alpha\beta} = \langle \chi_{\alpha\beta} | \Psi \rangle$. An operator X acting on H_C may likewise be expanded in terms of its matrix elements in this basis:

$$X = \sum_{\alpha, \alpha'} \sum_{\beta, \beta'} \langle \chi_{\alpha'\beta'} | X | \chi_{\alpha\beta} \rangle | \chi_{\alpha'\beta'} \rangle \langle \chi_{\alpha\beta} | \quad (2.18)$$

We allow operators that act on all of H_C , or on just one of its subsystems H_A or H_B . An operator A acting solely on H_A may be written explicitly as $A \otimes I$ to signify its effect on $H_A \otimes H_B = H_C$ - i.e., such an operator has the effect of the identity I when applied to states in H_B .

A important notion that shall be used later on is that of the *partial trace* of an operator. The partial trace refers to a trace carried out only over one of the subsystems H_A or H_B of the global system H_C . For an operator X acting on the system H_C , the partial trace over H_B is the operator acting on H_A given by:

$$\text{Tr}_B(X) = \sum_{\beta} \langle \eta_{\beta} | X | \eta_{\beta} \rangle \quad (2.19)$$

where the sum is over all states in the basis set $\{|\eta_{\beta}\rangle\}$. By substituting in the expansion for X over the states $|\chi_{\alpha\beta}\rangle$ in Eq. (2.18), we get an expansion in states:

$$\text{Tr}_B(X) = \sum_{\alpha, \alpha'} \sum_{\beta} \langle \chi_{\alpha'\beta} | X | \chi_{\alpha\beta} \rangle | \phi_{\alpha'} \rangle \langle \phi_{\alpha} | \quad (2.20)$$

which shows explicitly how the resulting operator can only act on H_A . Note that $|\chi_{\alpha,\beta}\rangle = |\phi_{\alpha}\rangle |\eta_{\beta}\rangle$.

When X happens to be the density operator ρ of the total system H_C , the resulting operator is known as a *reduced density operator*. Its role becomes clear when we consider the expectation value of an operator O_A that acts only on H_A - it is:

$$\langle O_A \rangle = \text{Tr}(\rho O_A) = \sum_{\alpha, \beta} \langle \chi_{\alpha, \beta} | \rho O_A | \chi_{\alpha, \beta} \rangle = \sum_{\alpha} \langle \phi_{\alpha} | \left(\sum_{\beta} \langle \eta_{\beta} | \rho | \eta_{\beta} \rangle \right) O_A | \phi_{\alpha} \rangle = \text{Tr}_A(\rho_A O_A) \quad (2.21)$$

where $\rho_A = \text{Tr}_B(\rho)$ is the reduced density operator found by tracing only over H_B . So we see that ρ_A acts as an effective density operator for O_A - we can calculate its operator expectation using the operator ρ_A and only a trace over the states H_A . We chose, for concreteness, to evaluate the trace using the basis $|\chi_{\alpha,\beta}\rangle$.

All is precisely analogous in H_B - for an operator O_B acting only on H_B , we have

$$\langle O_B \rangle = \text{Tr}_B(\rho_B O_B) \quad (2.22)$$

where now $\rho_B = \text{Tr}_A(\rho)$.

2.2.3 The Schmidt Decomposition and entanglement defined

Use of the basis states $|\chi_{\alpha\beta}\rangle$ (which we arrived at by using bases for H_A and H_B) provides an expansion of an arbitrary state $|\Psi\rangle$ in H_C over orthonormal states, as in Eq. (2.17). This uses up to $\text{Dim}(H_A) \times \text{Dim}(H_B)$ ('Dim' = dimension) states in its expansion. Here, we assume that we are working in Hilbert spaces of *finite* dimension. In [12], it is shown that an alternative expansion

$$|\Psi\rangle = \sum_{n=1}^r Y_n |\alpha_n\rangle |\beta_n\rangle \quad (2.23)$$

is possible, where $r \leq \text{Min}\{\text{Dim}(H_A), \text{Dim}(H_B)\}$, and the product states $|\alpha_n\rangle |\beta_n\rangle$ are still orthonormal. This uses fewer states in its expansion.

The smallest value of r for which this expansion is possible is called the *Schmidt rank* of the state $|\Psi\rangle$ of H_C , with the corresponding expansion being the *Schmidt decomposition*. This particular decomposition is useful for a number of reasons. One such reason is that the density and reduced density operators for the state $|\Psi\rangle$ have particularly simple forms – these are:

$$\rho = \sum_{m,n} Y_m Y_n^* |\alpha_m\rangle \langle \alpha_n| \otimes |\beta_m\rangle \langle \beta_n| \quad (2.24)$$

$$\rho_A = \text{Tr}_B(\rho) = \sum_n |Y_n|^2 |\alpha_n\rangle \langle \alpha_n| \quad (2.25)$$

$$\rho_B = \text{Tr}_A(\rho) = \sum_n |Y_n|^2 |\beta_n\rangle \langle \beta_n| \quad (2.26)$$

See that the two reduced density operators share the same coefficients.

Now, a product state in H_C evidently has Schmidt rank 1. We also know that, reverting now to the wavefunction form of a product state, we have:

$$\phi(x_1, x_2) = \psi(x_1)\psi'(x_2) \Rightarrow dp(a, b) = |\psi(a)|^2 |\psi'(b)| dx_1 dx_2 \quad (2.27)$$

where $dp(a, b)$ is the probability that the particle described by $\psi(x_1)$ is localised in an interval dx_1 about $x_1 = a$ and the particle described by $\psi'(x_2)$ is in an interval dx_2 about $x_2 = b$. Because of the way that single particle probabilities multiply in the above equation, knowledge of x_1 tells us *nothing* of x_2 - these two variables are completely uncorrelated.

On the other hand, *correlated states* such as the singlet state used in the BBCJPW protocol of Section 2.1 are not able to be written as a single product state – we say that such states are *not separable*. Hand in hand with this fact, we note that such states also have a Schmidt rank larger than 1. This motivates the definition of entanglement.

Definition: Entanglement

A pure state $|\Psi\rangle$ of H_C is called *entangled* if it has a Schmidt rank $r > 1$.

This definition may seem a little abstract in terms of what physical consequences exist for an entangled state. We therefore state a theorem (Theorem 6.4 of [12]) which relates entanglement to fluctuations in system operators. Given an operator A that acts on H_A only, we define the operator $\Delta A = A - \langle A \rangle$ to describe fluctuations of A about its mean. Similarly, ΔB is defined for an operator B acting on H_B alone. We then have the following.

Theorem

For a state $|\Psi\rangle$ of H_C , fluctuations ΔA and ΔB are *correlated* if $\langle \Psi | \Delta A \Delta B | \Psi \rangle \neq 0$. The state $|\Psi\rangle$ is entangled if, and only if, there are at least one pair of observables A, B having correlated quantum fluctuations.

So we see correlations in a quantum state goes hand-in-hand with it formally being entangled.

2.2.4 Maximal entanglement

We now briefly consider a system that does *not* partition into two subsystems H_A and H_B . Suppose we write the system density matrix ρ in the basis in which it is diagonal. Its eigenvalues then appear along its main diagonal. Let the dimension of the system Hilbert space be n , and suppose that ρ has \mathfrak{R} non-zero eigenvalues. If these \mathfrak{R} eigenvalues are all equal (to $\frac{1}{\mathfrak{R}}$ in order that the density operator may still have unit trace), then the state described by the density matrix is called a *maximally mixed state*.

Back in the two particle system H_C , we say that a *pure state* of H_C is *maximally entangled* if the reduced density operators ρ_A and ρ_B are each maximally mixed, as defined above, with the number of non-zero eigenvalues \mathfrak{R} in each being equal to the states' Schmidt rank r .

It is worth considering a small example to illustrate the physics thus far described.

Example

We reconsider the spin-singlet state Eq. (2.02)

$$|\Psi_{23}^-\rangle = \frac{1}{\sqrt{2}}(|+_2\rangle|-_3\rangle - |-_2\rangle|+_3\rangle) \quad (2.28)$$

at the heart of the BBCJPW protocol. Here H_A will be the 2-dimensional Hilbert space corresponding to the spin of Particle 2; in a similar manner H_B describes Particle 3. The full density operator is:

$$\begin{aligned} \rho &= |\Psi_{23}^-\rangle\langle\Psi_{23}^-| \\ &= \frac{1}{2}(|+_2\rangle\langle+_2| \otimes |-_3\rangle\langle-3| - |+_2\rangle\langle-2| \otimes |-_3\rangle\langle+3| - |-_2\rangle\langle+_2| \otimes |+_3\rangle\langle-3| + |-_2\rangle\langle-2| \otimes |+_3\rangle\langle+3|) \end{aligned} \quad (2.29)$$

This gives the reduced density operators (by performing partial traces):

$$\rho_A = \frac{1}{2}(|+_2\rangle\langle+_2| + |-_2\rangle\langle-2|), \quad \rho_B = \frac{1}{2}(|+_3\rangle\langle+3| + |-_3\rangle\langle-3|) \quad (2.30)$$

Both of these have the matrix form

$$\begin{pmatrix} 1/2 & 0 \\ 0 & 1/2 \end{pmatrix} \quad (2.31)$$

when written in their respective bases (namely $\{|+_2\rangle, |-_2\rangle\}$ and $\{|+_3\rangle, |-_3\rangle\}$). Additionally, the state $|\Psi_{23}^-\rangle$ has Schmidt rank 2 (in fact it is already Schmidt decomposed in the form written above). So we see that $|\Psi_{23}^-\rangle$ is an example of a maximally entangled state.

As we have already mentioned, entangled states are central to quantum teleportation. However, maximally entangled states have a special role – for example, it is noted in [1] that teleportation can only be perfectly achieved in the BBCJPW protocol if Alice and Bob share a *maximally* entangled spin state. This is both a necessary and sufficient condition for perfect teleportation in that protocol. The description given of the BBCJPW protocol in Section 2.1 used a spin-singlet state shared between Alice and Bob, which of course is maximally entangled as we have just seen. It is possible to use states other than the singlet state (which are also maximally

entangled) in that protocol as well. Use of a less-than-maximally entangled state will not result in perfect teleportation, a concept that, with a little adaptation depending on the teleportation protocol at hand, is quite generally true.

Our presentation of entanglement has been brief, and defined with a view towards quantum teleportation, where entanglement between two subsystems is needed. For example, we have not looked at entangled mixed states. Additionally, the Schmidt decomposition definition given turns out *not* to extend to entanglement between more than 2 subsystems so easily. We don't go into this here, however.

2.3 Continuous-variable Teleportation Protocols

Shortly after the BBCJPW protocol was established, an extension of this was proposed by Vaidman [6] involving the use of continuous variables. In this section we outline his protocol.

The extension proposed by Vaidman involves starting with Particles 2 and 3 in the EPR state described by

$$|\Psi_{23}\rangle = |Q_2 + Q_3 = 0, P_2 - P_3 = 0\rangle \quad (2.32)$$

where Q and P are a pair of *canonically conjugate* variables, which we define below. The use of this state highlights the departure from the BBCJPW protocol, for it involves 2 particles having correlations in *continuous variables* rather than just discrete spins.

Canonically Conjugate Variables

Let P and Q be Hermitian operators. We call P and Q ‘canonically conjugate’ if they satisfy the canonical commutation relation $[Q, P] = i\hbar$.

See Appendix C4 of [12]. Position and momentum are obvious examples – in this case, the state $|\Psi_{23}\rangle$ would correspond to two particles having the same momenta at ‘opposite’ positions $\pm x$.

We have an input Particle 1, and Alice receives Particles 1 and 2 as in the BBCJPW protocol. The state of Particle 1 is what is being teleported, and we write it as $\Psi(Q_1)$. Alice now measures the variables $Q_1 + Q_2$ and $P_1 - P_2$, obtaining results which we write as:

$$Q_1 + Q_2 = a, \quad P_1 - P_2 = b \quad (2.33)$$

We note that simultaneous measurement of these variables is possible because they commute as operators:

$$[\hat{Q}_1 + \hat{Q}_2, \hat{P}_1 - \hat{P}_2] = [\hat{Q}_1, \hat{P}_1] - [\hat{Q}_2, \hat{P}_2] = 0 \quad (2.34)$$

under the assumption that operators for Particle 1 and Particle 2 commute as well. Because Q and P are continuous variables, a and b can take on any values.

Alice’s measurement results, along with the correlations between Particles 2 and 3, allow us to eliminate Q_2 and P_2 in Eqs. (2.32) and (2.33) to see that

$$Q_1 - Q_3 = a, \quad P_1 - P_3 = b \quad (2.35)$$

The distributions of Q and P for Particle 3 are now determined, and related to those of Particle 1 by the above equations. The state of Particle 3 after Alice’s measurements is then precisely that of Particle 1, shifted in Q_3 by

an amount a , and also shifted in P_3 by an amount b . We note that (as operators), \hat{Q}_3 generates shifts in \hat{P}_3 -space, by virtue of them being canonically conjugate – to shift by an amount z in \hat{P}_3 -space, one applies the operator

$$\exp\left(\frac{i\hat{Q}_3 z}{\hbar}\right) \quad (2.36)$$

So the state of Particle 3 is now

$$\exp\left(\frac{i\hat{Q}_3 b}{\hbar}\right)\Psi(Q_3 + a) \quad (2.37)$$

where Ψ is the *same* function as it was for Particle 1. Bob's action is to now apply appropriate 'back-shifts' of this state in P_3 and Q_3 upon receiving the results a and b of Alice's measurements, to recover the input state of Particle 1.

Chapter 3

Quantum Optics Aspects

We now move on to look at teleportation protocols that are based on quantum optics. Such protocols make use of the unique properties of light only describable in a quantum treatment. We aim to cover much of the quantum-optical background needed in the following sections.

3.1 Introduction: Quantisation of the electromagnetic field

Our first task is to look at the quantised electromagnetic field. What is presented here is covered in Sections 4.1 and 4.2 of Loudon [13], and Section 2.1 of Walls [14].

Our starting point for the quantisation of the electromagnetic field is the classical Maxwell equations

$$\nabla \cdot B = 0 \quad (3.01)$$

$$\nabla \times E = -\frac{\partial B}{\partial t} \quad (3.02)$$

$$\nabla \cdot E = \frac{\rho}{\epsilon_0} \quad (3.03)$$

$$\nabla \times B = \mu_0 J + \mu_0 \epsilon_0 \frac{\partial E}{\partial t} \quad (3.04)$$

in SI units; for a region having certain current densities J and charge densities ρ , but without dielectrics. Use of the electrostatic potential ϕ and vector potential A satisfying

$$E = -\nabla\phi - \frac{\partial A}{\partial t} \text{ and } B = \nabla \times A \quad (3.05)$$

mean that the first two of Maxwell's equations, Eqs. (3.01) and (3.02), are automatically satisfied.

Helmholtz's Theorem tells us that an arbitrary vector field F (vanishing sufficiently quickly at infinity) can be decomposed into *transverse* and *longitudinal* components F_T and F_L as:

$$F = F_T + F_L, \text{ where } \nabla \cdot F_T = 0 \text{ and } \nabla \times F_L = 0 \quad (3.06)$$

We decompose the fields A , B , E and J in this manner. Additionally, we work in the *Coulomb Gauge*, specifying $\nabla \cdot A = 0$. The vector potential A is then entirely *transverse* (in the above Helmholtz decomposition sense).

Substitution of the potentials and use of the Coulomb gauge in Maxwell's equations above show that

$$\nabla^2 \phi = \frac{-\rho}{\epsilon_0} \quad (3.07)$$

from the third Maxwell equation, Eq. (3.03) (this is *Poisson's equation*); additionally we have

$$\left(\frac{1}{c^2} \frac{\partial^2}{\partial t^2} - \nabla^2 \right) A = \mu_0 J_T \quad (3.08)$$

$$\left(\frac{1}{c^2} \frac{\partial}{\partial t} \right) \nabla \phi = \mu_0 J_L \quad (3.09)$$

by taking transverse and longitudinal components of Eq. (3.04). Note that $\nabla \phi$ is entirely *longitudinal* because $\nabla \times (\nabla \phi) = 0$. We also have:

$$E_T = -\frac{\partial A}{\partial t} \quad (3.10)$$

$$E_L = -\nabla \phi \quad (3.11)$$

The free field

We now consider a *free electromagnetic field*, which is one in a region having $\rho = 0$ and $J_T = 0$. Fields A, B and E are then transverse only, though we don't bother to write a subscript T for this. The vector potential A satisfies a wave equation

$$\left(\frac{1}{c^2} \frac{\partial^2}{\partial t^2} - \nabla^2 \right) A = 0 \quad (3.12)$$

and we can determine E and B from

$$E = -\frac{\partial A}{\partial t}, \quad B = \nabla \times A. \quad (3.13)$$

The above manipulations of Maxwell's equations are still within the classical framework of electromagnetism. It is now that we turn our attention to quantisation.

Our first step is to expand the vector potential A over a series of *mode functions*. Conceptually, we are restricting ourselves to consideration of a free electromagnetic field in some finite volume V . We write

$$A(r, t) = A^+(r, t) + A^-(r, t) \quad (3.14)$$

where $A^+(r, t)$ and $A^-(r, t)$ are complex conjugates, respectively known as the *positive* and *negative* frequency parts of $A(r, t)$. Such an expansion is applicable to fields in general. We have:

$$A^+(r, t) = \sum_k c_k u_k(r) e^{-i\omega_k t} \quad (3.15)$$

The mode functions here are $u_k(r)$, with the c_k being complex expansion coefficients. The form of the mode functions can be found by substitution of Eq. (3.14) with Eq. (3.15) into Eq. (3.12).

Quantisation is now within our reach, and is achieved as follows: first, rewrite the coefficients c_k in terms of new coefficients a_k :

$$c_k = a_k \sqrt{\frac{\hbar}{2\omega_k \epsilon_0}} \quad (3.16)$$

This is just a rescaling that makes the a_k dimensionless. We then consider a_k and a_k^* not as complex expansion coefficients, but as *operators* a_k and a_k^\dagger satisfying the usual *boson commutation relations*. The vector potential is now:

$$A(\mathbf{r}, t) = \sum_k \sqrt{\frac{\hbar}{2\omega_k \epsilon_0}} (a_k u_k(\mathbf{r}) e^{-i\omega_k t} + a_k^\dagger u_k^*(\mathbf{r}) e^{i\omega_k t}) \quad (3.17)$$

These operators a_k and a_k^\dagger are annihilation and creation operators (respectively) for the mode described by the index k . The operator a_k^\dagger creates (adds) one photon in the mode k ; a_k removes one photon from that mode. The situation is completely analogous to that of the quantum harmonic oscillator.

From this $A(\mathbf{r}, t)$, we can determine $B(\mathbf{r}, t)$ and $E(\mathbf{r}, t)$ using Eq. (3.13). If these are substituted into the classical Hamiltonian

$$H = \frac{1}{2} \int d^3r \left(\epsilon_0 E(\mathbf{r}, t)^2 + \frac{1}{\mu_0} B(\mathbf{r}, t)^2 \right) \quad (3.18)$$

we get

$$H = \sum_k \hbar\omega_k \left(a_k^\dagger a_k + \frac{1}{2} \right) \quad (3.19)$$

which is again identical in form to the Hamiltonian for the quantum harmonic oscillator.

Form of the mode functions

The precise form of the $u_k(\mathbf{r})$ depends on what boundary conditions we give to our volume V . For example, in a cubic box of sidelength L having periodic boundary conditions, we have [14]:

$$u_k(\mathbf{r}) = \frac{1}{\sqrt{V}} \hat{e}_\lambda \exp(i\mathbf{k} \cdot \mathbf{r}), \quad \mathbf{k} = \frac{2\pi n_x}{L} \hat{\mathbf{x}} + \frac{2\pi n_y}{L} \hat{\mathbf{y}} + \frac{2\pi n_z}{L} \hat{\mathbf{z}} \quad (3.20)$$

where \hat{e}_λ ($\lambda = 1, 2$) are unit polarisation vectors. As usual n_x , n_y and n_z are integers. Here we are using k as a collective index to describe a particular value of λ and a particular wavevector \mathbf{k} .

3.2 Squeezed Light

Explicitly, the free electric field in the Coulomb gauge is:

$$E(\mathbf{r}, t) = \sum_k i \sqrt{\frac{\hbar\omega_k}{2\epsilon_0}} (a_k u_k(\mathbf{r}) e^{-i\omega_k t} - a_k^\dagger u_k^*(\mathbf{r}) e^{i\omega_k t}) = E^+(\mathbf{r}, t) + E^-(\mathbf{r}, t) \quad (3.21)$$

We now take a *single mode* of the electric field, and use the cubic box mode functions of Eq. (3.20). Then,

$$E(\mathbf{r}, t) = i \sqrt{\frac{\hbar\omega_k}{2\epsilon_0 V}} \hat{e}_\lambda (a_k e^{-i(\omega_k t - \mathbf{k} \cdot \mathbf{r})} - a_k^\dagger e^{i(\omega_k t - \mathbf{k} \cdot \mathbf{r})}) \quad (3.22)$$

We define new operators – the *quadrature phase* operators – as follows:

$$X = a_k + a_k^\dagger \quad (3.23)$$

$$Y = -i(a_k - a_k^\dagger) \quad (3.24)$$

This is the convention used in Walls [14], although it is possible to define these operators with slightly differing factors. We then have:

$$E(r, t) = \sqrt{\frac{\hbar\omega_k}{2\epsilon_0 V}} \hat{e}_\lambda (X \sin(\omega_k t - k \cdot r) - Y \cos(\omega_k t - k \cdot r)) \quad (3.25)$$

Because the a_k and a_k^\dagger obey boson commutation relations, we arrive at the following commutator for the quadrature phase operators:

$$[X, Y] = 2i \quad (3.26)$$

So we see that X and Y are *canonically conjugate* observables (up to scaling) as defined in Section 2.3, analogous to position and momentum. We also have the uncertainty relation

$$\Delta X \Delta Y \geq 1 \quad (3.27)$$

where $\Delta X = \sqrt{\langle (\Delta X)^2 \rangle}$ as usual. We now make the following definitions.

Definition.

A *minimum uncertainty state* of the electric field is one for which $\Delta X \Delta Y = 1$.

Among minimum uncertainty states, we may further distinguish between:

- States having $\Delta X = 1$ and $\Delta Y = 1$
- *Squeezed states*, with either:
 - $\Delta X < 1$, and hence $\Delta Y > 1$
 - $\Delta X > 1$, and hence $\Delta Y < 1$

The above definition contains the essence of what it means for a state to be squeezed – we have a state that saturates the quadrature uncertainty relation Eq. (3.27), and has reduced uncertainty in one quadrature at the expense of increased uncertainty in the other quadrature.

A well-known class of minimum uncertainty states are the so-called *coherent states*, denoted by $|\alpha\rangle$. These can be defined in a few ways – for example [14], as the states that result when the operator

$$D(\alpha) = \exp(\alpha a^\dagger - \alpha^* a) \quad (3.28)$$

for an arbitrary complex number α , acts on the vacuum state:

$$|\alpha\rangle \equiv D(\alpha)|0\rangle \quad (3.29)$$

This definition also implies that the coherent states $|\alpha\rangle$ satisfy $a|\alpha\rangle = \alpha|\alpha\rangle$, which itself can be considered an alternative definition for these states. Not only are these minimum uncertainty states, but they also have equal uncertainty in each quadrature. The operator $D(\alpha)$ known as the *displacement operator*, for one can think of it as ‘displacing’ the vacuum state to produce a coherent state.

The field quadratures X and Y provide us with a form of *phase space* to view states of light in. Evidently, states cannot be represented as points in such a phase space, because it is impossible to have a simultaneous exact

measurement of both quadratures, in light of Eq. (3.26). However, states can be represented as areas in such a phase space, where the area represents states allowable under fluctuations (or uncertainties) in the quadratures. Coherent states are then circles in this phase space, because they have equal uncertainty in each quadrature. The circle center is at the point $(\langle X \rangle, \langle Y \rangle)$, which for a coherent state is:

$$\langle X \rangle = 2\text{Re}(\alpha), \quad \langle Y \rangle = 2\text{Im}(\alpha) \quad (3.30)$$

In phase space, squeezed states are not represented by circular areas, for they have unequal uncertainties in each quadrature. They are narrower in one quadrature and correspondingly broader in the other. They can, in fact, be represented by *ellipses*. The precise reason why they are elliptically shaped is due to the fact that these phase space areas are actually contours of the *Wigner function* representing the states [14].

Squeezed states, like coherent states, can also be generated from the vacuum state by applying an appropriate operator. In particular, we may generate the squeezed state $|\alpha, \epsilon\rangle$, consisting of an ellipse of minor axis e^{-r} , and major axis e^r , centered on the spot defined by Eq. (3.30) with principle axes rotated by an angle ϕ relative to the usual quadrature phase-space axes. This is done in the following manner:

$$|\alpha, \epsilon\rangle = D(\alpha)S(\epsilon)|0\rangle \quad (3.31)$$

The operator $D(\alpha)$ is as it was before. The new operator here is the *unitary squeeze operator*, given by:

$$S(\epsilon) = \exp\left(\frac{1}{2}\epsilon^* a^2 + \frac{1}{2}\epsilon a^{\dagger 2}\right) \quad (3.32)$$

where the complex number ϵ sets the *degree of squeezing* r and the rotation angle ϕ :

$$\epsilon = r \exp(2i\phi) \quad (3.33)$$

The quadrature uncertainties give rise to tangible uncertainties in the quantised electric field. We find the electric field variance $\langle(\Delta E(r, t))^2\rangle$ is:

$$\frac{\hbar\omega_k}{2\epsilon_0 V} \left(\langle(\Delta X)^2\rangle \sin^2(\omega_k t - k \cdot r) + \langle(\Delta Y)^2\rangle \cos^2(\omega_k t - k \cdot r) - \left(\frac{\langle XY + YX \rangle}{2} - \langle X \rangle \langle Y \rangle \right) \sin(2\omega_k t - 2k \cdot r) \right) \quad (3.34)$$

Note that if the electric field is in a minimum uncertainty state, the third term above vanishes.

It is worth looking at some diagrams to get a picture of all these concepts that we have introduced – squeezed states, quadrature phase space, and uncertainties in the electric field.

We consider the *coherent state* $|\alpha = 2 + 0i\rangle$ to be in force at $t = 0$, and we ignore the any phase $-k \cdot r$ in the field. In this state, we have from Eq. (3.30) that $\langle X \rangle = 4$ and $\langle Y \rangle = 0$. We set the mode frequency $\omega_k = 2$, and plot the initial state in quadrature phase space, and a portion of its electric field over some time period, with the field uncertainty $\Delta E = \sqrt{\langle(\Delta E)^2\rangle}$ distributed evenly either side of the mean value for the electric field. The mean value of the electric field is of course

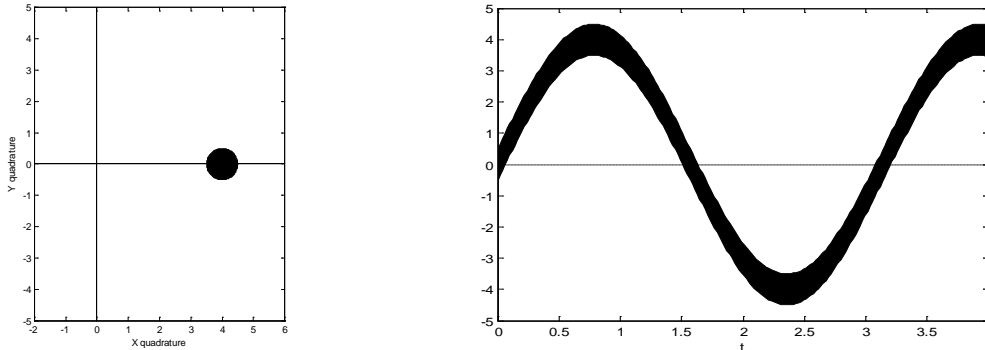
$$\langle E(r, t) \rangle = \sqrt{\frac{\hbar\omega_k}{2\epsilon_0 V}} \hat{e}_\lambda (\langle X \rangle \sin(\omega_k t - k \cdot r) - \langle Y \rangle \cos(\omega_k t - k \cdot r)) \quad (3.35)$$

We also consider some cases where we squeeze this initial coherent state.

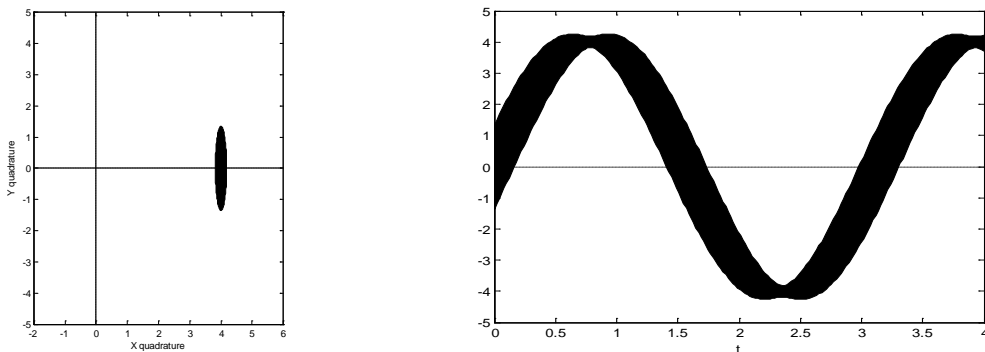
So far, we have introduced the quadrature operators X and Y effectively in the Schrodinger picture; in the Heisenberg picture, their time dependence means that the state in quadrature phase space orbits the origin at the mode frequency ω_k .

In the plots below, the left-hand picture shows the initial state described, in quadrature phase space. The right-hand plot shows a portion of the electric field (with its uncertainty as explained above), for some time interval.

The state $|\alpha = 2 + 0i\rangle$

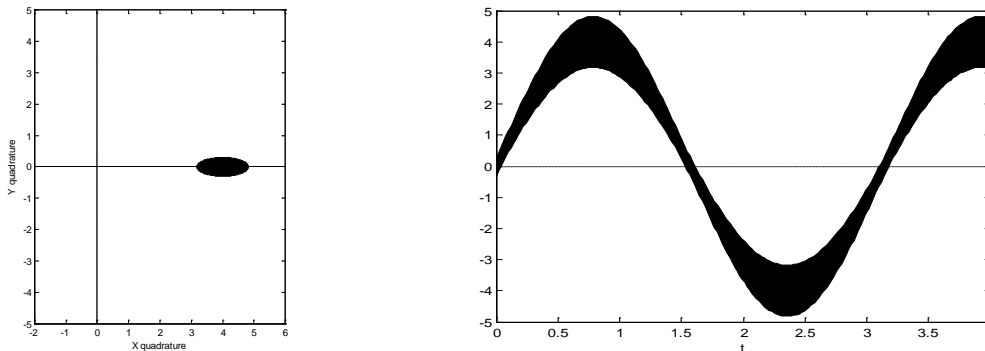


The state $|\alpha = 2 + 0i\rangle$, squeezed with $r = 1$



Notice that, compared to the unsqueezed state, the electric field amplitude is better defined here. This is an example of an *amplitude-squeezed* state.

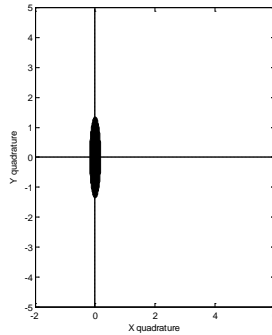
The state $|\alpha = 2 + 0i\rangle$, squeezed with $r = -0.5$



In this last case, note that the electric field's phase is better defined than in the unsqueezed case – this is an example of a *phase-squeezed* state.

A rather interesting type of squeezed state is that of the *squeezed vacuum*. The vacuum itself is exactly the same as the coherent state $|\alpha = 0 + 0i\rangle$. Hence, in quadrature phase space, it appears as a circle centered on the origin. As with the coherent state used in the above plots, it is possible to squeeze this vacuum state. We show an example below.

Squeezed vacuum with $r = 1$



Squeezed vacuum states will be of particular interest to us in optical teleportation protocols, as we shall see.

We note in closing that for the above plots, we have just set $\frac{\hbar c}{2\epsilon_0 V} = 1$ for convenience. This is quite generally the case, and most of the time we will just write an electric field in terms of its quadrature-phase operators as $\mathcal{E} = \mathcal{E}^X + i\mathcal{E}^Y$ (where the quadrature operators can now carry the time dependence) without regard to an overall constant.

3.3 Quantum optics description of a beamsplitter

As shall be seen below, beamsplitters also play an important role in optical teleportation protocols. The key property of these devices is they allow us to easily produce *linear superpositions* of input states. It is in this way that they are able to create the correlated states necessary for quantum teleportation to work. See, for example, Sections 3.2 and 5.7 of Loudon [13].

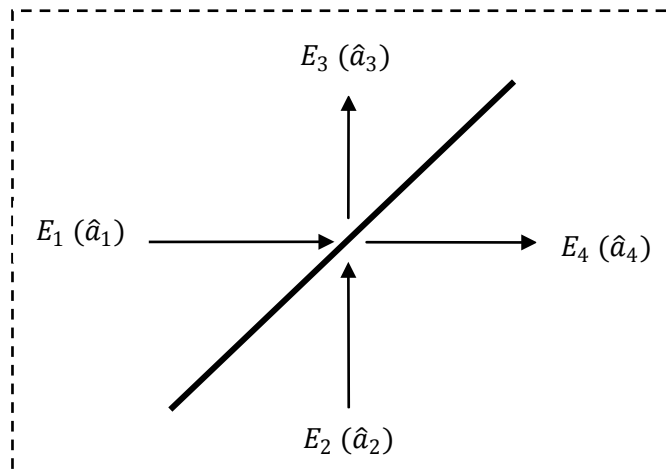


Figure 1. A beamsplitter.

Classically, we relate the output electric fields to the input fields via a matrix equation

$$\begin{pmatrix} E_3 \\ E_4 \end{pmatrix} = \begin{pmatrix} R_{31} & T_{32} \\ T_{41} & R_{42} \end{pmatrix} \begin{pmatrix} E_1 \\ E_2 \end{pmatrix} \quad (3.36)$$

showing that the output fields are linearly related to the input fields, with weights given by the constants R_{31}/R_{42} and T_{32}/T_{41} – these are the *reflection* and *transmission* coefficients respectively, which may be complex.

We next assume the beamsplitter to be *lossless* – i.e., *energy is conserved* between the input and output fields:

$$|E_1|^2 + |E_2|^2 = |E_3|^2 + |E_4|^2 \quad (3.37)$$

From these last two equations, we can derive:

$$|R_{31}|^2 + |T_{41}|^2 = 1 \quad (3.38)$$

$$|R_{42}|^2 + |T_{32}|^2 = 1 \quad (3.39)$$

$$R_{31}T_{32}^* + T_{41}R_{42}^* = 0 \quad (3.40)$$

We also get the result

$$|R_{31}| = |R_{42}|, \quad |T_{32}| = |T_{41}| \quad (3.41)$$

i.e. that the complex numbers R_{31}/R_{42} and T_{32}/T_{41} have *equal amplitudes*.

The above results are quite general. We simplify by taking the matrix elements of the above to be *symmetric* [13]; that is, R_{31} and R_{42} are assumed to have *equal (complex) phases*, the value of which is ϕ_R (they already have equal amplitudes due to Eq. (3.41)), and likewise for T_{32} and T_{41} (with equal phases ϕ_T). We then have, using Eqs. (3.38), (3.39) and (3.40):

$$|R|^2 + |T|^2 = 1 \quad (3.42)$$

$$RT^* + TR^* = 0 \quad (3.43)$$

where $R = |R_{31}| = |R_{42}|$ and $T = |T_{32}| = |T_{41}|$.

A final simplification occurs when the above is used to describe a *50/50 beamsplitter* – this is one for which R and T have equal magnitudes:

$$|R| = \frac{1}{\sqrt{2}}, \quad |T| = \frac{1}{\sqrt{2}} \quad (3.44)$$

whilst the phases ϕ_R and ϕ_T differ by $\pi/2$: $\phi_R - \phi_T = \frac{\pi}{2}$.

In fact, we will only be considering beamsplitters of this type in this report.

From a quantum optics perspective, the input fields have corresponding annihilation operators \hat{a}_1 and \hat{a}_2 , and output operators \hat{a}_3 and \hat{a}_4 , as seen in the diagram. These take the place of the electric fields in Eq. (3.36):

$$\begin{pmatrix} \hat{a}_3 \\ \hat{a}_4 \end{pmatrix} = \begin{pmatrix} R_{31} & T_{32} \\ T_{41} & R_{42} \end{pmatrix} \begin{pmatrix} \hat{a}_1 \\ \hat{a}_2 \end{pmatrix} \quad (3.45)$$

In the *symmetric case* described above, we have $\hat{a}_3 = R\hat{a}_1 + T\hat{a}_2$ and $\hat{a}_4 = T\hat{a}_1 + R\hat{a}_2$. The usual boson commutation relations hold for the input field operators:

$$[\hat{a}_1, \hat{a}_1^\dagger] = 1, \quad [\hat{a}_2, \hat{a}_2^\dagger] = 1 \quad (3.46)$$

Additionally, operators 1 and 2 are taken to be commuting. For the output field operators, we have

$$[\hat{a}_3, \hat{a}_3^\dagger] = [R\hat{a}_1 + T\hat{a}_2, R^*\hat{a}_1^\dagger + T^*\hat{a}_2^\dagger] = RR^*[\hat{a}_1, \hat{a}_1^\dagger] + TT^*[\hat{a}_2, \hat{a}_2^\dagger] = |R|^2 + |T|^2 \quad (3.47)$$

Likewise

$$[\hat{a}_4, \hat{a}_4^\dagger] = [T\hat{a}_1 + R\hat{a}_2, T^*\hat{a}_1^\dagger + R^*\hat{a}_2^\dagger] = |R|^2 + |T|^2 \quad (3.48)$$

And hence, in order to have the boson commutation relations hold for the *output* field operators as well, and by requiring operators 3 and 4 to commute (in the same manner that the input operators do), we find that

$$|R|^2 + |T|^2 = 1 \quad (3.49)$$

$$RT^* + TR^* = 0 \quad (3.50)$$

which are identical to Eqs. (3.42) and (3.43) describing the classical case.

In the classical case described above, *energy* was conserved at a lossless beamsplitter. In the quantum description, it might be reasonable on physical grounds for one to expect *total photon numbers* to be conserved at a lossless beamsplitter; this is indeed the case. To see, we write the number operators for the output fields in terms of operators for the input fields:

$$\hat{n}_3 = \hat{a}_3^\dagger \hat{a}_3 = (R^*\hat{a}_1^\dagger + T^*\hat{a}_2^\dagger)(R\hat{a}_1 + T\hat{a}_2) = |R|^2 \hat{a}_1^\dagger \hat{a}_1 + |T|^2 \hat{a}_2^\dagger \hat{a}_2 + R^*T \hat{a}_1^\dagger \hat{a}_2 + T^*R \hat{a}_2^\dagger \hat{a}_1 \quad (3.51)$$

and likewise for \hat{n}_4 . We then have:

$$\hat{n}_3 + \hat{n}_4 = [|R|^2 + |T|^2] (\hat{a}_1^\dagger \hat{a}_1 + \hat{a}_2^\dagger \hat{a}_2) + [R^*T + T^*R] (\hat{a}_1^\dagger \hat{a}_2 + \hat{a}_2^\dagger \hat{a}_1) = \hat{n}_1 + \hat{n}_2 \quad (3.52)$$

where we have used Eqs. (3.49) and (3.50).

3.4 Balanced Homodyne Detection

Balanced homodyne detection is yet another essential ingredient in optical teleportation protocols. We look into this now. What follows is taken from Section 6.11 of Loudon [13].

Consider the setup below.

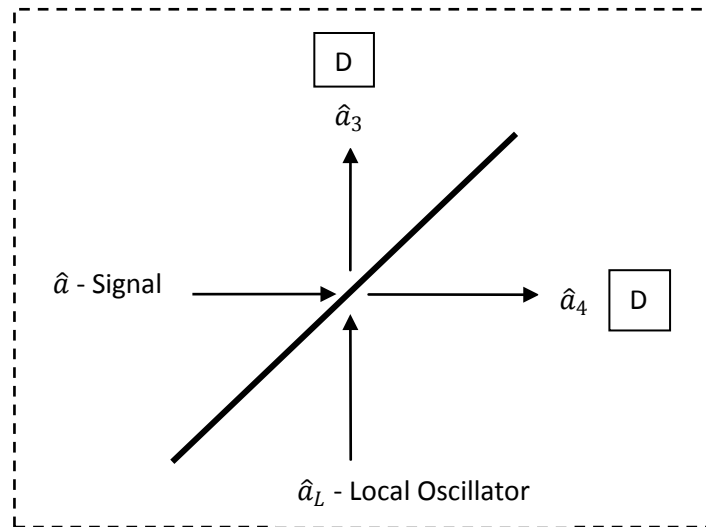


Figure 2. Setup for homodyne detection. The 'D's are detectors.

A 50/50 beamsplitter (as seen in the previous section) has two sources of light incident on it. One is a *signal source*, whose properties we wish to investigate. We associate with its field an annihilation operator $\hat{a}(t)$. The other is a *local oscillator* source, having annihilation operator $\hat{a}_L(t)$. We ensure that the frequency ω_L of the local oscillator matches up with that of the signal source.

What we want to consider is the signal corresponding to the *difference* in intensities of the two detectors, which in a quantum description amounts to differences in photon numbers detected over some observation period T . The annihilation operators for the two output branches of the beamsplitter are as defined in the diagram. This photon number difference is represented by the operator

$$M(t, \tau) = \int_t^{t+T} \left(\hat{a}_3^\dagger(t') \hat{a}_3(t') - \hat{a}_4^\dagger(t') \hat{a}_4(t') \right) dt' = i \int_t^{t+T} \left(\hat{a}^\dagger(t') \hat{a}_L(t') - \hat{a}_L^\dagger(t') \hat{a}(t') \right) dt' \quad (3.53)$$

The second equality comes from using the beamsplitter relations Eq. (3.45) for the symmetric beamsplitter to express the output operators in terms of the input ones. The balanced homodyne photocount is just the expectation value of this: $\langle M(t, \tau) \rangle$. We assume for simplicity that the detection process has unit efficiency.

Our general picture of the local oscillator is that it is a strong, coherent signal. We thus model it with a *coherent state* $|\alpha(t)\rangle$. Let the state be initially $|\alpha(0)\rangle = ||\alpha|e^{i\theta}\rangle$, where in this last we wrote the complex number α in terms of its magnitude and phase. Then, at a later time, we have $|\alpha(t)\rangle = ||\alpha|e^{i(-\omega_L t + \theta)}\rangle$. Now being a coherent state, this is an eigenstate of $\hat{a}_L(t)$. We hence find that

$$\langle M(t, \tau) \rangle = i|\alpha| \int_t^{t+T} \langle \hat{a}^\dagger(t') e^{i(-\omega_L t' + \theta)} - \hat{a}(t') e^{i(\omega_L t' - \theta)} \rangle dt' \quad (3.54)$$

But now since we have chosen the local oscillator frequency to match that of the signal frequency, this last is:

$$\langle M(t, \tau) \rangle = i|\alpha| \int_t^{t+T} \langle \hat{a}^\dagger e^{i(\theta)} - \hat{a} e^{i(-\theta)} \rangle dt' = i|\alpha| \int_t^{t+T} \langle \hat{a}^\dagger - \hat{a} \rangle \cos \theta + i \langle \hat{a}^\dagger + \hat{a} \rangle \sin \theta dt' \quad (3.55)$$

once we input the time dependence of the signal creation and annihilation operators.

Hence we see that by altering the local oscillator phase θ , we are able to measure values proportional to the quadrature expectation values - see Eqs. (3.23) and (3.24) defining the field quadratures.

It may be unclear why the local oscillator needs to be a *strong* signal. The reason is that allowing the local oscillator amplitude $|\alpha|$ to be large generally results in a large *signal-to-noise ratio* for the homodyne signal (i.e., the difference in signal between the two detectors), which is desirable. See Loudon Section 6.11 [13].

This is interesting situation. We have already seen in Section 3.2 that the field quadratures are canonically conjugate variables, like position and momentum. We also know that a pair of canonically conjugate variables, when measured appropriately, can achieve continuous variable quantum teleportation, as in the Vaidman protocol of Section 2.3. The balanced homodyne detector shows us that measurement of these variables can be physically realised in a quantum optics setup with relative ease. It is exactly this type of detection that is used to perform the measurements necessary in optical teleportation protocols.

3.5 Correlation Functions and Classification of Light

The quantum view of light is essentially one which realises that light consists of energy quanta – *photons*. We'll skirt over any difficulties in defining what photons actually are at present, although an excellent discussion on this point can be found in the Introduction of Loudon [13]. It is enough to think of them as energy quanta. This view isn't at odds with the classical view of course, which is that states of light are superpositions of perfectly coherent waves (i.e., waves of well defined phase and amplitude). The link is made by associating *photon numbers* with light intensity. The classical coherent waves, or their superpositions, can be viewed as the average behaviour over many photons. However, we shall see that the converse is not true. There exist states of light, describable in terms of photons, that *cannot* be described classically (i.e., as a superposition of coherent waves).

With this in mind, we now turn to look at photon statistics. Photon statistics provide us with one possible means of 'classifying' light. Our benchmark for perfectly stable light will be the usual classical one of a coherent electromagnetic wave of unchanging and well-defined phase and amplitude. By considering a length L of a beam of such light, and asking what the probability $P(n)$ of finding n photons in it is, we find that $P(n)$ obeys a *Poisson distribution* – that is, one having standard deviation $\Delta n = \sqrt{\bar{n}}$, where \bar{n} is the mean number of photons in the length L [10].

So a Poisson distribution pertains to light of perfectly constant intensity. One can see then, that if there are any intensity fluctuations in the light, we expect to obtain correspondingly larger fluctuations in photon numbers than $\sqrt{\bar{n}}$. Accordingly, we may classify light by its photon statistics in the following manner. Light is:

- *Sub-poissonian* if $\Delta n < \sqrt{\bar{n}}$
- *Poissonian* if $\Delta n = \sqrt{\bar{n}}$
- *Super-poissonian* if $\Delta n > \sqrt{\bar{n}}$

See, for example, Chapter 5 of [10].

Photon statistics are useful because of the connection between photon numbers and intensity. The photon statistics of a state of light give us a means of comparing intensity fluctuations to those found in perfectly coherent light. There are many examples of super-poissonian light. One such example is blackbody radiation. A *single mode* of the radiation field of blackbody radiation has

$$\Delta n = \sqrt{\bar{n} + \bar{n}^2} \quad (3.56)$$

which is evidently super-poissonian [10]. Here we are considering photon numbers in each mode of the field, rather than in a beam of length L . This result was mentioned in the Introduction of this report, with respect to the experiment of Hanbury-Brown and Twiss. Another interesting example is that of the squeezed vacuum. For such a state, we find [14]:

$$\Delta n = \sqrt{\bar{n}(1 + \cosh(2r))} \quad (3.57)$$

which is again super-poissonian when $r \neq 0$. Here r is the squeeze parameter introduced earlier, in Section 3.2. Sub-poissonian photon statistics have no classical analogue, for it isn't possible to consider electromagnetic waves that are more stable than the single coherent one having Poissonian statistics.

We now move on to look at the field correlation functions. There are two that are of chief significance for light; these are correlations in the electric fields, and correlations in the intensity. We begin with the former.

Classically, the *degree of first-order temporal coherence* is given by [13]:

$$g^{(1)}(\tau) = \frac{\langle E^*(t)E(t+\tau) \rangle}{\langle E^*(t)E(t) \rangle} \quad (3.58)$$

The denominator is solely a normalisation convention, and all physical significance is in the numerator – we are considering the correlation between the electric field at time t , and at a later time $t + \tau$. Implicitly, we are talking about *stationary* states here, where the value of $g^{(1)}$ depends on the time difference τ only, not on the measurement time t . The average value $\langle \dots \rangle$ is then taken to be an integral over a long time interval T , normalised by the length of that interval.

What physical meaning are we to derive from the value of $g^{(1)}(\tau)$? Well, evidently $g^{(1)}(0) = 1$ in all cases. The classical picture of a monochromatic, perfectly coherent light source is, as mentioned, one with perfectly stable amplitude in phase. For such light, $g^{(1)}(\tau) = 1$ for all times τ .

This is not the case for most light sources, which are realistically coherent only over a finite period of time, known as the *coherence time* τ_c . For such sources, $g^{(1)}(\tau)$ is close to 1 on timescales comparable to τ_c , however in the long run, it decays to 0 when $\tau \gg \tau_c$, corresponding to the fields $E(t)$ and $E(t + \tau)$ being uncorrelated. So the ‘closeness’ of $g^{(1)}(\tau)$ to 1 or 0 measures the light’s coherence, or incoherence (in electric fields) respectively, over the time interval τ .

A quantity that shall be of interest to us is the Fourier transform of the first-order correlation function, in the variable τ . It is shown in Section 3.5 of Loudon [13] that the Fourier transform of the first-order correlation function gives us the normalised power spectral density of the light. This connection is a form of the *Wiener-Khinchine Theorem*.

The next correlation function that is important is the *degree of second-order temporal coherence*, given by [13]:

$$g^{(2)}(\tau) = \frac{\langle \bar{I}(t)\bar{I}(t+\tau) \rangle}{\langle \bar{I}(t) \rangle^2} = \frac{\langle E^*(t)E^*(t+\tau)E(t+\tau)E(t) \rangle}{\langle E^*(t)E(t) \rangle^2} \quad (3.59)$$

Once more, the denominator is a normalisation constant. To be clear, note that \bar{I} refers to the long-time average light intensity in the manner

$$\bar{I}(t) = \frac{1}{2} \epsilon_0 c |E(t)|^2 \quad (3.60)$$

That is, \bar{I} is formed by fixing t and averaging over many cycles of the field having (fixed) electric field magnitude $|E(t)|$. In contrast, the angular brackets $\langle \dots \rangle$ refer to an average over t , where this field magnitude may vary.

Again, we ask what physical meaning can be derived from the value of $g^{(2)}(\tau)$. With perfectly coherent light as our benchmark, we find that $g^{(2)}(\tau) = 1$ for all values of τ , because such light has no variation in time of intensity. On the other hand, consider light that does have some variation in intensity. We write the intensity as

$$\bar{I}(t) = \langle \bar{I} \rangle + \Delta \bar{I}(t) \quad (3.61)$$

i.e., as a fixed mean value plus some fluctuation. It follows that

$$\langle \bar{I}(t)\bar{I}(t+\tau) \rangle = \langle \bar{I} \rangle^2 + \langle \Delta \bar{I}(t)\Delta \bar{I}(t+\tau) \rangle \quad (3.62)$$

where we note that the fluctuations $\Delta \bar{I}(t)$ and $\Delta \bar{I}(t + \tau)$ have expectation value zero. Hence:

$$g^{(2)}(0) = \frac{\langle \bar{I} \rangle^2 + \langle \Delta \bar{I}(0)^2 \rangle}{\langle \bar{I} \rangle^2} \geq 1 \quad (3.63)$$

So light that isn't coherent has a $g^{(2)}(0)$ larger than that of coherent light (i.e. 1). Note that this isn't necessarily true in a quantum description of light.

Classically, we also find that $g^{(2)}(\tau)$ has the following property [13]:

$$0 \leq g^{(2)}(\tau) \leq g^{(2)}(0) \quad (3.64)$$

for $\tau \neq 0$. That is, the second order correlation function never exceeds its value at $\tau = 0$.

Now, we find that the initial value $g^{(2)}(0)$ of the second order correlation function gives us another way of classifying light, instead of using photon statistics. We call the light:

- Bunched, if $g^{(2)}(0) > 1$
- Coherent, if $g^{(2)}(0) = 1$
- Antibunched, if $g^{(2)}(0) < 1$

Once again, see that antibunched light is not possible in a classical description of light, where the inequality given above (Eq. (3.63)) must be obeyed. We note in passing that the definition above for antibunched light is not the only one possible, but it is the definition used in this report. We have effectively defined antibunched light as light violating the classical inequality Eq. (3.63). Some authors (for example Loudon [13]) consider antibunched light to be light violating the *other* classical inequality above, Eq. (3.64). These two definitions are not equivalent. This 3-fold classification of light is not equivalent to the 3-fold one found using photon statistics [10]. However, we shall shortly introduce a parallel between the second-order correlation function and photon distributions.

We haven't yet mentioned anything about a quantum description of light, in particular, the quantised nature of the electric field seen previously hasn't yet been brought up. One may ask how the correlation functions Eqs. (3.58) and (3.59) change in the quantum picture. In fact, there is not much change in their form, and our interpretations of their values remain the same. We simply need to replace E with the positive frequency part E^+ of electric field operator (see Eq. (3.21)), which we saw when the field was quantised, and E^* with the Hermitian conjugate of this operator, namely E^- .

There is one slight caveat here though. Classically, the quantities E and E^* can be multiplied in any order – of course, they commute. The operators E^+ and E^- don't have this property, for they contain boson creation and annihilation operators, so the question arises as to what order we should write these operators down. In fact, we provided the correct order when we defined the correlation functions above. This particular order is known as *normal ordering* of the operators. Normal ordering of a group of operators is performed as follows:

- Creation operators should be written to the *left* of any annihilation operators.
- Where two creation operators are in a product, but at *different* times, the later time operator should appear to the *right* of the earlier time one.
- For two annihilation operators in a product at different times, the later time operator should appear to the *left* of the earlier time one.

We use the symbols $::$ when a normally ordered operator product is to be explicitly indicated. In writing down the second order correlation function, we don't generally bother to include them, for if we take $\tau > 0$ then the numerator as written in Eq. (3.59) is always normally ordered. Note that the definition of the second order correlation function implies the symmetry

$$g^{(2)}(\tau) = g^{(2)}(-\tau) \quad (3.65)$$

so we need only consider $\tau > 0$ anyway.

It is interesting to note that in spite of the similarity to the classical picture, going over to the quantum description means that the classical inequalities

$$g^{(2)}(\tau) \leq g^{(2)}(0) \quad (3.66)$$

$$g^{(2)}(0) \geq 1 \quad (3.67)$$

are not necessarily true at all. It is in this way that a quantum description of light can access states not describable by a classical picture.

A small speciality is to be made here with respect to our correlation functions. All of the correlations we will end up considering (for example, in the next chapter) are of the *steady state* type, in the sense that a long time limit is taken. We use a subscript *ss* notation to indicate this:

$$\langle A(t')B(t'') \rangle_{ss} = \lim_{T \rightarrow \infty} \langle A(T+t')B(T+t'') \rangle \quad (3.68)$$

So, for example, the first order correlation function in a quantum description in this long time limit would be written

$$g^{(1)}(\tau) = \frac{\langle E^-(\tau)E^+(0) \rangle_{ss}}{\langle E^-(0)E^+(0) \rangle_{ss}} \quad (3.69)$$

Taking such a long-time limit means that correlations $\langle \dots \rangle_{ss}$ are only ever dependent on time differences.

Photon Antibunching

We work only with steady-state quantities (in the sense of long-time limits and Eq. (3.68)) in what follows, as signified by the subscript *ss*.

The beauty of photon statistics is that they allow us to see what is happening with variations in the light intensity, due to the direct link between photon numbers and intensity. The correlation functions defined above may not afford such an easy physical interpretation – in particular, we are referring to the value $g_{ss}^{(2)}(0)$ which we stated was an alternative way of classifying light. As we noted before, the photon statistics and second order correlation function classifications of light aren't necessarily equivalent. It is true that our antibunching condition $g_{ss}^{(2)}(0) < 1$ implies sub-Poissonian photon statistics for *short* counting times [8]. However, these conditions are not equivalent in general. Here we explore then, what implications the antibunching inequality $g_{ss}^{(2)}(0) < 1$ has.

The meaning that $g_{ss}^{(2)}(0) < 1$ can be found by looking at an associated quantity – the *waiting time distribution* $w_{ss}(\tau)$ as defined in [8]. The waiting time distribution gives the probability distribution governing how the time intervals between photon detection pulses in a detector are distributed. That is, $w(\tau)$ is the probability that a given time interval between two *sequential* photopulses is of length τ . We introduce this because we have the important equivalence [8]:

$$g_{ss}^{(2)}(0) < 1 \Leftrightarrow w_{ss}(0) < w_{ss}(0)_{\text{Coherent}} \quad (3.70)$$

That is, antibunched light has a reduced probability of having successive photon counts (i.e., ones with zero wait time between them) than does coherent light of the same intensity. Loosely speaking, this implies an inability of the photons to ‘bunch’ – i.e. become very close together – hence the name ‘antibunching’.

The field of resonance fluorescence is an example of a state of light satisfying our antibunching condition. We have plotted $g^{(2)}(\tau)$ for the resonance fluorescence field in Section 5.3.

It is shown in [8] that, for perfect collection and detection efficiencies, the waiting time distribution for resonance fluorescence is given by

$$w_{ss}(\tau) = \gamma \exp\left(-\frac{\gamma\tau}{2}\right) \frac{Y^2}{2Y^2 - 1} \left(1 - \cosh(\delta'\tau)\right) \quad (3.71)$$

On the other hand, coherent light of the same intensity has a waiting time distribution:

$$w_{ss}(\tau) = \frac{\gamma}{2} \left(\frac{Y^2}{1 + Y^2}\right) \exp\left(-\frac{\gamma}{2} \left(\frac{Y^2}{1 + Y^2}\right) \tau\right) \quad (3.72)$$

Being probability distributions, we have the usual normalisation condition in all cases:

$$\int_0^{\infty} w_{ss}(\tau) d\tau = 1 \quad (3.73)$$

where we note that $w_{ss}(\tau) = 0$ for $\tau < 0$. We sample from these probability distributions a series of photopulse interval times². These are shown below.

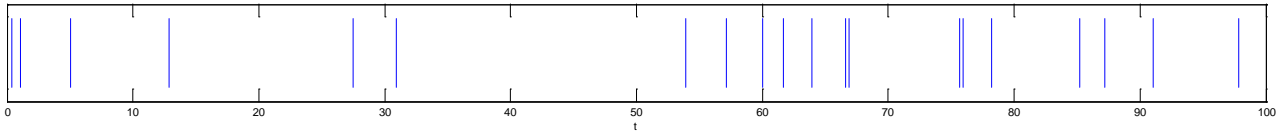


Figure 3. A series of photopulses from the coherent waiting time distribution above. We have taken $Y^2 = 1$ and $\gamma = 1$.

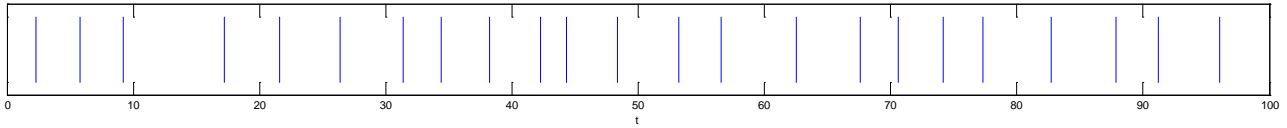


Figure 4. A series of photopulses from a resonance fluorescence waiting time distribution with $Y^2 = 1$ and $\gamma = 1$.

The meaning of ‘antibunched’ is quite easily visualised here. One sees that the spacing of photopulse intervals in the antibunched photopulse sequence is considerably more regular than that of the coherent source. In particular, it lacks photopulses that are very close together.

² Sampling can be done with the use of the cumulative density functions $W_{ss}(t) = \int_{-\infty}^t w_{ss}(\tau) d\tau$; this is the method we have used. These are $W_{ss}(t) = \gamma \frac{Y^2}{2Y^2 - 1} \left\{ \frac{2}{\gamma} \left(1 - \exp\left(-\frac{\gamma t}{2}\right)\right) + \frac{1}{2\delta'^2 - \frac{\gamma^2}{2}} \left(\gamma - \exp\left(-\frac{\gamma t}{2}\right) \left(2\delta' \sinh(\delta' t) + \gamma \cosh(\delta' t)\right)\right) \right\}$ for resonance fluorescence, and $W_{ss}(t) = 1 - \exp\left(-\frac{\gamma}{2} \left(\frac{Y^2}{1 + Y^2}\right) t\right)$ for coherent light.

Chapter 4

Correlation Functions

Certain correlation functions are needed in order to quantitatively implement the Furusawa protocol [2]. We present these now.

4.1 For squeezed vacuum fields

We have met squeezed vacuum states in Section 3.2. There are two types that we are interested in:

- Vacuum states squeezed in their X quadrature (i.e., with reduced fluctuations in that quadrature), the electric field of which we write as \mathcal{E}_{EPRx} .
- Vacuum states squeezed in their Y quadrature, whose electric field we write as \mathcal{E}_{EPRy} .

There is a slight change in notation here – the symbol \mathcal{E} in fact refers only to E^+ , the positive-frequency component of the electric field in Eq. (3.21). This should be noted in all that follows.

We then have the following correlation functions [7]:

$$\langle \mathcal{E}_{EPRx}^\dagger(\tau) \mathcal{E}_{EPRx}(0) \rangle_{ss} = \frac{\gamma_s}{4} \left(\frac{\lambda}{1-\lambda} e^{-\frac{\gamma_s}{2}(1-\lambda)|\tau|} - \frac{\lambda}{1+\lambda} e^{-\frac{\gamma_s}{2}(1+\lambda)|\tau|} \right) \quad (4.01)$$

$$\langle \mathcal{E}_{EPRy}^\dagger(\tau) \mathcal{E}_{EPRy}(0) \rangle_{ss} = \langle \mathcal{E}_{EPRx}^\dagger(\tau) \mathcal{E}_{EPRx}(0) \rangle_{ss} \quad (4.02)$$

$$\langle \mathcal{E}_{EPRx}^\dagger(\tau) \mathcal{E}_{EPRx}^\dagger(0) \rangle_{ss} = \frac{-\gamma_s}{4} \left(\frac{\lambda}{1-\lambda} e^{-\frac{\gamma_s}{2}(1-\lambda)|\tau|} + \frac{\lambda}{1+\lambda} e^{-\frac{\gamma_s}{2}(1+\lambda)|\tau|} \right) \quad (4.03)$$

$$\langle \mathcal{E}_{EPRy}^\dagger(\tau) \mathcal{E}_{EPRy}^\dagger(0) \rangle_{ss} = -\langle \mathcal{E}_{EPRx}^\dagger(\tau) \mathcal{E}_{EPRx}^\dagger(0) \rangle_{ss} \quad (4.04)$$

Here γ_s is the *squeezing bandwidth*, and $0 \leq \lambda < 1$ is a parameter that controls the degree of squeezing – it has a similar role to the parameter r we introduced for squeezed states. As $\lambda \rightarrow 1$ the squeezing becomes perfect. These correlation functions are valid for all $-\infty < \tau < \infty$.

The correlation functions given here have in fact been derived for a specific quantum-optical device, known as an *optical parametric oscillator*. Such a device consists of a ‘pump beam’ directed onto a non-linear crystal, which is capable of converting this into squeezed vacuum states. We don’t provide a description of the optical parametric oscillator here, but note that this is one important method by which squeezed vacuum states are generated in physical teleportation setups. This is why the correlation functions are expressed in terms of the parameters λ and γ_s , rather than parameters like r and ϕ seen in Section 3.2.

For the optical teleportation protocol of Furusawa *et al.* that we will be considering closely, the following linear combinations of the fields \mathcal{E}_{EPRx} and \mathcal{E}_{EPRy} will also be of importance:

$$\mathcal{E}_A = \frac{1}{\sqrt{2}}(\mathcal{E}_{EPRx} + \mathcal{E}_{EPRy}) \quad (4.05)$$

$$\mathcal{E}_B = \frac{1}{\sqrt{2}}(\mathcal{E}_{EPRx} - \mathcal{E}_{EPRy}) \quad (4.06)$$

We may relate correlations between the fields \mathcal{E}_A and \mathcal{E}_B back to the correlations between \mathcal{E}_{EPRx} and \mathcal{E}_{EPRy} ; for example, we have:

$$\langle \mathcal{E}_A(\tau)\mathcal{E}_A^\dagger(0) \rangle_{ss} = \langle \mathcal{E}_{EPRx}^\dagger(\tau)\mathcal{E}_{EPRx}(0) \rangle_{ss} + \delta(\tau) \quad (4.07)$$

$$\langle \mathcal{E}_A(\tau)\mathcal{E}_B(0) \rangle_{ss} = \langle \mathcal{E}_{EPRx}^\dagger(\tau)\mathcal{E}_{EPRx}(0) \rangle_{ss} \quad (4.08)$$

$$\langle \mathcal{E}_B^\dagger(\tau)\mathcal{E}_A^\dagger(0) \rangle_{ss} = \langle \mathcal{E}_{EPRx}^\dagger(\tau)\mathcal{E}_{EPRx}(0) \rangle_{ss} \quad (4.09)$$

$$\langle \mathcal{E}_B^\dagger(\tau)\mathcal{E}_B(0) \rangle_{ss} = \langle \mathcal{E}_{EPRx}^\dagger(\tau)\mathcal{E}_{EPRx}(0) \rangle_{ss} \quad (4.10)$$

These are just computed directly from the definitions of \mathcal{E}_A and \mathcal{E}_B in Eqs. (4.05) and (4.06), and the fact that all steady-state correlations $\langle \dots \rangle_{ss}$ depend only on time differences. To illustrate, we show Eq. (4.08):

$$\begin{aligned} \langle \mathcal{E}_A(\tau)\mathcal{E}_B(0) \rangle_{ss} &= \left\langle \frac{1}{\sqrt{2}}(\mathcal{E}_{EPRx}(\tau) + \mathcal{E}_{EPRy}(\tau)) \frac{1}{\sqrt{2}}(\mathcal{E}_{EPRx}(0) - \mathcal{E}_{EPRy}(0)) \right\rangle_{ss} \\ &= \frac{1}{2} \langle \mathcal{E}_{EPRx}(\tau)\mathcal{E}_{EPRx}(0) \rangle_{ss} + \frac{1}{2} \langle \mathcal{E}_{EPRy}(\tau)\mathcal{E}_{EPRy}(0) \rangle_{ss} \\ &= \langle \mathcal{E}_{EPRx}(\tau)\mathcal{E}_{EPRx}(0) \rangle_{ss} \\ &= \langle \mathcal{E}_{EPRx}^\dagger(\tau)\mathcal{E}_{EPRx}^\dagger(0) \rangle_{ss} \end{aligned}$$

The second inequality follows from the assumption that the fields \mathcal{E}_{EPRx} and \mathcal{E}_{EPRy} are uncorrelated; hence we have $\langle \mathcal{E}_{EPRx}(\tau)\mathcal{E}_{EPRy}(0) \rangle_{ss} = 0$, and so on. The third equality comes from Eq. (4.02).

The fourth equality comes from the steady state assumption and from the fact that correlation functions are even in τ ; explicitly:

$$\begin{aligned} \langle \mathcal{E}_{EPRx}(\tau)\mathcal{E}_{EPRx} \rangle &= \langle \mathcal{E}_{EPRx}(\tau)\mathcal{E}_{EPRx} \rangle^* \quad (\text{because the correlation functions are real}) \\ &= \langle \mathcal{E}_{EPRx}^\dagger \mathcal{E}_{EPRx}^\dagger(\tau) \rangle \\ &= \langle \mathcal{E}_{EPRx}^\dagger(-\tau)\mathcal{E}_{EPRx}^\dagger \rangle \quad (\text{by the stationary condition}) \\ &= \langle \mathcal{E}_{EPRx}^\dagger(\tau)\mathcal{E}_{EPRx}^\dagger \rangle \quad (\text{since the correlation functions are even in } \tau) \end{aligned}$$

The appearance of the delta function in Eq. (4.07) is due to the *antinormal ordering* of the operators in that correlation; exchanging their order costs a delta function which can be thought of as arising due to vacuum noise [7].

4.2 For resonance fluorescence

Testing of the central teleportation protocol of this report will, among other means, be done by teleporting the scattered field of resonance fluorescence. This field is of historical importance; it was in 1975 that H.J. Carmichael and D.F. Walls first predicted that *photon antibunching* (as in Section 3.5) would be observed in such a system, thus providing a physically realisable means for observing this unique quantum phenomenon. This was in fact precisely the system used by H.J. Kimble *et al.* in 1977, mentioned in Section 1.1.

We outline the quantum description of this system here. What follows is taken from [8].

It is possible to quote directly from [8] the correlation functions for the field of resonance fluorescence. However, we would also like to obtain correlation functions for the X and Y quadratures of this field. Doing so requires a minor modification of the calculation giving the field correlation functions, but it is necessary to trace the calculation through properly in order to do this. We choose here to start essentially from the beginning.

Our model of the atom is as a two-level system, having states $|1\rangle$ and $|2\rangle$ with energies E_1 and E_2 . The atomic Hamiltonian is

$$H_A = \frac{1}{2} \hbar \omega_A (|2\rangle\langle 2| - |1\rangle\langle 1|) \equiv \frac{1}{2} \hbar \omega_A \sigma_z \quad (4.11)$$

which takes this form due to the fact that we have shifted the zero of energy to be exactly halfway between E_1 and E_2 . We also introduce the atomic raising and lowering operators

$$\sigma_+ = |2\rangle\langle 1|, \quad \sigma_- = |1\rangle\langle 2| \quad (4.12)$$

The use of σ to denote these operators here is not accidental; the three operators σ_z , σ_+ and σ_- have analogies to the usual three Pauli spin matrices - hence they are sometimes referred to as *pseudo-spin operators*.

The expectation values of these operators relate to the elements of the system density operator ρ :

$$\langle \sigma_z \rangle = \text{Tr}(\rho \sigma_z) = \langle 2|\rho|2\rangle - \langle 1|\rho|1\rangle = \rho_{22} - \rho_{11} \quad (4.13)$$

$$\langle \sigma_+ \rangle = \langle 1|\rho|2\rangle = \rho_{12} \quad (4.14)$$

$$\langle \sigma_- \rangle = \langle 2|\rho|1\rangle = \rho_{21} \quad (4.15)$$

The resonance fluorescence system consists of a two-level atom excited by a strong incident laser mode whose energy matches the energy difference $E_2 - E_1$ between the two levels (i.e., is on resonance). The treatment of this system is as a *quantum open system*. This works as follows. We need to allow our system (i.e., the two level atom and laser) to interact with some form of external environment. This is done by considering the system S to be coupled to a large environmental system R (also called a *reservoir*) by some interaction. We describe the situation with a total Hamiltonian

$$H = H_S + H_R + H_{SR} \quad (4.16)$$

where H_S and H_R are the system and reservoir Hamiltonians, and H_{SR} describes the interaction.

We are interested in the system dynamics, and not that of the reservoir. The *total system* has some density operator, which we call χ , which obeys the differential equation

$$\frac{d\chi}{dt} = \frac{1}{i\hbar} [H, \chi] \quad (4.17)$$

with H given by Eq. (4.16). From χ we can, as usual, calculate operator expectation values and the like. But for operators that act only in the portion S of the total system, these quantities need only be calculated with the reduced density operator, which we met in Section 2.2.2:

$$\rho(t) = \text{Tr}_R[\chi(t)] \quad (4.18)$$

By performing the trace here over the reservoir states appropriately, we can derive a differential equation describing the time evolution of ρ only, without having to find χ . This is known as the *master equation* for the system S .

In the case of resonance fluorescence, we have a system Hamiltonian:

$$H_s = \frac{1}{2} \hbar \omega_A \sigma_z - dE(e^{-i\omega_A t} \sigma_+ + e^{i\omega_A t} \sigma_-) \quad (4.19)$$

The first term here is the 2-level atomic Hamiltonian seen in Eq. (4.11). The second term is due to the laser-atom interaction. We have treated the laser electric field classically, with this explicitly time-dependent Hamiltonian. The laser field at the atom side was taken to be $\mathbf{E} = \hat{e} 2E \cos(\omega_A t + \phi)$, and the interaction energy is then $-\mathbf{d} \cdot \mathbf{E}$, written down in the electric dipole and rotating wave approximations.

The reservoir with which our system interacts is simply the many modes of the electromagnetic field, whose Hamiltonian we write

$$H_R = \sum_{\mathbf{k}, \lambda} \hbar \omega_{\mathbf{k}} r_{\mathbf{k}, \lambda}^\dagger r_{\mathbf{k}, \lambda} \quad (4.20)$$

where the operators r and r^\dagger are precisely the photon annihilation and creation operators as seen before, for the given mode \mathbf{k}, λ .

The system-reservoir interaction Hamiltonian is given by

$$H_{SR} = \sum_{\mathbf{k}, \lambda} \hbar (\kappa_{\mathbf{k}, \lambda}^* r_{\mathbf{k}, \lambda}^\dagger \sigma_- + \kappa_{\mathbf{k}, \lambda} r_{\mathbf{k}, \lambda} \sigma_+) \quad (4.21)$$

where the κ are coupling constants that dictate the strength of coupling to each mode \mathbf{k}, λ .

From these Hamiltonians, it is possible to perform the reservoir trace explained above. We just quote here the result - the master equation for resonance fluorescence is given by:

$$\frac{d\rho}{dt} = -\frac{i\omega_A}{2} [\sigma_z, \rho] + \frac{i\Omega}{2} [e^{-i\omega_A t} \sigma_+ + e^{i\omega_A t} \sigma_-, \rho] + \frac{\gamma}{2} (2\sigma_- \rho \sigma_+ - \sigma_+ \sigma_- \rho - \rho \sigma_+ \sigma_-) \quad (4.22)$$

Here γ is the Einstein A coefficient for the two-level atom, and Ω the Rabi frequency (which effectively sets the strength of the driving laser).

A full derivation of this can be found in [8]. It is quite common to abbreviate the master equation as

$$\frac{d\rho}{dt} = \mathcal{L}\rho \quad (4.23)$$

where the operator \mathcal{L} is known as the *Liouvillian*.

By sandwiching the master equation between states $\langle 1 | \dots | 2 \rangle$, $\langle 2 | \dots | 1 \rangle$ and the like, and making use of Eqs. (4.13), (4.14) and (4.15), we can obtain time evolution equations for the operator expectation values:

$$\frac{d}{dt} \langle \sigma_+ \rangle = i\omega_A \langle \sigma_+ \rangle + i \frac{\Omega}{2} e^{i\omega_A t} \langle \sigma_z \rangle - \frac{\gamma}{2} \langle \sigma_+ \rangle \quad (4.24)$$

$$\frac{d}{dt} \langle \sigma_- \rangle = -i\omega_A \langle \sigma_- \rangle + i \frac{\Omega}{2} e^{-i\omega_A t} \langle \sigma_z \rangle - \frac{\gamma}{2} \langle \sigma_- \rangle \quad (4.25)$$

$$\frac{d}{dt} \langle \sigma_z \rangle = i\Omega e^{-i\omega_A t} \langle \sigma_+ \rangle - i\Omega e^{i\omega_A t} \langle \sigma_- \rangle + \gamma(\langle \sigma_z \rangle + 1) \quad (4.26)$$

For the system at hand, these are the *Optical Bloch Equations*. We can remove the explicit dependence on time by defining new operators:

$$\langle \tilde{\sigma}_+ \rangle = \langle \sigma_+ \rangle e^{-i\omega_A t}, \quad \langle \tilde{\sigma}_- \rangle = \langle \sigma_- \rangle e^{i\omega_A t} \quad (4.27)$$

The operator σ_z is left unchanged. Then we decompose these operators into a steady-state value, plus a fluctuating part:

$$\tilde{\sigma}_+ = \Delta \tilde{\sigma}_+ + \langle \tilde{\sigma}_+ \rangle_{ss}, \quad \tilde{\sigma}_- = \Delta \tilde{\sigma}_- + \langle \tilde{\sigma}_- \rangle_{ss}, \quad \sigma_z = \Delta \sigma_z + \langle \sigma_z \rangle_{ss} \quad (4.28)$$

much in the same way that was done in Section 2.2.3.

Now it turns out that we are interested in the operator correlation function $\langle \tilde{\sigma}_+(0) \tilde{\sigma}_-(\tau) \rangle_{ss}$. Note that as written, this is an *atomic* correlation function (involving atomic operators) rather than one for the field. However the two are certainly linked, as we shall see in Chapter 5. With the decomposition of Eq. (4.28), this correlation function will consist of two parts:

- $\langle \tilde{\sigma}_+ \rangle_{ss} \langle \tilde{\sigma}_- \rangle_{ss}$, independent of τ
- $\langle \Delta \tilde{\sigma}_+(0) \Delta \tilde{\sigma}_-(\tau) \rangle_{ss}$, dependent on τ

Upon taking the Fourier Transform, this first part will give a delta function – the *coherent spectrum* – whilst the remaining term gives the *incoherent spectrum*. The incoherent spectrum is the part we are interested in. We now need equations of motion for the Δ operators; they follow immediately from the Optical Bloch Equations Eqs. (4.24), (4.25) and (4.26):

$$\frac{d}{dt} \begin{pmatrix} \langle \Delta \tilde{\sigma}_- \rangle \\ \langle \Delta \tilde{\sigma}_+ \rangle \\ \langle \Delta \sigma_z \rangle \end{pmatrix} = \begin{pmatrix} -\frac{\gamma}{2} & 0 & -i \frac{Y\gamma}{2\sqrt{2}} \\ 0 & -\frac{\gamma}{2} & i \frac{Y\gamma}{2\sqrt{2}} \\ i \frac{Y\gamma}{\sqrt{2}} & i \frac{Y\gamma}{\sqrt{2}} & -\gamma \end{pmatrix} \begin{pmatrix} \langle \Delta \tilde{\sigma}_- \rangle \\ \langle \Delta \tilde{\sigma}_+ \rangle \\ \langle \Delta \sigma_z \rangle \end{pmatrix} \equiv \mathbf{M} \begin{pmatrix} \langle \Delta \tilde{\sigma}_- \rangle \\ \langle \Delta \tilde{\sigma}_+ \rangle \\ \langle \Delta \sigma_z \rangle \end{pmatrix} \equiv \mathbf{M} \langle \Delta \mathbf{s} \rangle \quad (4.29)$$

In dealing with the resonance fluorescence spectrum, it is convenient to define the parameter

$$Y = \frac{\sqrt{2}\Omega}{\gamma} \quad (4.30)$$

This has been used in writing Eq. (4.29), note.

Now Eq. (4.29) shows us that, for the set of operators $\Delta \tilde{\sigma}_-$, $\Delta \tilde{\sigma}_+$ and $\Delta \sigma_z$, the time rate-of-change of operator expectation values are *linear* in the operator expectation values themselves. Such a situation is amenable to analysis under a useful theorem known as the *quantum regression theorem*.

The Quantum Regression Theorem

We give the statement of this theorem as seen in [8]. Suppose there exists a set of system operators A_μ , $\mu = 1, 2, \dots$, which are *complete*. By this, we mean to say that for an arbitrary operator O , we have the following:

$$\text{Tr}_S (A_\mu (\mathcal{L}O)) = \sum_\lambda M_{\mu\lambda} \text{Tr}_S (A_\lambda O) \quad (4.31)$$

for each μ , where \mathcal{L} is the master equation Liouvillian of Eq. (4.23). The $M_{\mu\lambda}$ are constants. It follows that these complete operators satisfy the following:

$$\frac{d}{dt} \langle \mathbf{A} \rangle = \mathbf{M} \langle \mathbf{A} \rangle \quad (4.32)$$

where \mathbf{M} is the matrix having elements $M_{\mu\lambda}$, and \mathbf{A} is a column vector of the operators A_μ . Then, the quantum regression theorem is the statement

$$\frac{d}{d\tau} \langle O_1(t) \mathbf{A}(t + \tau) \rangle = \mathbf{M} \langle O_1(t) \mathbf{A}(t + \tau) \rangle \quad (4.33)$$

where O_1 is an arbitrary operator acting on the *system* (not the reservoir) alone. This last is valid for $\tau > 0$ only, note.

Loosely speaking, we are allowed to ‘multiply’ Eq. (4.32) by the operator O_1 , take it inside the expectation value brackets, and consider the lot as a new differential equation in τ rather than t . The quantum regression theorem is significant, as a common way of finding operator correlation functions is to solve the differential equation Eq. (4.33) arising from the regression theorem’s application.

‘The’ regression theorem is a little misleading, for the quantum regression theorem has many different forms. We have presented the form most relevant to the situation at hand.

We apply it immediately. We see that three operators $\Delta\tilde{\sigma}_-$, $\Delta\tilde{\sigma}_+$ and $\Delta\sigma_z$ satisfy Eq. (4.32); it turns out that they are also complete in the sense of Eq. (4.31). The quantum regression theorem then applied to Eq. (4.29) thus gives:

$$\frac{d}{d\tau} \langle \Delta\tilde{\sigma}_+(0) \Delta \mathbf{s}(\tau) \rangle_{ss} = \mathbf{M} \langle \Delta\tilde{\sigma}_+(0) \Delta \mathbf{s}(\tau) \rangle_{ss} \quad (4.34)$$

which is a differential equation in τ . The vector $\mathbf{s}(\tau)$ is the column vector of operators $[\sigma_-, \sigma_+, \sigma_z]^T$. This differential equation has solution:

$$\langle \Delta\tilde{\sigma}_+(0) \Delta \mathbf{s}(\tau) \rangle_{ss} = \mathbf{S}^{-1} \exp(\boldsymbol{\lambda} \tau) \mathbf{S} \langle \Delta\tilde{\sigma}_+(0) \Delta \mathbf{s}(0) \rangle_{ss} \quad (4.35)$$

where \mathbf{S} is a matrix that diagonalises \mathbf{M} , and $\boldsymbol{\lambda}$ is the resulting matrix of eigenvalues. Explicitly,

$$\boldsymbol{\lambda} = \underbrace{\begin{pmatrix} \frac{1}{2} & \frac{1}{2} & 0 \\ -i\frac{\sqrt{2}}{Y\gamma}\left(\frac{1}{2} + \frac{\gamma}{8\delta}\right) & i\frac{\sqrt{2}}{Y\gamma}\left(\frac{1}{2} + \frac{\gamma}{8\delta}\right) & -\frac{1}{2\delta} \\ -i\frac{\sqrt{2}}{Y\gamma}\left(\frac{1}{2} - \frac{\gamma}{8\delta}\right) & i\frac{\sqrt{2}}{Y\gamma}\left(\frac{1}{2} - \frac{\gamma}{8\delta}\right) & \frac{1}{2\delta} \end{pmatrix}}_{\mathbf{S}} \underbrace{\begin{pmatrix} -\frac{\gamma}{2} & 0 & -i\frac{Y\gamma}{2\sqrt{2}} \\ 0 & -\frac{\gamma}{2} & i\frac{Y\gamma}{2\sqrt{2}} \\ i\frac{Y\gamma}{\sqrt{2}} & i\frac{Y\gamma}{\sqrt{2}} & -\gamma \end{pmatrix}}_{\mathbf{M}} \underbrace{\begin{pmatrix} 1 & i\frac{Y\gamma}{2\sqrt{2}} & i\frac{Y\gamma}{2\sqrt{2}} \\ 1 & -i\frac{Y\gamma}{2\sqrt{2}} & -i\frac{Y\gamma}{2\sqrt{2}} \\ 0 & \frac{\gamma}{4} - \delta & \frac{\gamma}{4} + \delta \end{pmatrix}}_{\mathbf{S}^{-1}} \quad (4.36)$$

This gives:

$$\lambda = \begin{pmatrix} -\frac{\gamma}{2} & 0 & 0 \\ 0 & -\frac{3\gamma}{4} + \delta & 0 \\ 0 & 0 & -\frac{3\gamma}{4} - \delta \end{pmatrix} \quad (4.37)$$

The constant δ is given by:

$$\delta = \frac{\gamma}{4} \sqrt{1 - 8Y^2} \quad (4.38)$$

It remains only to find the ‘initial condition’ $\langle \Delta\tilde{\sigma}_+(0)\Delta\mathbf{s}(0) \rangle_{ss}$. This is given by [8]:

$$\langle \Delta\tilde{\sigma}_+(0)\Delta\mathbf{s}(0) \rangle_{ss} = \begin{pmatrix} \langle \Delta\tilde{\sigma}_+(0)\Delta\tilde{\sigma}_-(0) \rangle_{ss} \\ \langle \Delta\tilde{\sigma}_+(0)\Delta\tilde{\sigma}_+(0) \rangle_{ss} \\ \langle \Delta\tilde{\sigma}_+(0)\Delta\sigma_z(0) \rangle_{ss} \end{pmatrix} = \frac{1}{2} \frac{Y^2}{(1+Y^2)^2} \begin{pmatrix} Y^2 \\ 1 \\ i\sqrt{2}Y \end{pmatrix} \quad (4.39)$$

Eq. (4.39) is obtained by solving the Optical Bloch Equations and taking the steady state solution.

We at last have our correlation functions:

$$\begin{aligned} \langle \Delta\tilde{\sigma}_+(0)\Delta\tilde{\sigma}_-(\tau) \rangle_{ss} &= \frac{1}{4} \frac{Y^2}{Y^2 + 1} \exp\left(-\frac{\gamma}{2}\tau\right) \\ &\quad - \frac{1}{8} \frac{Y^2}{(Y^2 + 1)^2} \left(1 - Y^2 + (1 - 5Y^2) \frac{\gamma}{4\delta}\right) \exp\left(-\left(\frac{3\gamma}{4} - \delta\right)\tau\right) \\ &\quad - \frac{1}{8} \frac{Y^2}{(Y^2 + 1)^2} \left(1 - Y^2 - (1 - 5Y^2) \frac{\gamma}{4\delta}\right) \exp\left(-\left(\frac{3\gamma}{4} + \delta\right)\tau\right) \end{aligned} \quad (4.40)$$

We also have:

$$\begin{aligned} \langle \Delta\tilde{\sigma}_+(0)\Delta\tilde{\sigma}_+(\tau) \rangle_{ss} &= \frac{1}{4} \frac{Y^2}{Y^2 + 1} \exp\left(-\frac{\gamma}{2}\tau\right) \\ &\quad + \frac{1}{8} \frac{Y^2}{(Y^2 + 1)^2} \left(1 - Y^2 + (1 - 5Y^2) \frac{\gamma}{4\delta}\right) \exp\left(-\left(\frac{3\gamma}{4} - \delta\right)\tau\right) \\ &\quad + \frac{1}{8} \frac{Y^2}{(Y^2 + 1)^2} \left(1 - Y^2 - (1 - 5Y^2) \frac{\gamma}{4\delta}\right) \exp\left(-\left(\frac{3\gamma}{4} + \delta\right)\tau\right) \end{aligned} \quad (4.41)$$

This is identical to the correlation function Eq. (4.40), but for the sign changes in the second and third terms. We shall see later that this correlation function is used to calculate the aforementioned quadrature correlation functions. Looking ahead, we shall find that because the sign changes between the two correlation functions Eq. (4.40) and Eq. (4.41), one quadrature correlation function will carry the central resonance fluorescence peak, whilst the other quadrature correlation function will carry the flanking sidepeaks.

Both of these correlation functions are real, in spite of the fact that δ can be complex for Y sufficiently large (see Eq. (4.38)). To see this explicitly, note that whenever δ is complex, it is purely imaginary, and in this case the second and third terms in Eqs. (4.40) and (4.41) are complex conjugates, which evidently sum to a real number for each correlation function.

Now it is clear that, upon taking the Fourier Transform of the correlation function Eq. (4.40) (which corresponds to the field correlation function), a three-peaked spectrum will result, from the three exponentials in that equation. Our analysis so far has been quite formal – using the regression theorem to derive correlations in the output field – so one may wonder if a *physical* interpretation exists for the three-peaked spectrum. After all, our model for the atom contains only two levels, and at first glance doesn't appear to accommodate three distinct transitions. In fact, such an interpretation does exist, and is known as the *dressed-states model* for the atom [8]. This replaces our three-part semiclassical Hamiltonian given by Eqs. (4.16), (4.19), (4.20) and (4.21) with the following:

$$H = \frac{1}{2} \hbar \omega_A \sigma_z + \hbar \omega_A a^\dagger a + \hbar (\kappa a \sigma_+ + \kappa^* a^\dagger \sigma_-) \quad (4.42)$$

This is a fully quantised Hamiltonian, known as the *Jaynes-Cummings Hamiltonian*. See that the driving laser is no longer being treated as classical – its energy appears explicitly as the term $\hbar \omega_A a^\dagger a$. The third term in Eq. (4.42) represents the atom-laser interaction. For simplicity, we have taken the atom to only interact with the laser mode, rather than allowing it to interact with all the modes of the electromagnetic field, which we had done previously. This is quite reasonable if the laser is very intense.

The *dressed states* referred to are the eigenstates of this Hamiltonian when there is no interaction (i.e. when $\kappa = 0$), and are product states involving the atomic states $|1\rangle$ and $|2\rangle$ and photon number states for the laser field. There is some degeneracy among these levels; see the diagram below. When $\kappa \neq 0$, we find that the degeneracy is lifted, and the resulting states split in such a way that only 3 distinct transitions (in terms of energy size) are possible – these are exactly the transitions responsible for the 3-peaked spectrum mentioned earlier.

It is possible to show [8], that each energy level is split symmetrically by a total amount $\hbar \Omega$, where Ω is the Rabi frequency as before, provided that the laser field is strong (in particular, it has a very large mean photon number). It is possible to find the energy splitting exactly, without having to assume a large mean photon number, however.

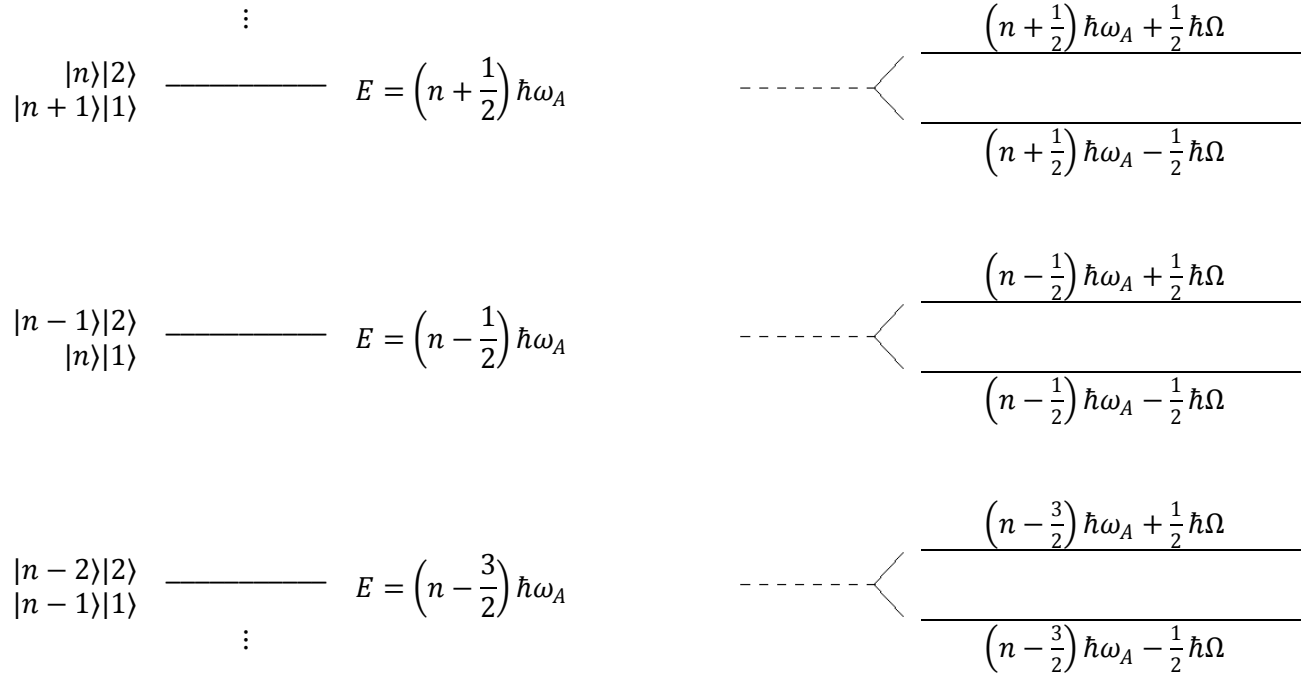


Figure 5. Left: The Jaynes-Cummings ‘ladder’ of states are the eigenstates of Eq. (4.42) when $\kappa = 0$. Note the degeneracy. Right: The degeneracy is lifted once we consider interactions. The new ladder of states appears to have many possible transitions, but in fact only 3 are unique.

Chapter 5

The optical protocol of Furusawa *et al.*

5.1 Description

The Furusawa protocol [2] begins with two generating cavities that produce squeezed light. These are *optical parametric oscillators*, which we met when presenting the vacuum correlation functions in Section 4.1. One of the cavities generates vacuum states that are squeezed in the x -direction, whose field we write \mathcal{E}_{EPRx} (again as we did in Section 4.1), whilst the other generates vacuum states squeezed in the y -direction (\mathcal{E}_{EPRy}). Be aware of the convention mentioned in Section 4.1, whereby \mathcal{E} refers only to the positive-frequency part of the electric field.

These two fields are mixed at a 50/50 beamsplitter, seen in Section 3.3. The symmetric superposition

$$\mathcal{E}_A = \frac{1}{\sqrt{2}}(\mathcal{E}_{EPRx} + \mathcal{E}_{EPRy}) \quad (5.01)$$

is distributed to Alice, whilst the antisymmetric superposition

$$\mathcal{E}_B = \frac{1}{\sqrt{2}}(\mathcal{E}_{EPRx} - \mathcal{E}_{EPRy}) \quad (5.02)$$

is distributed to Bob. The two fields \mathcal{E}_A and \mathcal{E}_B are correlated.

Alice mixes her received field \mathcal{E}_A with the input field \mathcal{E}_{in} which is to be teleported, at a different 50/50 beamsplitter, and then makes measurements of the X and Y quadratures of the two outputs of this beamsplitter. She measures the X quadrature of one of the outputs, and the Y -quadrature of the other, employing balanced homodyne detection (Section 3.4) to do so. Ultimately, she is measuring the quantities

$$\frac{1}{\sqrt{2}}(\mathcal{E}_{in}^X + \mathcal{E}_A^X), \quad \frac{1}{\sqrt{2}}(\mathcal{E}_{in}^Y - \mathcal{E}_A^Y) \quad (5.03)$$

where the superscript indicates the appropriate quadrature of its associated field.

Bob receives the field \mathcal{E}_B as well as the results of Alice's measurements. To perform teleportation, Bob needs to modify his field dependent on Alice's measurement results. In fact, he wishes to add to his field

$$\mathcal{E}_B = \mathcal{E}_B^X + i\mathcal{E}_B^Y \quad (5.04)$$

a particular type of *displacement*, consisting of the following:

- Addition of $\mathcal{E}_{in}^X + \mathcal{E}_A^X$ to his X -quadrature \mathcal{E}_B^X
- Addition of $\mathcal{E}_{in}^Y - \mathcal{E}_A^Y$ to his Y -quadrature \mathcal{E}_B^Y

We will show shortly that such a displacement results in perfect teleportation in appropriate limits. In total, Bob adds to his field \mathcal{E}_B the following quantity

$$F_A * \sqrt{2} \left(\frac{1}{\sqrt{2}} (\mathcal{E}_{in}^X + \mathcal{E}_A^X) + \frac{i}{\sqrt{2}} (\mathcal{E}_{in}^Y - \mathcal{E}_A^Y) \right) \quad (5.05)$$

The function F_A is the *impulse response* describing any filtering that is done by Alice in the process of making her measurements. For the case where Alice's measurements don't filter the fields in any way, the convolution above isn't needed. In any practical setup however, we note that Alice's measurements will always include some kind of cut-off (i.e. at least some indirect filtering) due to the apparatus she is using; hence, the convolution is shown for completeness.

After Bob has implemented his displacement as described above, his field is

$$\begin{aligned} \mathcal{E}_{out} &= F_B * (\mathcal{E}_B + F_A * (\mathcal{E}_{in} + \mathcal{E}_A^*)) \\ &= \mathcal{E}_B^b + \mathcal{E}_{in}^{ab} + \mathcal{E}_A^{*ab} \end{aligned} \quad (5.06)$$

Just as was the case with Alice, we have included the possibility of filtering by Bob: F_B is the impulse response of any filter that Bob may be using, which he applies after displacing his field as in Eq. (5.05).

We have abbreviated the convolutions (i.e., the filtering) by using a superscript a for filtering by Alice, and a superscript b for that by Bob. Note that, due to the commutativity of the convolution, it does not matter what order these are applied in:

$$\mathcal{E}^{ab} = F_A * F_B * \mathcal{E} = (F_A * F_B) * \mathcal{E} = (F_B * F_A) * \mathcal{E} = \mathcal{E}^{ba}, \text{ etc} \quad (5.07)$$

In the limit of *no filtering by Alice and Bob* (equivalently, allowing the bandwidth of any such filtering to become large), we find

$$\begin{aligned} \mathcal{E}_{out} &= \mathcal{E}_{in} + (\mathcal{E}_B + \mathcal{E}_A^*) \\ &= \mathcal{E}_{in} + \frac{1}{\sqrt{2}} (\mathcal{E}_{EPRx} - \mathcal{E}_{EPRy}) + \frac{1}{\sqrt{2}} (\mathcal{E}_{EPRx}^* + \mathcal{E}_{EPRy}^*) \\ &= \mathcal{E}_{in} + \sqrt{2} \mathcal{E}_{EPRx}^X - i\sqrt{2} \mathcal{E}_{EPRy}^Y \end{aligned} \quad (5.08)$$

Hence, for *large squeezing* of \mathcal{E}_{EPRx} in its X -quadrature and of \mathcal{E}_{EPRy} in its Y -quadrature, we have the result that $\mathcal{E}_{out} \rightarrow \mathcal{E}_{in}$, i.e. the teleportation becomes perfect. This is the reason for the particular choice Eq. (5.05) for Bob's displacement.

This protocol was successfully implemented by Furusawa *et al.* [2]. Formally, the quality of the teleportation can be quantified by a number known as the *fidelity*, which ranges from 0 to 1. A fidelity of 1 indicates perfect teleportation. It is explained in [2] that for teleportation of coherent states, the fidelity F cannot exceed 0.5 in this protocol without the use of entanglement. Furusawa *et al.* report an experimental fidelity of $F = 0.58 \pm 0.02$, which is highly indicative of the quantum nature of the teleportation.

5.2 First Order Correlation Functions for the output field

We are interested in correlations in the output field \mathcal{E}_{out} . The first order correlation function was defined already in Section 3.5, Eq. (3.69).

We look now at the numerator of Eq. (3.69), and use the equation for the output field Eq. (5.06) to get:

$$\begin{aligned}
 \langle \mathcal{E}_{out}^\dagger(\tau) \mathcal{E}_{out} \rangle &= \langle (\mathcal{E}_B^{\dagger b}(\tau) + \mathcal{E}_{in}^{\dagger ab}(\tau) + \mathcal{E}_A^{ab}(\tau)) (\mathcal{E}_B^b + \mathcal{E}_{in}^{ab} + \mathcal{E}_A^{\dagger ab}) \rangle \\
 &= \langle \mathcal{E}_{in}^{\dagger ab}(\tau) \mathcal{E}_{in}^{ab} \rangle + \langle (\mathcal{E}_B^{\dagger b}(\tau) + \mathcal{E}_A^{ab}(\tau)) (\mathcal{E}_B^b + \mathcal{E}_A^{\dagger ab}) \rangle \\
 &= \langle \mathcal{E}_{in}^{\dagger ab}(\tau) \mathcal{E}_{in}^{ab} \rangle + \langle \mathcal{E}_B^{\dagger b}(\tau) \mathcal{E}_B^b \rangle + \langle \mathcal{E}_B^{\dagger b}(\tau) \mathcal{E}_A^{\dagger ab} \rangle + \langle \mathcal{E}_A^{ab}(\tau) \mathcal{E}_B^b \rangle + \langle \mathcal{E}_A^{ab}(\tau) \mathcal{E}_A^{\dagger ab} \rangle \\
 &= \langle \mathcal{E}_{in}^{\dagger ab}(\tau) \mathcal{E}_{in}^{ab}(0) \rangle_{ss} + 4 \text{ vacuum terms}
 \end{aligned} \tag{5.09}$$

The second inequality above follows from the assumption that there is no correlation between the input field \mathcal{E}_{in} and the squeezed fields \mathcal{E}_{EPRx} and \mathcal{E}_{EPRy} .

So, in the most general case which considers filtering by both Alice and Bob, the first-order correlation function for the output field consists of that for the input field (with filtering), plus 4 extra terms involving the squeezed vacuum fields.

5.2.1 Gaussian Filtering in the absence of filtering by Alice

We move on now to consider the following situation:

- *No* filtering by Alice
- *Gaussian* filtering by Bob

The numerator of our first order correlation function simplifies in the absence of filtering by Alice:

$$\begin{aligned}
 \langle \mathcal{E}_{out}^\dagger(\tau) \mathcal{E}_{out}(0) \rangle_{ss} &= \langle \mathcal{E}_{in}^{\dagger b}(\tau) \mathcal{E}_{in}^b(0) \rangle_{ss} \\
 &\quad + \langle \mathcal{E}_B^{\dagger b}(\tau) \mathcal{E}_B^b(0) \rangle_{ss} + \langle \mathcal{E}_B^{\dagger b}(\tau) \mathcal{E}_A^{\dagger b}(0) \rangle_{ss} + \langle \mathcal{E}_A^b(\tau) \mathcal{E}_B^b(0) \rangle_{ss} + \langle \mathcal{E}_A^b(\tau) \mathcal{E}_A^{\dagger b}(0) \rangle_{ss} \\
 &= \langle \mathcal{E}_{in}^{\dagger b}(\tau) \mathcal{E}_{in}^b(0) \rangle_{ss} + 4 \text{ vacuum terms}
 \end{aligned} \tag{5.10}$$

To begin with, we shall concern ourselves only with the 4 vacuum terms in Eq. (5.10).

We let the Gaussian filter impulse response (in time) be

$$g(t) = C e^{-dt^2} \tag{5.11}$$

where C and d are related constants. We note that $d > 0$ as well.

Let also $\mathcal{E}(t)$ be an arbitrary signal in time that is ‘switched on’ at some time $t = t_0$, and is zero for $t < t_0$.

Gaussian filtering of such a signal then involves the convolution integral

$$(C e^{-dt^2}) * \mathcal{E}(t) = C \int_{t_0}^{\infty} e^{-d(t-t')^2} \mathcal{E}(t') dt' \tag{5.12}$$

A note is in order at this point. Unlike a Lorentzian filter, whose impulse response is *causal*, the Gaussian filter impulse response is *acausal*. This means that the Gaussian filtering process described is slightly artificial.

We now consider evaluation of the last of the vacuum terms in Eq. (5.10). Firstly,

$$\begin{aligned}\mathcal{E}_A^b(\tau+t)\mathcal{E}_A^{\dagger b}(t) &= \int_{t_0}^{\infty} C e^{-d(\tau+t-t')^2} \mathcal{E}_A(t') dt' \int_{t_0}^{\infty} C e^{-d(t-t'')^2} \mathcal{E}_A^{\dagger}(t'') dt'' \\ &= \int_{t_0}^{\infty} \int_{t_0}^{\infty} \exp\left[-d(\tau+t-t')^2 - d(t-t'')^2\right] \mathcal{E}_A(t') \mathcal{E}_A^{\dagger}(t'') dt' dt''\end{aligned}$$

And hence:

$$\langle \mathcal{E}_A^b(\tau+t)\mathcal{E}_A^{\dagger b}(t) \rangle = \int_{t_0}^{\infty} \int_{t_0}^{\infty} \exp\left[-d(\tau+t-t')^2 - d(t-t'')^2\right] \langle \mathcal{E}_A(t') \mathcal{E}_A^{\dagger}(t'') \rangle dt' dt'' \quad (5.13)$$

Now, we wish only to work with fields in their steady-states. The LHS correlation function in Eq. (5.13) can be made into a steady-state one by allowing the field ‘switch-on’ time t_0 to go to minus infinity – i.e., allowing the fields to have been ‘switched on’ for a long time period. We also take the fields appearing in the integrand of Eq. (5.13) to be in their steady-state as well. Overall, what we get from Eq. (5.13) is the following:

$$\langle \mathcal{E}_A^b(\tau)\mathcal{E}_A^{\dagger b}(0) \rangle_{ss} = \lim_{t_0 \rightarrow -\infty} \int_{t_0}^{\infty} \int_{t_0}^{\infty} \exp\left[-d(\tau+t-t')^2 - d(t-t'')^2\right] \langle \mathcal{E}_A(t') \mathcal{E}_A^{\dagger}(t'') \rangle_{ss} dt' dt'' \quad (5.14)$$

In taking the limit, we expect the parameter t to become superfluous. We are able to find the expectation value $\langle \mathcal{E}_A(t') \mathcal{E}_A^{\dagger}(t'') \rangle_{ss}$ in terms of the correlation functions given in Section 4.1. One first notes that:

$$\langle \mathcal{E}_A(t') \mathcal{E}_A^{\dagger}(t'') \rangle_{ss} = \langle \mathcal{E}_A(|t' - t''|) \mathcal{E}_A^{\dagger}(0) \rangle_{ss} \quad (5.15)$$

which is a consequence of the correlation functions being both even in time, and dependent only on time differences. We may then use Eq. (4.07) for the RHS of Eq. (5.15) above.

Looking at the correlation functions presented in Section 4.1, we see that the RHS of Eq. (5.15) involves linear combinations of exponentials like $\exp(-\eta|t|)$, where η is a constant. We thus consider the integral

$$I(C, d, \tau, \eta) = \lim_{t_0 \rightarrow -\infty} C^2 \int_{t_0}^{\infty} \int_{t_0}^{\infty} \exp\left[-d(\tau+t-t')^2 - d(t-t'')^2\right] \exp(-\eta|t' - t''|) dt' dt'' \quad (5.16)$$

and then we can use linearity to work out the correlation function Eq. (5.14).

The procedure just shown can be repeated for all 4 vacuum terms appearing in Eq. (5.10). We note that some of the vacuum terms will require the use of delta functions $\delta(t)$ (see Eq. (4.07)), for which we will need an integral similar to Eq. (5.16), namely

$$I_{\delta}(C, d, \tau, \eta) = \lim_{t_0 \rightarrow -\infty} C^2 \int_{t_0}^{\infty} \int_{t_0}^{\infty} \exp\left[-d(\tau+t-t')^2 - d(t-t'')^2\right] \delta(t' - t'') dt' dt'' \quad (5.17)$$

The absolute value is not required since the delta function is even.

Details regarding the evaluation of $I(C, d, \tau, \eta)$ are given in Appendix B. The result is

$$I(C, d, \tau, \eta) = C^2 \frac{\pi}{2d} \exp\left(\frac{\eta^2}{2d} + \eta\tau\right) \left[\operatorname{erf}\left(\frac{-\eta - d\tau}{\sqrt{2d}}\right) + 1 \right] + C^2 \frac{\pi}{2d} \exp\left(\frac{\eta^2}{2d} - \eta\tau\right) \left[1 - \operatorname{erf}\left(\frac{\eta - d\tau}{\sqrt{2d}}\right) \right] \quad (5.18)$$

For consistency, we have evaluated $I_\delta(C, d, \tau, \eta)$ in two ways. The first is to use a particular definition of the delta function in terms of an appropriate limit of functions (see [7]), namely:

$$\lim_{\eta \rightarrow \infty} \frac{\eta}{2} \exp(-\eta|t|) = \delta(t) \quad (5.19)$$

We hence have the result

$$I_\delta(C, d, \tau) = \lim_{\eta \rightarrow \infty} \frac{\eta}{2} I(C, d, \tau, \eta) \quad (5.20)$$

This limit can be evaluated using L'Hopital's Rule. Alternatively, we can simply evaluate the integral defining $I_\delta(C, d, \tau)$ directly – Eq. (5.17). Both methods give

$$I_\delta(C, d, \tau) = C^2 \sqrt{\frac{\pi}{2d}} \exp\left(\frac{-d\tau^2}{2}\right) \quad (5.21)$$

Now we note that the integral $I(C, d, \tau, \eta)$ effectively ‘filters’ the function $\exp(-\eta t)$, that function being a generic feature in the correlation functions defined in Section 4.1. From the Gaussian impulse response also given above, Eq. (5.11), we see that d controls the bandwidth of the Gaussian filtering. As $d \rightarrow \infty$, i.e. as the filtering bandwidth becomes very large, we expect the filter to have no effect – we should recover our input function. By making the choice

$$C = \sqrt{\frac{d}{\pi}} \quad (5.22)$$

we get the expected result

$$\lim_{d \rightarrow \infty} I(C, d, \tau, \eta) = \exp(-\eta\tau) \quad (5.23)$$

It is also possible to define the delta function as a limit of Gaussians as follows [17]:

$$\delta(x) = \lim_{\epsilon \rightarrow 0} \frac{1}{2\sqrt{\pi\epsilon}} \exp\left(-\frac{x^2}{4\epsilon}\right) \quad (5.24)$$

From this, we also get the result

$$\lim_{d \rightarrow \infty} I_\delta(C, d, \tau) = \delta(\tau) \quad (5.25)$$

with the choice for C as given in Eq. (5.22). Such a result is expected for precisely the same reasons given above – that is, I_δ effectively filters a delta function, which we expect to get back in the regime of very large filtering bandwidths.

In what follows, we shall stick with the notation that has C as an argument in the integrals I and I_δ , mainly to distinguish these integrals from the corresponding ones for Lorentzian filtering to be introduced in the next section. However, C is not really an extra variable since it is related to d , and in all that follows we will not be considering any values for C other than $C = \sqrt{d/\pi}$.

5.2.2 Lorentzian Filtering in the absence of filtering by Alice

Relevant integrals for the following situation:

- No filtering by Alice
- Lorentzian filtering by Bob

are derived by Noh in [7]. For completeness, we state the results here. The impulse response in time of Bob's Lorentzian filter is given by

$$l(t) = \gamma_B u(t) \exp(-\gamma_B t) \quad (5.26)$$

where γ_B is his filter bandwidth. Here $u(t)$ is the unit step:

$$u(t) = \begin{cases} 0, & t < 0 \\ 1, & t > 0 \end{cases} \quad (5.27)$$

The presence of this unit step means that the Lorentzian filter is *causal*, as we explained earlier.

The integrals $I(C, d, \tau, \eta)$ and $I_\delta(C, d, \tau)$ of Eqs. (5.16) and (5.17) above were evaluated for Gaussian filtering. Going through the same process for Lorentzian filtering gives

$$I(\gamma_B, \tau, \eta) = \frac{\gamma_B \eta}{\eta^2 - \gamma_B^2} \exp(-\gamma_B \tau) + \frac{\gamma_B^2}{\gamma_B^2 - \eta^2} \exp(-\eta \tau) \quad (5.28)$$

$$I_\delta(\gamma_B, \tau) = \frac{\gamma_B}{2} \exp(-\gamma_B \tau) \quad (5.29)$$

In all above (and in the following) equations, the replacements $I(C, d, \tau, \eta) \rightarrow I(\gamma_B, \tau, \eta)$ and $I_\delta(C, d, \tau) \rightarrow I_\delta(\gamma_B, \tau)$ take us from Gaussian filtering over to Lorentzian filtering by Bob. We'll take γ_B to represent Lorentzian filter bandwidths, and d to indicate Gaussian filter bandwidths, in order to make it clear which type of filtering is being used.

These equations will be used in plots below to test the effectiveness of Gaussian filtering against Lorentzian filtering.

5.2.3 Spectrum of the teleported vacuum

We now consider the teleporter output when there is no input state. We then have only the four vacuum terms in our first-order correlation function Eq. (5.10):

$$\langle \mathcal{E}_{out}^\dagger(\tau) \mathcal{E}_{out}(0) \rangle_{ss(VAC)} = \langle \mathcal{E}_B^{\dagger b}(\tau) \mathcal{E}_B^b(0) \rangle_{ss} + \langle \mathcal{E}_B^{\dagger b}(\tau) \mathcal{E}_A^{\dagger b}(0) \rangle_{ss} + \langle \mathcal{E}_A^b(\tau) \mathcal{E}_B^b(0) \rangle_{ss} + \langle \mathcal{E}_A^b(\tau) \mathcal{E}_A^{\dagger b}(0) \rangle_{ss} \quad (5.30)$$

If we use our integrals, namely Eqs. (5.16) and (5.17) defined in the previous section, we can evaluate Eq. (5.30). The correlation functions of Section 4.1 are needed, as shown in the previous section. The result is:

$$\langle \mathcal{E}_{out}^\dagger(\tau) \mathcal{E}_{out}(0) \rangle_{ss(VAC)} = \frac{-\lambda \gamma_s}{1 + \lambda} I\left(C, d, \frac{\gamma_s}{2}(1 + \lambda), \tau\right) + I_\delta(C, d, \tau) \quad (5.31)$$

This gives us the unnormalised first order correlation function for no input field.

We shall define the *optical spectrum* as:

$$S(\omega) = \frac{1}{2\pi} \int_{-\infty}^{\infty} d\tau \langle \mathcal{E}_{out}^\dagger(\tau) \mathcal{E}_{out} \rangle \exp(i\omega\tau) \quad (5.32)$$

which is a Fourier transform of the unnormalised correlation function. This is really the normalised power spectral density, mentioned in Section 3.5.

Now, we see that the correlation functions for the vacuum terms are linear in the integrals $I(C, d, \tau, \eta)$ and $I_\delta(C, d, \tau)$. Hence, in order to look at the spectrum, it is only necessary to take the Fourier transform of these integrals.

All the correlation functions we shall ever meet in this report are *even* in τ . Essentially, this is a consequence of us insisting on the use of *normal ordering* in all correlation functions, and the fact that the correlation functions we will be working with are all *real*. Now for a function $f(\tau)$ that is real and even in time, we have the result

$$\frac{1}{2\pi} \int_{-\infty}^{\infty} d\tau f(\tau) \exp(i\omega\tau) = \frac{1}{2\pi} 2\text{Re} \left(\int_0^{\infty} f(\tau) \exp(i\omega\tau) \right) \quad (5.33)$$

where the Re indicates the real part. Now define

$$SI(C, d, \omega, \eta) = \frac{1}{2\pi} \int_0^{\infty} d\tau I(C, d, \tau, \eta) \exp(i\omega\tau) \quad (5.34)$$

$$SI_\delta(C, d, \omega) = \frac{1}{2\pi} \int_0^{\infty} d\tau I_\delta(C, d, \tau) \exp(i\omega\tau) \quad (5.35)$$

Then, if we want to look at the correlation function spectrum, it is only necessary to replace the integrals I and I_δ wherever they occur with the functions SI and SI_δ , and take twice the real part of the resulting overall expression. This also holds true later on, when we consider teleporting the resonance fluorescence field. These functions are given by:

$$SI(C, d, \omega, \eta) = \frac{C^2}{4d} \left(\frac{2\eta}{\omega^2 + \eta^2} \exp\left(-\frac{\omega^2}{2d}\right) \left(1 + \text{erf}\left(\frac{i\omega}{\sqrt{2d}}\right)\right) + \frac{2\omega i}{\omega^2 + \eta^2} \exp\left(\frac{\eta^2}{2d}\right) \left(1 - \text{erf}\left(\frac{\eta}{\sqrt{2d}}\right)\right) \right) \quad (5.36)$$

And

$$SI_\delta(C, d, \omega) = \frac{C^2}{4d} \exp\left(-\frac{\omega^2}{2d}\right) \left(1 + \text{erf}\left(\frac{i\omega}{\sqrt{2d}}\right)\right) \quad (5.37)$$

We now look at some vacuum spectra below. For comparison, plots are shown with Lorentzian filtering as well. The comparison here is done by matching the filter half-widths. Recall that d was used as the parameter controlling the Gaussian filtering bandwidth, while γ_B was used for Lorentzian filtering. To relate the two, note that under our version of the Fourier transform that we are using for spectra, namely $S(\omega) = \frac{1}{2\pi} \int_{-\infty}^{\infty} f(t) e^{i\omega t} dt$, we have the following:

$$\gamma_B u(t) \exp(-\gamma_B t) \leftrightarrow \frac{1 + \frac{\omega}{\gamma_B} i}{2\pi \left(1 + \left(\frac{\omega}{\gamma_B}\right)^2\right)} \quad (5.38)$$

and³

³ See, for example, entry (23) p121 of [20].

$$\sqrt{\frac{d}{\pi}} \exp(-dt^2) \leftrightarrow \frac{1}{2\pi} \exp\left(-\frac{\omega^2}{4d}\right) \quad (5.39)$$

The Fourier convolution theorem reads, under our particular definition for the Fourier Transform:

$$f * g \leftrightarrow 2\pi FG \quad (5.40)$$

where \leftrightarrow denotes a Fourier Transform pair. In frequency space then, these filters halve in amplitude at $\omega = \pm\gamma_B$ and $\omega = \pm\sqrt{4d\log(2)}$ respectively. Matching half-widths then gives

$$d = \frac{\gamma_B^2}{4\log(2)} \quad (5.41)$$

In the figures below, we have worked in terms of γ_B , and calculated the appropriate d from Eq. (5.41). The degree of squeezing has been set at $\lambda = 0.9$ for these plots. The right-hand figure is zoomed in around the $\omega = 0$ part of the spectrum.

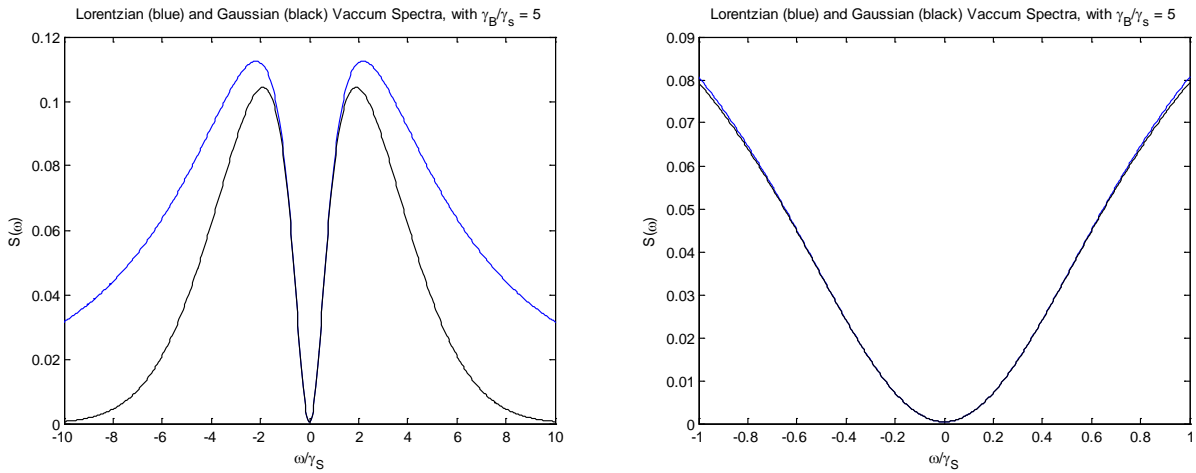


Figure 6: Teleported vacuum spectra with $\gamma_B/\gamma_s = 5$

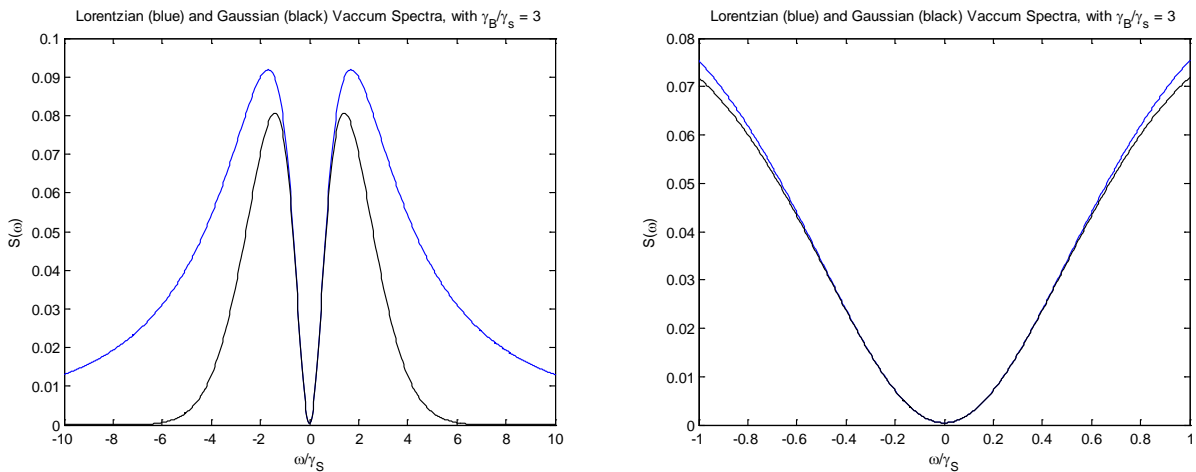


Figure 7: Teleported vacuum spectra with $\gamma_B/\gamma_s = 3$

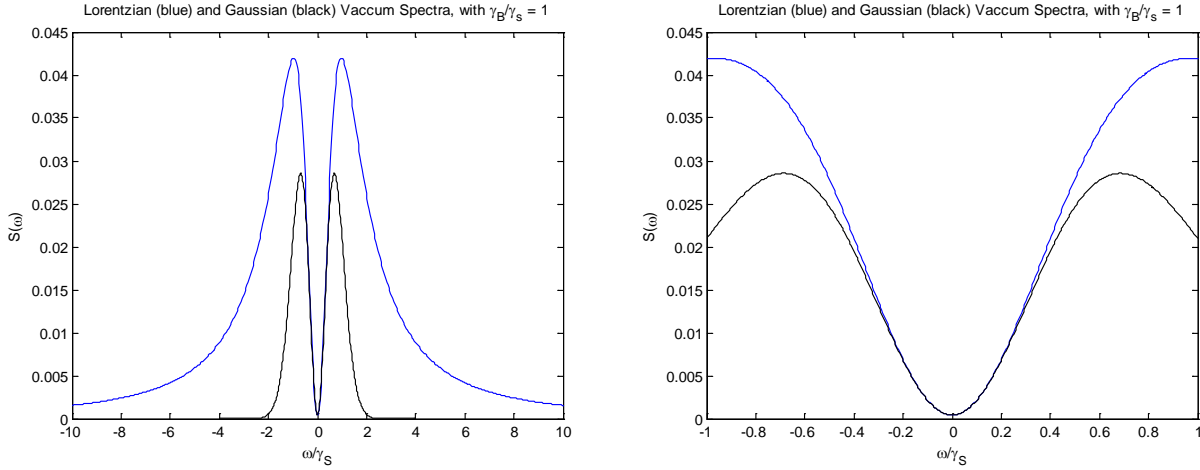


Figure 8: Teleported vacuum spectra with $\gamma_B/\gamma_s = 1$

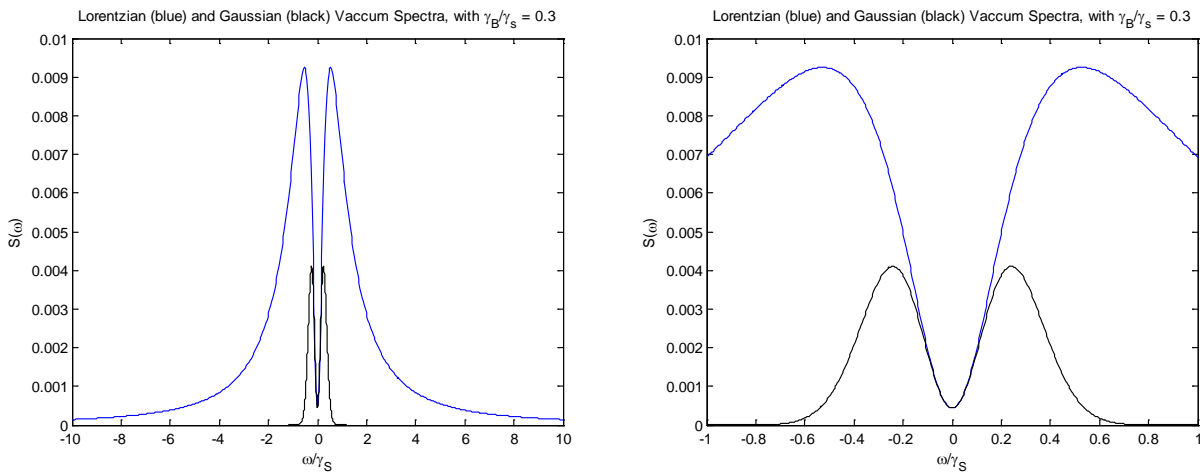


Figure 9: Teleported vacuum spectra with $\gamma_B/\gamma_s = 0.3$

The general teleported vacuum spectrum consists of a ‘vacuum dip’ region centered around $\omega = 0$, where the vacuum noise is reduced almost to zero, flanked either side by two broad peaks (‘sidepeaks’).

We can see that for filtering bandwidths by Bob that are larger than the squeezing bandwidth, i.e. $\gamma_B > \gamma_s$, the central region around $\omega = 0$ is much the same between Gaussian and Lorentzian filters. This is to be expected – Bob’s bandwidth is not yet narrow enough to start cutting significantly into the vacuum dip region. However, we see that the Gaussian filter is better at cutting out the higher frequency noise, which is expected due to the fact that it decays much quicker than does the Lorentzian in frequency space, at higher frequencies. As γ_B is decreased relative to the squeezing bandwidth, the Gaussian filter begins to reduce the vacuum sidepeak noise much sooner than does the Lorentzian filter (each filter having the same half-width). For $\gamma_B < \gamma_s$, we see considerable noise reduction by the Gaussian filter. It does not reduce the noise right in the centre at $\omega = 0$, however – the two filters still match in performance there. The vacuum dip region also narrows as the filter bandwidth is decreased.

5.2.4 Spectrum of the teleported resonance fluorescence field

Further testing of the Gaussian filter shall now be done by looking at teleporting a resonance fluorescence spectrum. The output field correlation function now has an additional term since we are not just inputting a vacuum:

$$\langle \mathcal{E}_{out}^\dagger(\tau) \mathcal{E}_{out}(0) \rangle_{ss} = \langle \mathcal{E}_{in}^{\dagger b}(\tau) \mathcal{E}_{in}^b(0) \rangle_{ss} + \langle \mathcal{E}_{out}^\dagger(\tau) \mathcal{E}_{out}(0) \rangle_{ss(VAC)} \quad (5.42)$$

Evaluating $\langle \mathcal{E}_{in}^{\dagger b}(\tau) \mathcal{E}_{in}^b(0) \rangle_{ss}$, and then its spectrum, is done in exactly the same way as for $\langle \mathcal{E}_B^{\dagger b}(\tau) \mathcal{E}_B^b(0) \rangle_{ss}$ and others in Sections 5.2.1 and 5.2.3. There is a slight difference, however. We want to make use of the correlation functions of Section 4.2, but as we saw before, those correlation functions are given in terms of atomic raising and lowering operators. What we need then is a relationship between \mathcal{E}_{in} and the atomic raising and lowering operators. This relationship is as follows:

$$\mathcal{E}_{in} = \sqrt{\gamma_{in}} \sigma_- + \mathcal{E}_{in} \quad (5.43)$$

where \mathcal{E}_{in} is a vacuum field operator. This is an example of an ‘input-output’ relationship - see for example, Section 7.1 of Walls [14]. Such a relationship expresses a cavity output field in terms of input fields and atomic operators. Our notation is perhaps a little unclear, for we have used ‘in’ on the LHS of Eq. (5.43) because this is the field that is input into the teleporter, but it is really the ‘output’ field in the sense used in the input-output relationship just mentioned. Ultimately, assuming that we normally order our operators, the first-order field correlation functions are obtained from the atomic operator correlation functions simply by multiplying by γ_{in} , the *input bandwidth* of the field, and changing γ to γ_{in} . From Eq. (4.40),

$$\begin{aligned} \langle \mathcal{E}_{in}^\dagger(\tau) \mathcal{E}_{in}(0) \rangle_{ss} &= \sqrt{\gamma_{in}} \sqrt{\gamma_{in}} \langle \tilde{\sigma}_+(\tau) \tilde{\sigma}_-(0) \rangle_{ss} \\ &= \frac{\gamma_{in}}{4} \frac{Y^2}{Y^2 + 1} \exp\left(-\frac{\gamma_{in}}{2} \tau\right) \\ &\quad - \frac{\gamma_{in}}{8} \frac{Y^2}{(Y^2 + 1)^2} \left(1 - Y^2 + (1 - 5Y^2) \frac{\gamma_{in}}{4\delta}\right) \exp\left(-\left(\frac{3\gamma_{in}}{4} - \delta\right) \tau\right) \\ &\quad - \frac{\gamma_{in}}{8} \frac{Y^2}{(Y^2 + 1)^2} \left(1 - Y^2 - (1 - 5Y^2) \frac{\gamma_{in}}{4\delta}\right) \exp\left(-\left(\frac{3\gamma_{in}}{4} + \delta\right) \tau\right) \end{aligned} \quad (5.44)$$

The first equality is the application of Eq. (5.43), along with the fact that we are normally ordering, so that the second term on the RHS of Eq. (5.43), \mathcal{E}_{in} , can be ignored.

Note that we have skipped over a small fact here. Eq. (4.40) was really only defined for $\tau > 0$, due to the way the quantum regression theorem was applied. It follows that Eq. (5.44) is valid only for $\tau < 0$, where it is understood that $|\tau|$ is to be used on the RHS of that equation. But, taking the complex conjugate of Eq. (4.40) and using the fact that it is real shows us that Eq. (4.40) is equally valid for $\tau < 0$, with the replacement $\tau \rightarrow |\tau|$. So we find that Eq. (5.44) is in fact valid for all τ .

What we then want is the filtered version of this: $\langle \mathcal{E}_{in}^{\dagger b}(\tau) \mathcal{E}_{in}^b(0) \rangle_{ss}$. However, Eq. (5.16) shows us how to filter a generic exponential $\exp(-\eta|\tau|)$, and Eq. (5.44) is merely a linear combination of three such exponentials, so this is easily done.

We may, in a similar manner, use Eqs. (4.41) and (5.43) to obtain the *normally-ordered* quadrature correlation functions. We first compute $\langle \mathcal{E}_{in}^\dagger(\tau) \mathcal{E}_{in}^\dagger(0) \rangle_{ss}$ - this will be identical to Eq. (5.44), but for a sign change on the second and third terms. Then, expressing the field X and Y quadratures (\mathcal{E}_{in}^X and \mathcal{E}_{in}^Y) in terms of the fields themselves, we have $\langle : \mathcal{E}_{in}^X(\tau) \mathcal{E}_{in}^X(0) : \rangle_{ss} = \frac{1}{2} \{ \langle \mathcal{E}_{in}^\dagger(\tau) \mathcal{E}_{in}(0) \rangle_{ss} + \langle \mathcal{E}_{in}^\dagger(\tau) \mathcal{E}_{in}^\dagger(0) \rangle_{ss} \}$ and $\langle : \mathcal{E}_{in}^Y(\tau) \mathcal{E}_{in}^Y(0) : \rangle_{ss} = \frac{1}{2} \{ \langle \mathcal{E}_{in}^\dagger(\tau) \mathcal{E}_{in}(0) \rangle_{ss} - \langle \mathcal{E}_{in}^\dagger(\tau) \mathcal{E}_{in}^\dagger(0) \rangle_{ss} \}$.

In all that follows, we set the resonance fluorescence spectrum parameters as:

- $Y = 8$ (recall this is proportional to the Rabi frequency, as in Eq. (4.30), and so sets the laser intensity)
- $\lambda = 0.9$ (degree of squeezing)
- $\gamma_{in}/\gamma_s = 0.01$ (ratio of input to squeezing bandwidths)

Note that γ_{in} is not the sole parameter that controls the total width of the resonance fluorescence spectrum. According to our dressed states model (Section 4.2), the distance between the two side peaks is 2Ω (almost; but due to the influence of the middle peak this is not exact), and Ω depends on both γ_{in} and Y . However, γ_{in} does control the linewidth of each of the three peaks.

With these parameters, the object of our teleportation thus appears as follows.

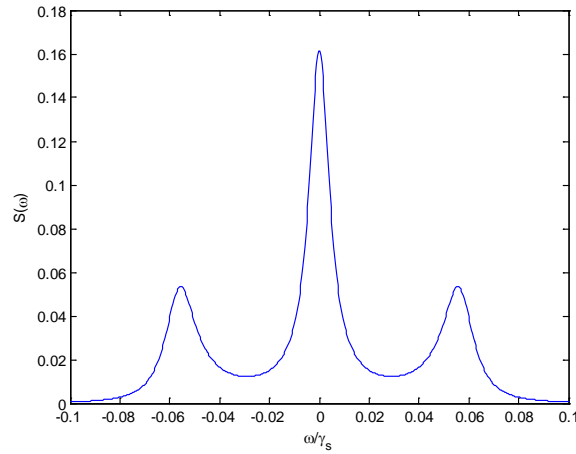


Figure 10. The resonance fluorescence spectrum with parameters given above.

For actual computation purposes, we have just set $\gamma_s = 1$. This gives a frequency scale that is in units of ω/γ_s , as indicated (if one was to consider arbitrary values of γ_s).

We expect that this spectrum will ‘sit’ inside the vacuum spectrum dip seen before in our vacuum plots. The fact that this dip is not perfectly free of vacuum noise (which is a result of imperfect squeezing) means that our input field will of course be modified a little upon teleporting.

The quadrature correlation functions have the following spectra:

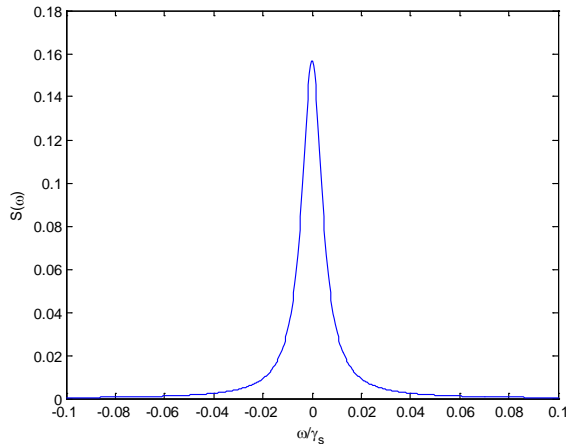


Figure 11. The spectrum of $\langle : \mathcal{E}_{in}^X(\tau) \mathcal{E}_{in}^X(0) : \rangle_{ss}$.

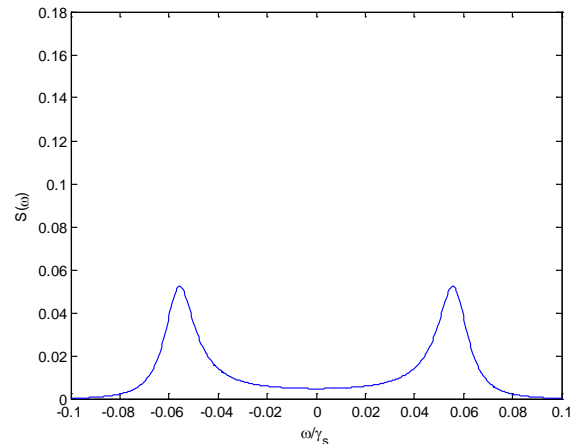


Figure 12. The spectrum of $\langle : \mathcal{E}_{in}^Y(\tau) \mathcal{E}_{in}^Y(0) : \rangle_{ss}$.

We see that one quadrature contains the central peak (the X quadrature), while the Y quadrature contains the two sidepeaks as mentioned in Section 4.2.

We now plot the teleported spectrum for a few values of Bob's filtering bandwidth, to get a feel for the parameters involved. As was the case with the vacuum spectra, we have matched half-widths for the Lorentzian and Gaussian filters.

The left-hand plot in each case shows the teleported spectrum under Lorentzian filtering (blue) and Gaussian filtering (black). The right-hand plot is a residual one, and subtracts away from the teleported spectra the spectrum of the input resonance fluorescence field. Obviously, if the teleportation is perfect, this residual plot should just be a flat line at 0 (indicated by the dashed line where appropriate). We should like it to be as close to this as possible.

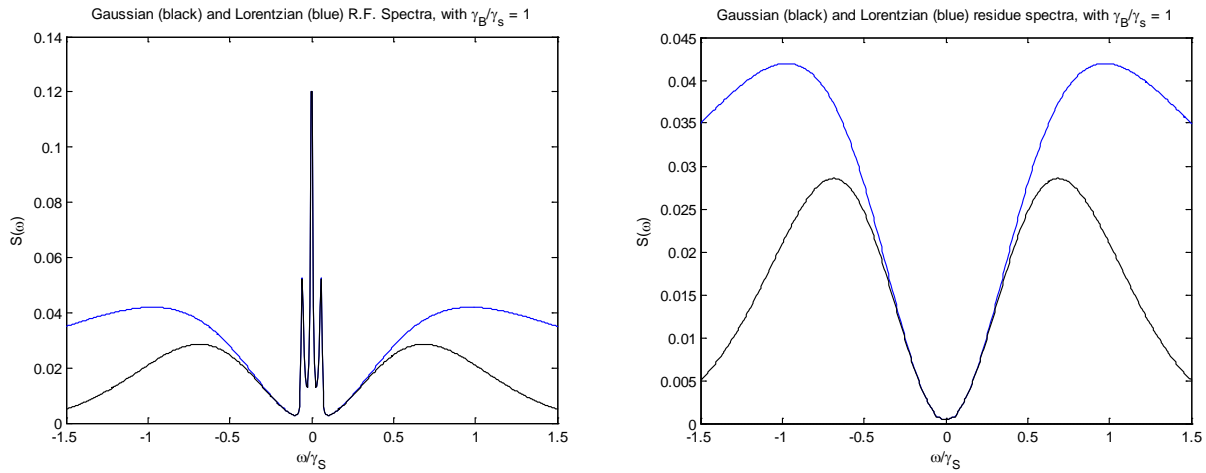


Figure 13: Teleported resonance fluorescence spectra with $\gamma_B/\gamma_s = 1$.

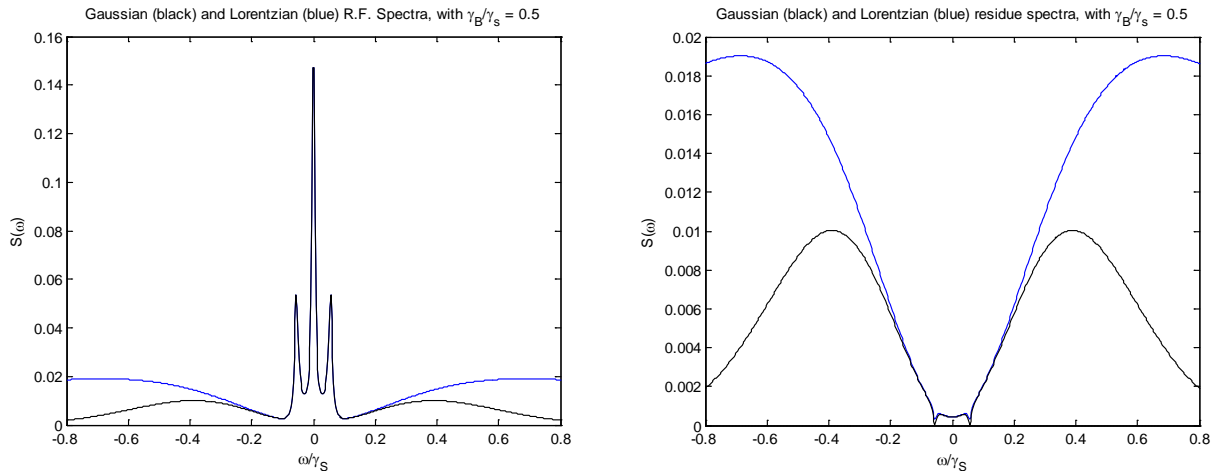


Figure 14: Teleported resonance fluorescence spectra with $\gamma_B/\gamma_s = 0.5$.

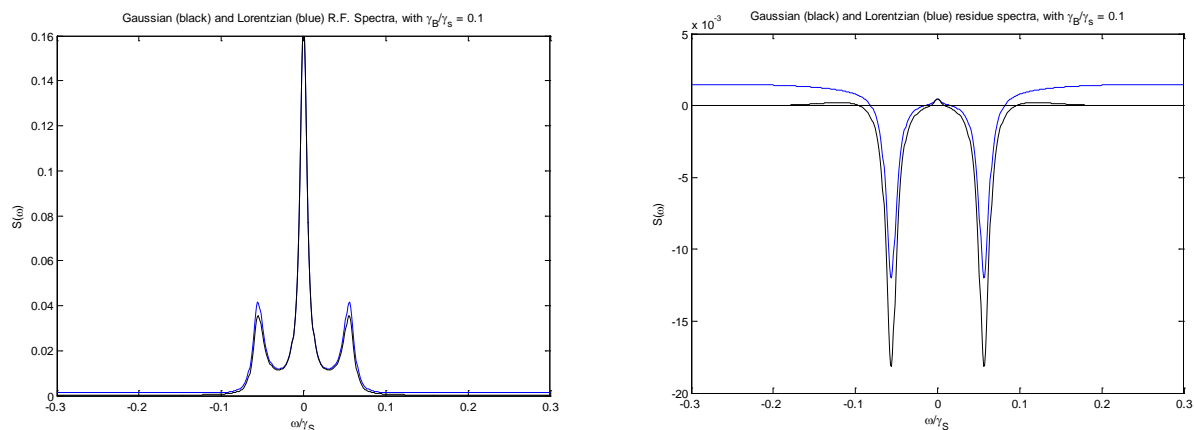


Figure 15: Teleported resonance fluorescence spectra with $\gamma_B/\gamma_S = 0.1$.

In the first plot, where $\gamma_B/\gamma_S = 1$, our filters are not yet cutting into the resonance fluorescence spectrum – see that subtracting away the original spectrum leaves behind just a filtered vacuum (see Fig. 8). When $\gamma_B/\gamma_S = 0.5$ this is no longer the case: there are two small dips in the residue plot, either side of $\omega = 0$, corresponding to our filters beginning to cut into the actual sidepeaks of the input spectrum. By the time $\gamma_B/\gamma_S = 0.1$, this sidepeak loss is severe, and much more so for the Gaussian filter. On the other hand, one can see that the Gaussian filter has, for this value of γ_B/γ_S , cut the noise in the spectrum wings almost to zero.

It is clear that there is a trade-off here: we need to balance the elimination of vacuum noise against the loss of input signal, especially in the sidepeaks.

Loss of signal in the spectrum sidepeaks

We investigate specifically this sidepeak signal loss now. For the non-teleported spectrum having $\gamma_{in}/\gamma_S = 0.01$ and $Y = 8$, we numerically find the sidepeaks to be located at

$$\frac{\omega}{\gamma_S} = \pm 0.05565275$$

See Fig. 10. Note that this is offset just slightly from the Rabi frequency here, which is $\frac{\gamma_{in}Y}{\sqrt{2}} = 0.0565685$ (in units of $1/\gamma_S$), which due to overlap of the three Lorentzian peaks, as stated earlier.

The following plot shows the difference between the teleported spectrum and the input spectrum for resonance fluorescence, evaluated at the location of the right-hand sidepeak in the input spectrum. The sign of this difference is such that a *positive* value means that the teleported sidepeak is *larger* than the input sidepeak. It is seen that for a given filter half-width, Gaussian filtering results in a larger sidepeak loss. Conversely, this does mean that if we are prepared to accept a certain amount of sidepeak loss, a Gaussian filter of larger half-width can be used compared to Lorentzian filtering.

The blue curve corresponds to Lorentzian filtering, while the black curve is for Gaussian filtering.

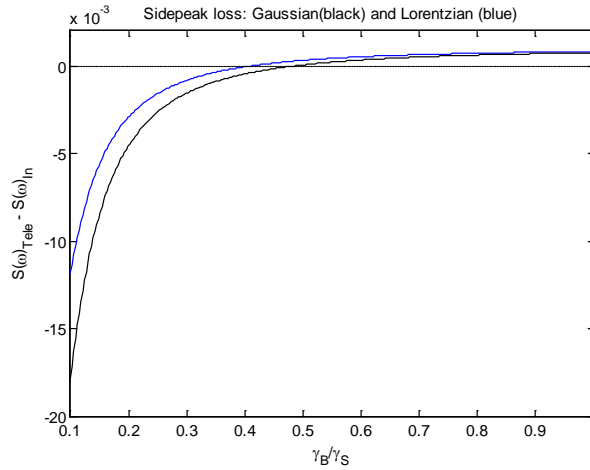


Figure 16. Sidepeak loss in the right-hand sidepeak of the teleported resonance fluorescence field.

This plot of sidepeak loss is deceptive. Technically, the tip of the sidepeak appears to be perfectly teleported at approximately $\frac{\gamma_B}{\gamma_S} = 0.41$ for Lorentzian filtering, and $\frac{\gamma_B}{\gamma_S} = 0.48$ for Gaussian filtering (i.e., where these curves cross the dashed line in Fig. 16 above). However, upon removal of the vacuum noise, we realise that this ‘perfectly’ teleported sidepeak is in fact the result of the teleportation protocol letting in vacuum noise at the sidepeak location. For a fairer comparison, we remove the vacuum noise that is being let in, and zero in on the part of the spectrum that actually came from the input spectrum only. The result of this comparison is shown in the figures below. We notice that these plots are always less than zero, since some input signal is *always* lost. The right-hand figure is a zoomed-in version of the left-hand one.

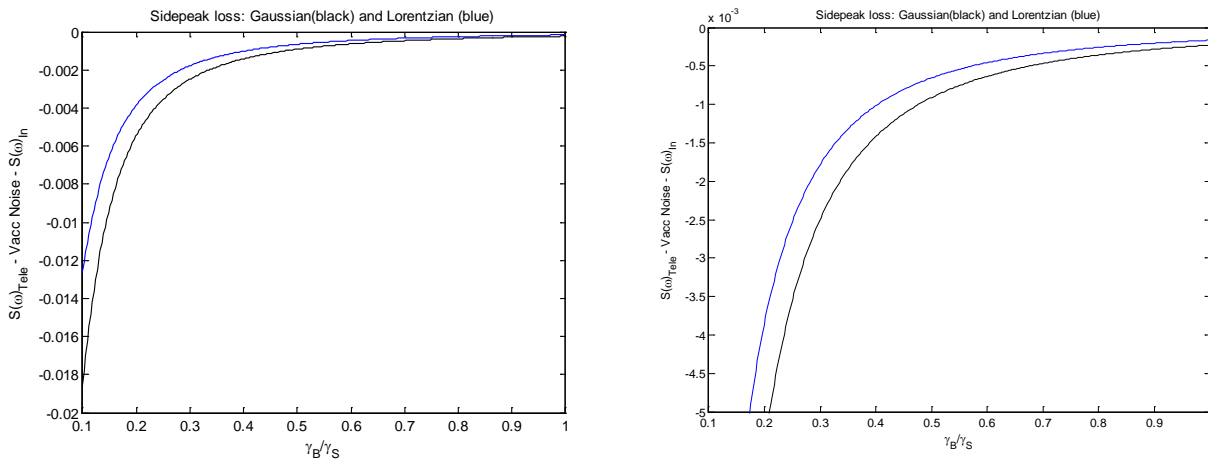


Figure 17. Sidepeak loss comparison, after removing the vacuum noise, in the resonance fluorescence spectrum.

Our conclusions are unchanged however – for a given filtering half-width, Gaussian filtering results in greater sidepeak loss than does Lorentzian filtering.

Vacuum noise let in during teleportation

In our plots showing the total output resonance fluorescence spectrum, Figs. 13 – 15, we see that a certain amount of vacuum noise is always present in the spectrum wings. These give rise to very broad vacuum noise peaks that flank the triple-peaked resonance fluorescence spectrum in the centre.

Below, the plot shows the largest value of this vacuum noise, as a function of the filtering half-width. See that the Gaussian filter has, in all cases, a lower maximum amount of vacuum noise than does Lorentzian filtering. We compute this largest value of vacuum noise by calculating a teleported spectrum, subtracting away the original spectrum, and finding the largest value of the noise that remains. This corresponds to the height of the flanking broad peaks, less any signal present at that location.

As usual, the blue curve pertains to Lorentzian filtering; the black curve is for Gaussian filtering.

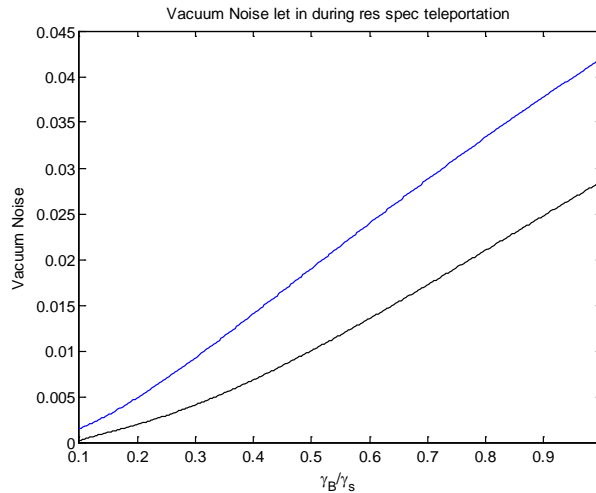


Figure 18. The largest value of the vacuum noise let in by each filter type during resonance fluorescence teleportation.

As explained before, there is always a trade-off in teleportation. We wish to set our filtering so that it cuts out as much vacuum noise as possible, without eating away at the edges of the input spectrum (in the case of resonance fluorescence, the sidepeaks). We expect the relationship between these two quantities to be an inverse one – if we are cutting out a lot of the vacuum noise, then our filtering must be strict and the sidepeak loss must be large. Conversely, if we are prepared to let in a bit more vacuum noise, then we can have less sidepeak loss. Below, the plot shows the sidepeak loss as a function of the maximum vacuum noise let in, for each filter type. The ‘sidepeak loss’ is the *actual* loss in input signal, and *excludes* any vacuum noise.

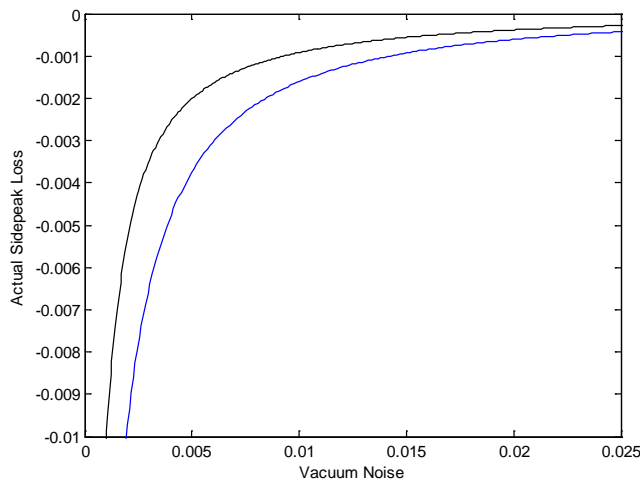


Figure 19: The trade-off plot. (Actual) Sidepeak loss versus maximum amount of vacuum noise let in.

We can see the superiority of Gaussian filtering here. Given a particular value for the maximum vacuum noise let in, we see that a Gaussian filter can do the job with *less* sidepeak loss than a Lorentzian filter (we are not saying anything about the half-widths involved, however – these won't necessarily be the same for each filter). Conversely, if we set the amount of sidepeak loss that we are prepared to accept, then use of a Gaussian filter gives a smaller value for the maximum vacuum noise let in.

Teleported Y-quadrature correlation functions

The teleported sidepeaks are made up of 3 parts: some overlap from the central peak, some vacuum noise, and of course the original spectrum (but now filtered) – the ‘signal’ part of the teleported sidepeak. We remove the influence of the central peak by comparing the Y quadrature correlation function for the teleported field with the Y quadrature correlation function for the input field (Fig. 12).

The location of the sidepeaks in the Y quadrature spectrum are:

$$\frac{\omega}{\gamma_s} = \pm 0.0556776436283$$

See that this differs very slightly from the value found previously for the total spectrum sidepeaks, since we no longer have the overlap effect of the central spectrum peak.

When we calculate the Y quadrature correlation function for the teleported field, we find that it contains half the vacuum noise present in the total output field correlation function. The other half is present in the X quadrature.

The plot below shows the ratio of the teleported sidepeak height (*minus* vacuum noise first) to the input sidepeak height. As usual, Gaussian is black and Lorentzian is blue. The fact that the Gaussian curve lies below that of the Lorentzian indicates that, for a fixed quality of teleportation (for example, if we want the *signal* part of the teleported sidepeaks to be at least 96% of the input signal), a Gaussian filter of *larger* half-width does the same job as a Lorentzian filter of *smaller* half-width.

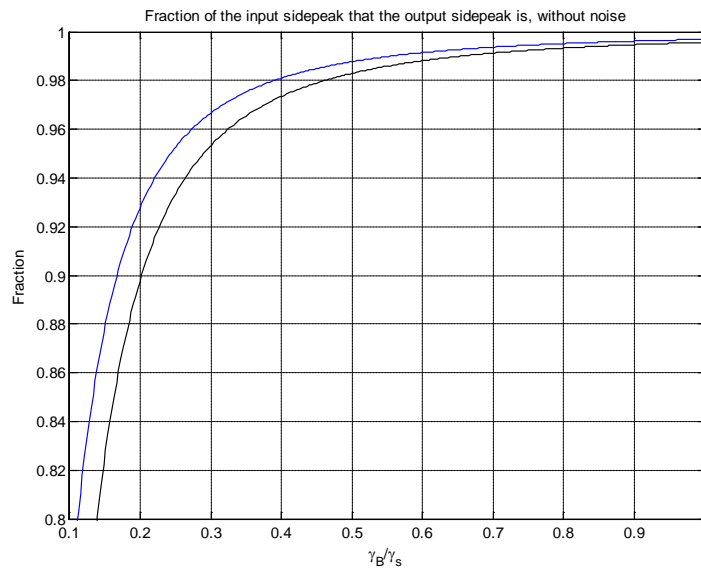


Figure 20. The signal part of the teleported sidepeak divided by the actual (input) height of the sidepeak.

We repeat the above plot, but now consider the *total* teleported sidepeak height (including vacuum noise) as a fraction of the input sidepeak.

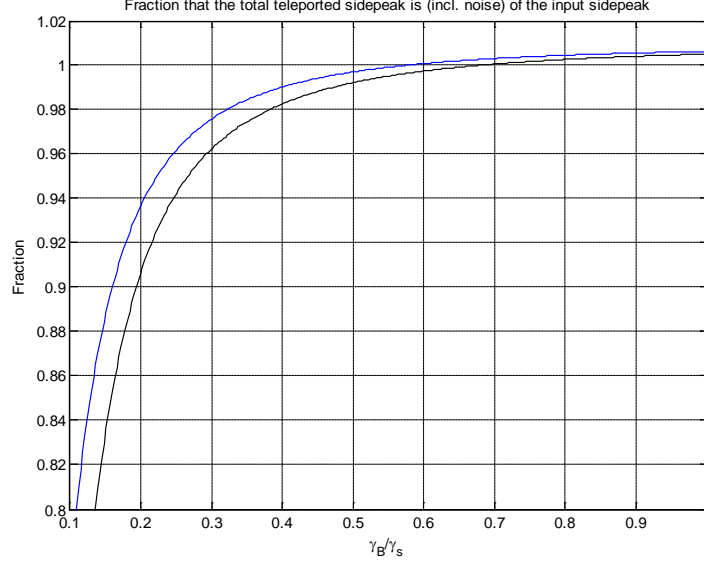


Figure 21. The total teleported sidepeak height divided by the actual (input) height of the sidepeak.

As expected, our inclusion of vacuum noise eventually gives us *higher* teleported sidepeaks than were originally input.

5.2.5 Analytical work with the first-order correlation function

We expect that in certain limits, the Furusawa teleportation protocol outlined should yield perfect teleportation of the first order correlation function, among other things. In this section, we work analytically with the first-order correlation functions to highlight this more explicitly.

Our expression for the vacuum part of the correlation function is Eq. (5.31), under Gaussian filtering:

$$\langle \mathcal{E}_{out}^\dagger(\tau) \mathcal{E}_{out}(0) \rangle_{ss(VAC)} = \frac{-\lambda \gamma_s}{1 + \lambda} I\left(C, d, \frac{\gamma_s}{2}(1 + \lambda), \tau\right) + I_\delta(C, d, \tau) \quad (5.45)$$

where we will be taking $C = \sqrt{\frac{d}{\pi}}$ as usual. Written out in full using Eqs. (5.18) and (5.21), this is:

$$\begin{aligned} \langle \mathcal{E}_{out}^\dagger(\tau) \mathcal{E}_{out}(0) \rangle_{ss(VAC)} &= \frac{-\lambda \gamma_s}{2(1 + \lambda)} \exp\left(\frac{\gamma_s(1 + \lambda)}{2} \left(\frac{\gamma_s}{d} \left(\frac{1 + \lambda}{4}\right) + \tau\right)\right) \left[1 - \operatorname{erf}\left(\frac{\gamma_s}{\sqrt{d}} \left(\frac{1 + \lambda}{2\sqrt{2}}\right) + \tau \sqrt{\frac{d}{2}}\right)\right] \\ &+ \frac{-\lambda \gamma_s}{2(1 + \lambda)} \exp\left(\frac{\gamma_s(1 + \lambda)}{2} \left(\frac{\gamma_s}{d} \left(\frac{1 + \lambda}{4}\right) - \tau\right)\right) \left[1 - \operatorname{erf}\left(\frac{\gamma_s}{\sqrt{d}} \left(\frac{1 + \lambda}{2\sqrt{2}}\right) - \tau \sqrt{\frac{d}{2}}\right)\right] \\ &+ \sqrt{\frac{d}{2\pi}} \exp\left(\frac{-d\tau^2}{2}\right) \end{aligned} \quad (5.46)$$

No approximations have been made so far.

We would like to make the approximation $\gamma_s \gg d$ – that is, Bob’s Gaussian filter bandwidth d should be ‘well within’ the squeezed bandwidth of light used in teleportation. Provided that the input bandwidth γ_{in} is also well within d , i.e. $d \gg \gamma_{in}$, we expect that this, along with the requirement $\lambda \rightarrow 1$ (i.e. perfect squeezing), should yield perfect teleportation. These conditions on the bandwidths involved in teleportation are reported on by Noh in [7].

A quick way of doing this is simply to take $\gamma_s \rightarrow \infty$, i.e. to consider that the squeezing bandwidth is quite large. Since the two integrals $I(C, d, \eta, \tau)$ and $I_\delta(C, d, \tau)$ are related by

$$\lim_{\eta \rightarrow \infty} \frac{\eta}{2} I(C, d, \eta, \tau) = I_\delta(C, d, \tau) \quad (5.47)$$

we have that:

$$\lim_{\gamma_s \rightarrow \infty} \frac{-\lambda \gamma_s}{1 + \lambda} I\left(C, d, \frac{\gamma_s}{2}(1 + \lambda), \tau\right) = \frac{-4\lambda}{(1 + \lambda)^2} I_\delta(C, d, \tau) \quad (5.48)$$

Hence:

$$\lim_{\gamma_s \rightarrow \infty} \langle \mathcal{E}_{out}^\dagger(\tau) \mathcal{E}_{out}(0) \rangle_{ss(VAC)} = \left(1 - \frac{4\lambda}{(1 + \lambda)^2}\right) I_\delta(C, d, \tau) \quad (5.49)$$

This expression is true in the case where I and I_δ have been evaluated for Lorentzian filters, because Eq. (5.47) holds for Lorentzian filtering as well. In fact, this approximation doesn’t depend on the explicit form of our filtering.

It gives us an approximate expression for $\langle \mathcal{E}_{out}^\dagger(\tau) \mathcal{E}_{out}(0) \rangle_{ss(VAC)}$ in the large γ_s regime; for Gaussian filtering, this is:

$$\langle \mathcal{E}_{out}^\dagger(\tau) \mathcal{E}_{out}(0) \rangle_{ss(VAC)} \approx \sqrt{\frac{d}{2\pi}} \left(1 - \frac{4\lambda}{(1 + \lambda)^2}\right) \exp\left(\frac{-d\tau^2}{2}\right) \quad (5.50)$$

If we now allow $\lambda \rightarrow 1$, this expression vanishes. By considering that $d \gg \gamma_{in}$, we see that Bob’s filtering won’t ‘clip’ any of the input signal, so that we may consider the input field \mathcal{E}_{in} as approximately unfiltered the teleporter output. We then have approximately:

$$g_{out}^{(1)}(\tau) = \frac{g_{in}^{(1)}(\tau) \langle \mathcal{E}_{in}^\dagger(0) \mathcal{E}_{in}(0) \rangle_{ss} + \langle \mathcal{E}_{out}^\dagger(\tau) \mathcal{E}_{out}(0) \rangle_{ss(VAC)}}{\langle \mathcal{E}_{in}^\dagger(0) \mathcal{E}_{in}(0) \rangle_{ss} + \langle \mathcal{E}_{out}^\dagger(0) \mathcal{E}_{out}(0) \rangle_{ss(VAC)}} \quad (5.51)$$

where we have removed superscripted b ’s on the \mathcal{E}_{in} ’s in accordance with the approximation $d \gg \gamma_{in}$. Hence, under the approximations:

- $\gamma_s \rightarrow \infty$,
- $\lambda \rightarrow 1$, and
- $d \gg \gamma_{in}$

the terms $\langle \dots \rangle_{VAC}$ vanish, and we see that $g_{out}^{(1)}(\tau) \rightarrow g_{in}^{(1)}(\tau)$; i.e. the first order correlation functions of the input field are recovered at the teleporter output.

Now as mentioned, this result doesn't depend explicitly on the type of filtering used. To obtain a teleportation limit that is more relevant to Gaussian filtering, we instead take the limit $\gamma_s \gg d$ by considering the limit $\frac{\gamma_s}{d} \rightarrow \infty$, or equivalently $\frac{d}{\gamma_s} \rightarrow 0$.

Then, taking τ to have some finite value, we see that allowing $\frac{\gamma_s}{d} \rightarrow \infty$ in the expression Eq. (5.46) means that the error function arguments become very large. Now for $x \gg 1$, we have the approximation

$$\text{erf}(x) \approx 1 - \frac{1}{x\sqrt{\pi}} \exp(-x^2) \quad (5.52)$$

One can see the quality of this approximation in the first-order correlation function by viewing the plots in Appendix A.

If we make the approximation Eq. (5.52) for both the error functions appearing in Eq. (5.46), we get the relation:

$$\langle \mathcal{E}_{out}^\dagger(\tau) \mathcal{E}_{out}(0) \rangle_{ss(VAC)} \approx \sqrt{\frac{d}{2\pi}} \left(1 - \frac{4\lambda}{(1+\lambda)^2 - 4\left(\frac{d}{\gamma_s}\right)^2 \tau^2} \right) \exp\left(\frac{-d\tau^2}{2}\right) \quad (5.53)$$

for Gaussian filtering in the $\frac{\gamma_s}{d} \rightarrow \infty$ limit. This is consistent with Eq. (5.50) – it is similar in form, but has an extra term in the denominator. Hence we see that under the approximations:

- $\gamma_s/d \rightarrow \infty$, or $d/\gamma_s \rightarrow 0$,
- $\lambda \rightarrow 1$, and
- $d \gg \gamma_{in}$

we again have $g_{out}^{(1)}(\tau) \rightarrow g_{in}^{(1)}(\tau)$.

A small note: one can see that Eq. (5.53) is undefined when $\tau = \frac{\gamma_s}{2d}(1+\lambda)$. This is not a problem however, for the approximation we took was only meant to be valid when $\frac{\gamma_s}{d} \gg \tau$, and $\tau = \frac{\gamma_s}{2d}(1+\lambda)$ falls outside this range of validity.

The equivalent expression to Eq. (5.53) for Lorentzian filtering is given in [7]:

$$\langle \mathcal{E}_{out}^\dagger(\tau) \mathcal{E}_{out} \rangle_{VAC} \approx \gamma_B \left(\frac{1}{2} \left(1 - \frac{4\lambda}{(1+\lambda)^2} \right) \exp(-\gamma_B \tau) - \frac{4\lambda}{(1+\lambda)^3} \left(\frac{\gamma_B}{\gamma_s} \right) \exp\left(-\frac{\gamma_s}{2}(1+\lambda)\tau\right) \right) \quad (5.54)$$

5.3 Second-Order Correlation Functions for the output field

The second order correlation function for the output field is

$$g_{out}^{(2)} = \frac{\langle \mathcal{E}_{out}^\dagger(0) \mathcal{E}_{out}^\dagger(\tau) \mathcal{E}_{out}(\tau) \mathcal{E}_{out}(0) \rangle_{ss}}{\langle \mathcal{E}_{out}^\dagger(0) \mathcal{E}_{out}(0) \rangle_{ss}^2} \quad (5.55)$$

As in Eq. (5.06), $\mathcal{E}_{out} = \mathcal{E}_B^b + \mathcal{E}_{in}^{ab} + \mathcal{E}_A^{*ab}$ in the general case of filtering by both Alice and Bob.

Our task will be to evaluate the numerator – the denominator can be computed by setting $\tau = 0$ in Eq. (5.42), and making use of Eq. (5.31) and the filtered version of Eq. (5.44).

The input second-order correlation function looks like, for the parameters of Section 5.2.4:

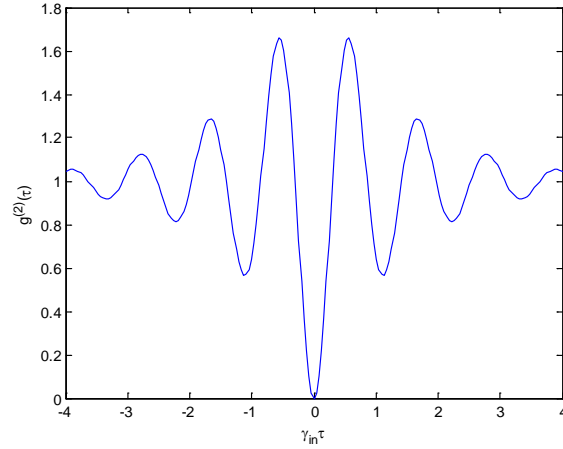


Figure 22. The second order correlation function for the resonance fluorescence field.

See Eq. (2.152) of Carmichael [8]. Notice the highly antibunched result $g^{(2)}(0) = 0$.

5.3.1 Vacuum terms in the second order correlation function

Let us write the squeezed fields in terms of their quadratures:

$$\mathcal{E}_{EPRx} = \mathcal{E}_{EPRx}^X + i\mathcal{E}_{EPRx}^Y \quad (5.56)$$

$$\mathcal{E}_{EPRy} = \mathcal{E}_{EPRy}^X + i\mathcal{E}_{EPRy}^Y \quad (5.57)$$

For such fields, both the X and Y quadratures are random variables with a *Gaussian distribution*. It follows that \mathcal{E}_A and \mathcal{E}_B (which are linear combinations of the squeezed fields \mathcal{E}_{EPRx} and \mathcal{E}_{EPRy}) are complex Gaussian random variables as well. We now state a theorem that will simplify the evaluation of second-order correlation functions involving \mathcal{E}_A and \mathcal{E}_B .

The Gaussian Moment Theorem

We present here the Gaussian Moment Theorem (also known as the Gaussian moment factorisation) as given in Section 2.8.1 of [11].

The Gaussian Moment Theorem states that for N Gaussian-distributed random variables X_1, X_2, \dots, X_N , moments to any order involving these variables can be reduced to combinations of second-order moments alone, provided the variables themselves have zero mean.

That is, if $\langle X_1 \rangle = \langle X_2 \rangle = \dots = \langle X_N \rangle = 0$, then we have:

$$\langle X_1 X_2 \dots X_N \rangle = \begin{cases} \frac{N!}{\left(\frac{N}{2}\right)! 2^{N/2}} \{ \langle X_1 X_2 \rangle \langle X_3 X_4 \rangle \dots \}_{sym}, & \text{for } N \text{ even} \\ 0, & \text{for } N \text{ odd} \end{cases}$$

By *sym*, we mean the symmetrised form of the product.

The particular result we need from this theorem is that, for variables X_i , $i = 1,2,3,4$ satisfying the conditions of the theorem,

$$\langle X_1 X_2 X_3 X_4 \rangle = \langle X_1 X_2 \rangle \langle X_3 X_4 \rangle + \langle X_1 X_4 \rangle \langle X_2 X_3 \rangle + \langle X_1 X_3 \rangle \langle X_2 X_4 \rangle \quad (5.58)$$

This result does apply to our vacuum fields, which of course have zero mean. If one applies this Theorem to the numerator of Eq. (5.55), it is possible to write that numerator as [7]:

$$\begin{aligned} & \langle \mathcal{E}_{in}^{\dagger b}(0) \mathcal{E}_{in}^{\dagger b}(\tau) \mathcal{E}_{in}^b(\tau) \mathcal{E}_{in}^b(0) \rangle_{ss} + 2 \langle \mathcal{E}_{in}^{\dagger b}(\tau) \mathcal{E}_{in}^b(0) \rangle_{ss} \langle \mathcal{E}_{out}^{\dagger}(\tau) \mathcal{E}_{out}(0) \rangle_{ss(VAC)} \\ & + 2 \langle \mathcal{E}_{in}^{\dagger b}(0) \mathcal{E}_{in}^b(0) \rangle_{ss} \langle \mathcal{E}_{out}^{\dagger}(0) \mathcal{E}_{out}(0) \rangle_{ss(VAC)} + \langle \mathcal{E}_{out}^{\dagger}(\tau) \mathcal{E}_{out}(0) \rangle_{ss(VAC)}^2 + \langle \mathcal{E}_{out}^{\dagger}(0) \mathcal{E}_{out}(0) \rangle_{ss(VAC)}^2 \end{aligned} \quad (5.59)$$

where it is assumed that the input field is the resonance fluorescence one.

All the terms involving VAC can already be evaluated with the results obtained earlier in first-order correlation functions. It remains only to evaluate the first term of Eq. (5.59).

5.3.2 The non-vacuum term in the second order correlation function

Operator equation

We begin by extending the analysis of Section 4.2. Consider an operator $X(t)$ that satisfies the same resonance fluorescence master equation as the system density operator. Note that, unlike ρ , the operator X may not have unit trace. That is,

$$\frac{dX}{dt} = -\frac{i\omega_A}{2} [\sigma_z, X] + \frac{i\Omega}{2} [e^{-i\omega_A t} \sigma_+ + e^{i\omega_A t} \sigma_-, X] + \frac{\gamma}{2} (2\sigma_- X \sigma_+ - \sigma_+ \sigma_- X - X \sigma_+ \sigma_-) \quad (5.60)$$

From this, we derive equations of motion for the matrix elements of X in the $|1\rangle, |2\rangle$ basis:

$$\frac{d}{dt} X_{11} = \frac{i\Omega}{2} e^{i\omega_A t} X_{21} - \frac{i\Omega}{2} e^{-i\omega_A t} X_{12} + \gamma X_{22} \quad (5.61)$$

$$\frac{d}{dt} X_{22} = \frac{i\Omega}{2} e^{-i\omega_A t} X_{12} - \frac{i\Omega}{2} e^{i\omega_A t} X_{21} - \gamma X_{22} \quad (5.62)$$

$$\frac{d}{dt} X_{12} = i\omega_A X_{12} + \frac{i\Omega}{2} e^{i\omega_A t} (X_{22} - X_{11}) - \frac{\gamma}{2} X_{12} \quad (5.63)$$

$$\frac{d}{dt} X_{21} = -i\omega_A X_{21} - \frac{i\Omega}{2} e^{-i\omega_A t} (X_{22} - X_{11}) - \frac{\gamma}{2} X_{21} \quad (5.64)$$

The first two equations show that $\frac{d}{dt} (X_{11} + X_{22}) = 0$, so the trace of X is preserved in time:

$$X_{11}(t) + X_{22}(t) = X_{11}(0) + X_{22}(0) \quad (5.65)$$

Due to this equation, we needn't work with the four separate equations Eqs. (5.61) – (5.64), reducing them instead to three. We may write them collectively as:

$$\frac{d}{dt} \begin{pmatrix} U \\ V \\ W \end{pmatrix} = \begin{pmatrix} -\frac{\gamma}{2} & 0 & -\frac{i\Omega}{2} \\ 0 & -\frac{\gamma}{2} & \frac{i\Omega}{2} \\ -i\Omega & i\Omega & -\gamma \end{pmatrix} \begin{pmatrix} U \\ V \\ W \end{pmatrix} - \gamma \begin{pmatrix} 0 \\ 0 \\ X_{11}(0) + X_{22}(0) \end{pmatrix} \quad (5.66)$$

where:

$$\begin{aligned} U &= \tilde{X}_{21} = X_{21} e^{i\omega_A t} \\ V &= \tilde{X}_{12} = X_{12} e^{-i\omega_A t} \\ W &= X_{22} - X_{11} \end{aligned}$$

Let us write this equation as

$$\frac{d}{dt} \mathbf{x} = \mathbf{M} \mathbf{x} + \mathbf{b} \quad (5.67)$$

We then have the solution

$$\mathbf{x}(t) = -\mathbf{M}^{-1} \mathbf{b} + \mathbf{S}^{-1} \exp(\lambda t) [\mathbf{S} \mathbf{x}(0) + \mathbf{S} \mathbf{M}^{-1} \mathbf{b}] \quad (5.68)$$

Once more, \mathbf{S} is a matrix that diagonalises \mathbf{M} , and $\lambda = \mathbf{S} \mathbf{M} \mathbf{S}^{-1}$. In fact, we do not need to re-diagonalise anything, for the matrices \mathbf{S} and \mathbf{M} are precisely the same as those in Eq. (4.36), which we have already diagonalised. We thus obtain full solutions to Eqs. (5.61)–(5.64). These are listed in Appendix C.

Structure of the calculation

We want to evaluate the correlation

$$\langle \mathcal{E}_{in}^{\dagger b}(0) \mathcal{E}_{in}^{\dagger b}(\tau) \mathcal{E}_{in}^b(\tau) \mathcal{E}_{in}^b(0) \rangle_{ss} \quad (5.69)$$

which is not reducible to first-order moments by the Gaussian moment theorem (for the resonance fluorescence field at least). It is evaluated by a method due to Noh [7]. In [7], the Eq. (5.69) was evaluated taking into account filtering by both Alice and Bob. In the regime of no filtering by Alice, it is slightly simpler to evaluate, and we outline the calculation here.

We begin with the case of Lorentzian filtering by Bob (and no filtering by Alice). Then, we have for $\langle \mathcal{E}_{in}^{\dagger b}(0) \mathcal{E}_{in}^{\dagger b}(\tau) \mathcal{E}_{in}^b(\tau) \mathcal{E}_{in}^b(0) \rangle_{ss}$ the expression:

$$\gamma_B^4 \gamma_{in}^2 \lim_{t_0 \rightarrow -\infty} e^{-\gamma_B(4t+2\tau)} \int_{t_0}^t dt_1 \int_{t_0}^{t+\tau} dt_2 \int_{t_0}^{t+\tau} dt_3 \int_{t_0}^t dt_4 \langle : \sigma_+(t_1) \sigma_+(t_2) \sigma_-(t_3) \sigma_-(t_4) : \rangle e^{\gamma_B(t_1+t_2+t_3+t_4)} \quad (5.70)$$

The parameter t is expected to disappear upon taking the limit indicated. Note that we wish to have normal ordering of operators in the integrand, in accordance with the rules of Section 3.5, as indicated by the explicit colons : : .

The procedure for evaluating this works as follows:

- Break the region of integration in Eq. (5.70) up into the $4 \times 3 \times 2 \times 1 = 24$ regions of integration corresponding to all possible different time orderings of t_1, t_2, t_3, t_4 .
- Apply the quantum regression theorem⁴ to calculate $\langle : \sigma_+(t_1)\sigma_+(t_2)\sigma_-(t_3)\sigma_-(t_4) : \rangle$ in each of the 24 cases.
- Perform the integration indicated above, changing the integration bounds to reflect the particular time ordering. Call the result W_i , where i runs from 1 to 24.
- Sum all 24 W_i to obtain the overall integral.

We are quite fortunate, though. It turns out that it isn't necessary to apply the quantum regression theorem 24 times over. Instead it is applied to 3 *master cases*, and by allowing our integration to be a little general in each of these 3 cases, we can find the integral in Eq. (5.70) for all 24 time orderings. We do this now.

Master Case 1. $t_2 > t_3 > t_1 > t_4$

One finds, upon applying the quantum regression theorem, that [7]:

$$\langle : \sigma_+(t_1)\sigma_+(t_2)\sigma_-(t_3)\sigma_-(t_4) : \rangle = \sum_{i,j,k=1}^4 P_{ijk}^{(1)} \exp(-\gamma_k \tau_1) \exp(-\gamma_j \tau_2) \exp(-\gamma_i \tau_3) \quad (5.71)$$

The $P_{ijk}^{(1)}$ are constant coefficients that are linear combinations of products of elements of the vectors F^+, F^-, G^+, G^-, H, I and J defined in Appendix C. See equations B.20a-c of [7]; for completeness we have listed them in Appendix D. The (1) indicates master case 1.

The variables τ_1, τ_2 and τ_3 correspond to the three positive time differences

$$\tau_1 = t_1 - t_4, \quad \tau_2 = t_3 - t_1, \quad \tau_3 = t_2 - t_3 \quad (5.72)$$

We now wish to perform the integration implied by Eq. (5.70), but with the particular time ordering indicated. We define a function $S_1(x, y, z, w | a, b, c)$ by:

$$\gamma_B^4 \gamma_{in}^2 \lim_{t_0 \rightarrow -\infty} e^{-\gamma_B(4t+x+y+z+w)} \int_{t_0}^{t+x} dt_1 \int_{t_0}^{t+y} dt_2 \int_{t_0}^{t+z} dt_3 \int_{t_0}^{t+w} dt_4 e^{-a\tau_1 - b\tau_2 - c\tau_3 + \gamma_B(t_1+t_2+t_3+t_4)} \quad (5.73)$$

where the subscript '1' indicates the integration is to be performed under the time constraints of master case 1 – i.e., $t_2 > t_3 > t_1 > t_4$. To incorporate this time ordering, the integration should be written

$$\int_{t_0}^{m_{xyzw}} dt_4 \int_{t_4}^{m_{xyz}} dt_1 \int_{t_1}^{m_{yz}} dt_3 \int_{t_3}^y dt_2 \quad (5.74)$$

Changing integration variables from t_1, t_2, t_3, t_4 to $\tau_1, \tau_2, \tau_3, t_4$, we find that the integral part of Eq. (5.73) is:

$$\int_{t_0}^{t+m_{xyzw}} dt_4 \int_0^{(t+m_{xyz})-t_4} d\tau_1 \int_0^{(t+m_{yz})-(\tau_1+t_4)} d\tau_2 \int_0^{(t+y)-(\tau_1+\tau_2+t_4)} d\tau_3 \quad (5.75)$$

whilst the integrand becomes

$$e^{(3\gamma_B - a)\tau_1 + (2\gamma_B - b)\tau_2 + (\gamma_B - c)\tau_3 + (4\gamma_B)t_4} \quad (5.76)$$

⁴ This is a generalisation of the quantum regression theorem presented in Section 4.2.

The limit part in front still needs to be taken. We have followed the notation of [7]: m_{xyzw} indicates the *smallest* of x, y, z and w , and so on. There is also a small simplification – it will in fact always be the case that 2 of x, y, z and w are 0, whilst the remaining two are then τ . Hence, we have $m_{xyzw} = m_{xyz} = 0$ above.

Now define

$$W_1(x, y, z, w) = \sum_{i,j,k=1}^4 P_{ijk}^{(1)} S_1(x, y, z, w | \gamma_k, \gamma_j, \gamma_i) \quad (5.77)$$

The contribution to $\langle \mathcal{E}_{in}^{\dagger b}(0) \mathcal{E}_{in}^{\dagger b}(\tau) \mathcal{E}_{in}^b(\tau) \mathcal{E}_{in}^b(0) \rangle_{ss}$ from the region $t_2 > t_3 > t_1 > t_4$ is then $W_1(0, \tau, \tau, 0)$.

Master Case 2. $t_2 > t_3 > t_4 > t_1$

We proceed exactly as in master case 1. In this new time regime, one finds

$$\langle : \sigma_+(t_1) \sigma_+(t_2) \sigma_-(t_3) \sigma_-(t_4) : \rangle = \sum_{i,j,k=1}^4 P_{ijk}^{(2)} \exp(-\gamma_k \tau_1) \exp(-\gamma_j \tau_2) \exp(-\gamma_i \tau_3) \quad (5.78)$$

where the constants $P_{ijk}^{(2)}$ differ from $P_{ijk}^{(1)}$. The τ variables differ now; they are

$$\tau_1 = t_4 - t_1, \quad \tau_2 = t_3 - t_4, \quad \tau_3 = t_2 - t_3 \quad (5.79)$$

Define $S_2(x, y, z, w | a, b, c)$ by the integral given in Eq. (5.73), but now carried out with $t_2 > t_3 > t_4 > t_1$.

The integration should be written, to include this new time ordering, as:

$$\int_{t_0}^{t+m_{xyzw}} dt_1 \int_0^{(t+m_{yzw})-t_1} d\tau_1 \int_0^{(t+m_{yz})-(\tau_1+t_1)} d\tau_2 \int_0^{(t+y)-(\tau_1+\tau_2+t_1)} d\tau_3 \quad (5.80)$$

whilst the integrand becomes

$$e^{(3\gamma_B - a)\tau_1 + (2\gamma_B - b)\tau_2 + (\gamma_B - c)\tau_3 + (4\gamma_B)t_1} \quad (5.81)$$

The limit is still taken. Remember that τ_1, τ_2 and τ_3 here are defined by Eq. (5.79), *not* Eq. (5.72).

With the realisation that $m_{xyzw} = m_{yzw} = 0$ for all the cases we will be considering (as explained in master case 1), we find (noting that t_1 and t_4 are just dummy integration variables) that S_1 and S_2 are exactly the same functions. Thus, in spite of the new time ordering being considered here, there is no need to do any new integration. However, we shall continue to distinguish the two functions notationally, even though they are the same. Define

$$W_2(x, y, z, w) = \sum_{i,j,k=1}^4 P_{ijk}^{(2)} S_2(x, y, z, w | \gamma_k, \gamma_j, \gamma_i) \quad (5.82)$$

The contribution to $\langle \mathcal{E}_{in}^{\dagger b}(0) \mathcal{E}_{in}^{\dagger b}(\tau) \mathcal{E}_{in}^b(\tau) \mathcal{E}_{in}^b(0) \rangle_{ss}$ from the region $t_2 > t_3 > t_4 > t_1$ is then $W_2(0, \tau, \tau, 0)$.

Master Case 3. $t_2 > t_1 > t_3 > t_4$

In this new time ordering, we have

$$\langle : \sigma_+(t_1) \sigma_+(t_2) \sigma_-(t_3) \sigma_-(t_4) : \rangle = \sum_{i,j,k=1}^4 P_{ijk}^{(3)} \exp(-\gamma_k \tau_1) \exp(-\gamma_j \tau_2) \exp(-\gamma_i \tau_3) \quad (5.83)$$

where the constants $P_{ijk}^{(3)}$ again can differ from $P_{ijk}^{(1)}$ and $P_{ijk}^{(2)}$. The τ variables are now:

$$\tau_1 = t_3 - t_4, \quad \tau_2 = t_1 - t_3, \quad \tau_3 = t_2 - t_1 \quad (5.84)$$

As before, define $S_3(x, y, z, w | a, b, c)$ by the integral given in Eq. (5.73), but now carried out with $t_2 > t_1 > t_3 > t_4$. The integration in Eq. (5.73) should be written, to include this new time ordering, as:

$$\int_{t_0}^{t+m_{xyzw}} dt_4 \int_0^{(t+m_{xyz})-t_4} d\tau_1 \int_0^{(t+m_{xy})-(\tau_1+t_4)} d\tau_2 \int_0^{(t+y)-(\tau_1+\tau_2+t_4)} d\tau_3 \quad (5.85)$$

whilst the integrand becomes

$$e^{(3\gamma_B - a)\tau_1 + (2\gamma_B - b)\tau_2 + (\gamma_B - c)\tau_3 + (4\gamma_B)t_4} \quad (5.86)$$

The limit is still taken.

Once more, this integral is almost entirely identical to that defining S_1 . We see that S_3 is exactly the same function as S_1 , but with the constant m_{yz} now replaced by m_{xy} - compare Eq. (5.85) with Eq. (5.75). Again, we don't need to do any new integration here. Define

$$W_3(x, y, z, w) = \sum_{i,j,k=1}^4 P_{ijk}^{(3)} S_3(x, y, z, w | \gamma_k, \gamma_j, \gamma_i) \quad (5.87)$$

The contribution to $\langle \mathcal{E}_{in}^{+b}(0) \mathcal{E}_{in}^{+b}(\tau) \mathcal{E}_{in}^b(\tau) \mathcal{E}_{in}^b(0) \rangle_{ss}$ from the region $t_2 > t_1 > t_3 > t_4$ is then $W_3(0, \tau, \tau, 0)$.

The remaining time orderings

Note that, for all 3 master cases, we have

$$\langle : \sigma_+(t_1) \sigma_+(t_2) \sigma_-(t_3) \sigma_-(t_4) : \rangle = \langle \sigma_+(t_1) \sigma_+(t_2) \sigma_-(t_3) \sigma_-(t_4) \rangle \quad (5.88)$$

i.e., no changes need to be made to normally order the 4-operator product in the $\langle \dots \rangle$. Let us consider a time ordering where this is not the case: the ordering $t_1 > t_3 > t_2 > t_4$. Then,

$$\langle : \sigma_+(t_1) \sigma_+(t_2) \sigma_-(t_3) \sigma_-(t_4) : \rangle = \langle \sigma_+(t_2) \sigma_+(t_1) \sigma_-(t_3) \sigma_-(t_4) \rangle \quad (5.89)$$

If we imagine now performing the integration implied by Eq. (5.70) for this particular time ordering, we find that upon changing the order of integration from $dt_1 dt_2 dt_3 dt_4$ to $dt_2 dt_1 dt_3 dt_4$ (without changing the integration bounds), that the result of the integration is just $W_1(\tau, 0, \tau, 0)$. Note that the variables t_1, t_2, t_3 and t_4 are only dummy variables, and one can relabel t_2 as t_1 and t_1 and t_2 to further highlight the connection.

We also note that complex conjugation of the operator expectation $\langle \dots \rangle$ takes the Hermitian conjugate of the 4-operator product inside. Consider $W_1(0, \tau, \tau, 0)$, which evaluates Eq. (5.70) in the regime $t_2 > t_3 > t_1 > t_4$. The operator expectation is normally ordered as in Eq. (5.88). Then, taking the complex conjugate, $W_1^*(0, \tau, \tau, 0)$ again evaluates Eq. (5.70), but with a new integrand $\langle \sigma_+(t_4) \sigma_+(t_3) \sigma_-(t_2) \sigma_-(t_1) \rangle e^{\gamma_B(t_1+t_2+t_3+t_4)}$ (still with the time ordering $t_2 > t_3 > t_1 > t_4$). Then, if we relabel the dummy integration variables in the following way:

$$t_4 \rightarrow t_1, \quad t_3 \rightarrow t_2, \quad t_2 \rightarrow t_3, \quad t_1 \rightarrow t_4$$

we see that $W_1^*(0, \tau, \tau, 0)$ in fact evaluates Eq. (5.70) with the time ordering $t_3 > t_2 > t_4 > t_1$.

The normal ordering and complex conjugation just mentioned allow us to extend our 3 master cases to cover all 24 time orderings. Each master case covers 4 time orderings by taking advantage of normal ordering, which extends to 8 time orderings by taking the complex conjugate of each. Given that there are 3 master cases, we get $8 \times 3 = 24$ time orderings in total, without any repetitions. To make this explicit, we now give a table showing all 24 time orderings, and the appropriate function with which to evaluate each. The 3 master cases are indicated in bold. For convenience, we just provide the t subscripts – i.e., $1 > 2 > 3 > 4$ means $t_1 > t_2 > t_3 > t_4$.

Time ordering	Relevant W -function	Time ordering	Relevant W -function
$1 > 2 > 3 > 4$	$W_3(\tau, 0, \tau, 0)$	$3 > 1 > 2 > 4$	$W_2^*(\tau, 0, \tau, 0)$
$1 > 2 > 4 > 3$	$W_3(\tau, 0, 0, \tau)$	$3 > 1 > 4 > 2$	$W_1^*(\tau, 0, \tau, 0)$
$1 > 3 > 2 > 4$	$W_1(\tau, 0, \tau, 0)$	$3 > 2 > 1 > 4$	$W_2^*(0, \tau, \tau, 0)$
$1 > 3 > 4 > 2$	$W_2(\tau, 0, \tau, 0)$	$3 > 2 > 4 > 1$	$W_1^*(0, \tau, \tau, 0)$
$1 > 4 > 2 > 3$	$W_1(\tau, 0, 0, \tau)$	$3 > 4 > 1 > 2$	$W_3^*(\tau, 0, \tau, 0)$
$1 > 4 > 3 > 2$	$W_2(\tau, 0, 0, \tau)$	$3 > 4 > 2 > 1$	$W_3^*(0, \tau, \tau, 0)$
$2 > 1 > 3 > 4$	$W_3(\mathbf{0}, \tau, \tau, \mathbf{0})$	$4 > 1 > 2 > 3$	$W_2^*(\tau, 0, 0, \tau)$
$2 > 1 > 4 > 3$	$W_3(0, \tau, 0, \tau)$	$4 > 1 > 3 > 2$	$W_1^*(\tau, 0, 0, \tau)$
$2 > 3 > 1 > 4$	$W_1(\mathbf{0}, \tau, \tau, \mathbf{0})$	$4 > 2 > 1 > 3$	$W_2^*(0, \tau, 0, \tau)$
$2 > 3 > 4 > 1$	$W_2(\mathbf{0}, \tau, \tau, \mathbf{0})$	$4 > 2 > 3 > 1$	$W_1^*(0, \tau, 0, \tau)$
$2 > 4 > 3 > 1$	$W_2(0, \tau, 0, \tau)$	$4 > 3 > 1 > 2$	$W_3^*(\tau, 0, 0, \tau)$
$2 > 4 > 1 > 3$	$W_1(0, \tau, 0, \tau)$	$4 > 3 > 2 > 1$	$W_3^*(0, \tau, 0, \tau)$

The correlation function can then be calculated succinctly as

$$\langle \mathcal{E}_{in}^{\dagger b}(0) \mathcal{E}_{in}^{\dagger b}(\tau) \mathcal{E}_{in}^b(\tau) \mathcal{E}_{in}^b(0) \rangle_{ss} = \sum_{n=1}^4 [W_n(0, \tau, \tau, 0) + W_n(0, \tau, 0, \tau) + W_n(\tau, 0, \tau, 0) + W_n(\tau, 0, 0, \tau)] + \text{CC} \quad (5.90)$$

where CC indicates the complex conjugate of the first term.

Application to Gaussian filtering

There is no difference in the structure of the calculation when we go over to Gaussian filtering. We find that

$\langle \mathcal{E}_{in}^{\dagger b}(0) \mathcal{E}_{in}^{\dagger b}(\tau) \mathcal{E}_{in}^b(\tau) \mathcal{E}_{in}^b(0) \rangle_{ss}$ is given by

$$C^4 \gamma_{in}^2 \lim_{t_0 \rightarrow -\infty} \int_{t_0}^{\infty} dt_1 \int_{t_0}^{\infty} dt_2 \int_{t_0}^{\infty} dt_3 \int_{t_0}^{\infty} dt_4 \langle : \sigma_+(t_1) \sigma_+(t_2) \sigma_-(t_3) \sigma_-(t_4) : \rangle e^{-d(t-t_1)^2 - d(t+\tau-t_2)^2 - d(t+\tau-t_3)^2 - d(t-t_4)^2} \quad (5.91)$$

We need only to redefine our functions S_1 , S_2 and S_3 . We have, for $S_1(x, y, z, w|a, b, c)$, the function:

$$C^4 \gamma_{in}^2 \lim_{t_0 \rightarrow -\infty} \int_{t_0}^{\infty} dt_1 \int_{t_0}^{\infty} dt_2 \int_{t_0}^{\infty} dt_3 \int_{t_0}^{\infty} dt_4 e^{-a\tau_1 - b\tau_2 - c\tau_3 - d((t+x)-t_1)^2 - d((t+y)-t_2)^2 - d((t+z)-t_3)^2 - d((t+w)-t_4)^2} \quad (5.92)$$

where the integration is to be done in the time ordering $t_2 > t_3 > t_1 > t_4$. Recall that $C = \sqrt{\frac{d}{\pi}}$. The τ variables are still defined by Eq. (5.72). Incorporating the time ordering can be done by rewriting the integration as

$$\int_{t_0}^{\infty} dt_4 \int_{t_4}^{\infty} dt_1 \int_{t_1}^{\infty} dt_3 \int_{t_3}^{\infty} dt_2 \quad (5.93)$$

Or, in terms of the variables τ_1, τ_2, τ_3 and t_4 :

$$\int_{t_0}^{\infty} dt_4 \int_0^{\infty} d\tau_1 \int_0^{\infty} d\tau_2 \int_0^{\infty} d\tau_3 \quad (5.94)$$

The integrand becomes, in these variables:

$$e^{-a\tau_1 - b\tau_2 - c\tau_3 - d((t+x) - (\tau_1 + t_4))^2 - d((t+y) - (\tau_1 + \tau_2 + \tau_3 + t_4))^2 - d((t+z) - (\tau_1 + \tau_2 + t_4))^2 - d((t+w) - t_4)^2} \quad (5.95)$$

For $S_2(x, y, z, w|a, b, c)$, we must evaluate Eq. (5.92) with the time ordering $t_2 > t_3 > t_4 > t_1$. The integral part should be written

$$\int_{t_0}^{\infty} dt_1 \int_0^{\infty} d\tau_1 \int_0^{\infty} d\tau_2 \int_0^{\infty} d\tau_3 \quad (5.96)$$

where the τ variables are given by Eq. (5.79) now. The integrand is

$$e^{-a\tau_1 - b\tau_2 - c\tau_3 - d((t+x) - t_1)^2 - d((t+y) - (\tau_1 + \tau_2 + \tau_3 + t_1))^2 - d((t+z) - (\tau_1 + \tau_2 + t_1))^2 - d((t+w) - (\tau_1 + t_1))^2} \quad (5.97)$$

Lastly, for $S_3(x, y, z, w|a, b, c)$, we evaluate Eq. (5.92) with time ordering $t_2 > t_1 > t_3 > t_4$. The integral part is

$$\int_{t_0}^{\infty} dt_4 \int_0^{\infty} d\tau_1 \int_0^{\infty} d\tau_2 \int_0^{\infty} d\tau_3 \quad (5.98)$$

with the τ variables given by Eq. (5.84); the integrand is

$$e^{-a\tau_1 - b\tau_2 - c\tau_3 - d((t+x) - (\tau_1 + \tau_2 + t_4))^2 - d((t+y) - (\tau_1 + \tau_2 + \tau_3 + t_4))^2 - d((t+z) - (\tau_1 + t_4))^2 - d((t+w) - t_4)^2} \quad (5.99)$$

Comparison of the 3 master case integrands given by Eqs. (5.95), (5.97) and (5.99) show us that in fact, once $S_1(x, y, z, w|a, b, c)$ is found, we have:

$$S_2(x, y, z, w|a, b, c) = S_1(w, y, z, x|a, b, c) \quad (5.100)$$

$$S_3(x, y, z, w|a, b, c) = S_1(z, y, x, w|a, b, c) \quad (5.101)$$

So our only work is done in evaluating $S_1(x, y, z, w|a, b, c)$.

There appears to be at least some difficulty in evaluating this integral. The process (Appendix B) for evaluating the two-time filtering integral doesn't generalise easily to cover the integral here. Looking ahead to Appendix B, it is noted that the integral was only possible because we allowed $t_0 \rightarrow -\infty$ prior to doing the second integration, rather than taking that limit post-integration. That was not a problem at the time, and it allowed us to make use of the result in Aside 2 of that Appendix. However, one sees that we cannot do the same thing here, for the lower bounds (for example, in Eq. (5.93)) are *not* $-\infty$, and must be kept general.

Due to time constraints, we have not performed this integration. The aim of this section has been to outline the process for calculating the second-order correlation function, showing how it works in the regime of no filtering

by Alice. For further details, see Appendices B and C of [7], although note that [7] considers the more general case of filtering by Alice, and hence is much more involved than the calculation presented above. Also note that we have not used the symbols W and S in the same context as [7].

5.4 Other filtering possibilities

One of the conclusions from our investigations in Gaussian filtering was that a Gaussian filter of larger bandwidth is capable of providing essentially the same performance as a Lorentzian of smaller bandwidth. There is another way of achieving a similar result, and that is by cascading several Lorentzian filters of larger bandwidth to create an overall filter of smaller bandwidth. From a theoretical point of view, this is also slightly more appealing than Gaussian filtering because we don't have the problem of an acausal impulse response. We can show briefly how this works.

In frequency space, the real part of a Lorentzian filter having bandwidth γ_B is

$$\frac{1}{1 + \left(\frac{\omega}{\gamma_B}\right)^2} \quad (5.102)$$

excluding a multiplicative factor of $\frac{1}{2\pi}$ arising from our particular Fourier transform (see Eq. (5.38)). The half-width of this filter is precisely γ_B .

If we cascade n such filters, of identical half-width γ_B , the resulting filter is (in frequency space)

$$\frac{1}{\left(1 + \left(\frac{\omega}{\gamma_B}\right)^2\right)^n} \quad (5.103)$$

which has an overall half-width of

$$\gamma_B \sqrt[n]{\sqrt{2} - 1} \quad (5.104)$$

which is *smaller* than γ_B when $n > 1$.

Chapter 6

Conclusions and future directions

Summary of the dissertation

Chapter 1 set forth the structure of the dissertation, and clarified a little what quantum teleportation actually is, distinguishing it clearly from any notions of far-fetched science fiction. With that out of the way, Chapter 2 moved on to look at the original Bennett *et al.* protocol of [1], this being of historical significance and also key in highlighting many of the important ingredients in quantum teleportation. One such ingredient of particular note was entanglement, which was also explored in detail, before covering Vaidman's teleportation protocol for continuous variables [6].

Chapter 3 set off in a different direction altogether, covering many of the unique properties of light describable only in a true quantum setting, in preparation for the description of the Furusawa protocol of Chapter 5 [2].

Chapter 4 gave the correlation functions for squeezed vacuum fields, as generated by an optical parametric oscillator, and we also worked through in detail the calculation of the resonance fluorescence field correlation functions, both to compute the field quadrature correlation functions that would be used in Chapter 5, and to highlight some of the interesting physics behind the calculation, such as the Quantum Regression Theorem.

Chapter 5 contained the bulk of the numerical work in this dissertation. We provided the integrals necessary for Gaussian filtering in the Furusawa protocol, going on to compare both the vacuum and resonance fluorescence spectra that resulted from matched-bandwidth Lorentzian and Gaussian filtering. We then ventured on to explore how much vacuum noise each filter type lets in, and how well each filter is capable of teleporting the signal part of the fluorescence spectrum sidepeaks.

We also covered the details needed to evaluate the second-order correlation function for the resonance fluorescence field, but were unable to put this into practice at the time of writing.

Conclusions

By looking at the vacuum spectra of Chapter 5 (Figs. 6 – 9) we were able to see that Gaussian filtering is more successful at cutting out vacuum noise in the spectrum wings, compared to Lorentzian filtering of the same half-width. Hand-in-hand with this, we saw that in teleporting the resonance fluorescence field, the maximum amount of vacuum noise let in by a Lorentzian filter is always greater than that found with a Gaussian filter of the same half-width (Fig. 18).

As one may well have expected, we found an inverse relationship between sidepeak loss in the teleported resonance fluorescence spectrum, and maximum vacuum noise let in during teleportation – that is, a small sidepeak loss necessarily went hand-in-hand with a larger amount of vacuum noise let in. However, as was seen in Fig. 19, the Gaussian filter still performed better than its Lorentzian counterpart – it was seen that for a given amount of vacuum noise let in, use of a Gaussian filter resulted in less sidepeak loss.

The Gaussian filter also performed better when it came to considering the amount of input signal (rather than vacuum noise) present in the teleported sidepeaks. This was investigated by looking at the sidepeak loss using the input/output fields Y correlation functions. There we saw that, if one wishes the teleported sidepeak signal (less any vacuum noise let in) to be some given percentage ($<100\%$) of the input signal, a Gaussian filter of larger half-width can achieve the same result Lorentzian filtering of a smaller half-width. See Fig. 20. This was also the case for the *total* output spectrum (not just its Y correlation); see Fig. 17.

The filtering integrals of Eqs. (5.18) and (5.21) had derivations that were reasonably involved – see Appendix A. However, we were able to show analytically that, in certain limits, perfect teleportation can indeed be obtained with these integrals, as one means of a check on our work (Section 5.2.5). We showed briefly how cascaded Lorentzian filters afford a means of creating an overall filter of less half-width from filters of larger half-widths.

Future Directions

There are a few extensions of the work done in this report, which we mention briefly here.

The method outlined in Section 5.3 could be properly implemented to look at the teleported second order correlation function under Gaussian filtering. It would be interesting to see whether or not the Gaussian's ability to cut out high frequency noise very effectively allows the second order correlation function to be teleported with better quality than in Lorentzian filtering.

The possibility of using other filter types could be followed up on. We mentioned in Section 5.4 the possibility of using cascaded Lorentzian filtering. Not only does this generate a filter of smaller overall half-width from a series of larger half-width filters, it also gives a filter that falls off faster at higher frequencies than an ordinary Lorentzian filter, and is not acausal. One could explore first-order and second-order correlation functions for these.

Appendices

Appendix A

We give a few properties of the error function here. A good list of error function properties is given in [18].

The *error function* is a non-elementary function defined by

$$\operatorname{erf}(z) = \frac{2}{\sqrt{\pi}} \int_0^z \exp(-t^2) dt$$

For small arguments $x \ll 1$, the error function can be calculated from

$$\begin{aligned} \operatorname{erf}(x) &= \frac{1}{\sqrt{\pi}} \exp(-x^2) \sum_{n=0}^{\infty} \frac{(2x)^{2n+1}}{(2n+1)!!} \\ &= \frac{2}{\sqrt{\pi}} \exp(-x^2) \left(x + \frac{2x^3}{3} + \frac{4x^5}{15} + \dots \right) \end{aligned}$$

The error function has the asymptotic series (as $x \rightarrow \infty$)

$$\begin{aligned} \operatorname{erf}(x) &\sim 1 - \frac{\exp(-x^2)}{\sqrt{\pi}} \sum_{n=0}^{\infty} \frac{(-1)^n (2n-1)!!}{2^n} x^{-(2n+1)} \\ &= 1 - \frac{\exp(-x^2)}{\sqrt{\pi}} \left(\frac{1}{x} - \frac{1}{2x^3} + \frac{3}{4x^5} + \dots \right) \end{aligned}$$

The RHS is hence an approximation to the error function for large arguments; we have used the first term of this series in previous sections.

The integral definition for the error function above is valid for complex arguments. In terms of actually computing its value for complex arguments, it is convenient to split into real and imaginary parts. Write

$$\operatorname{erf}(a + ib) = \frac{2}{\sqrt{\pi}} \int_0^{a+bi} \exp(-t^2) dt$$

Upon making the substitution $t = (a + ib)u$, and writing the resulting complex exponential in terms of cosines and sines, this becomes

$$\begin{aligned} \operatorname{erf}(a + bi) &= \frac{2}{\sqrt{\pi}} \int_0^1 \exp((b^2 - a^2)u^2) (a \cos(2abu^2) + b \sin(2abu^2)) du \\ &\quad + i \frac{2}{\sqrt{\pi}} \int_0^1 \exp((b^2 - a^2)u^2) (b \cos(2abu^2) - a \sin(2abu^2)) du \end{aligned}$$

which involves only real-valued integrals. Computationally, when required, these integrals were performed numerically in Matlab. This was done using the `quad` function which uses adaptive Simpson quadrature, and has a numerical error of $< 10^{-6}$.

For purely imaginary arguments:

$$\operatorname{erf}(bi) = ib \frac{2}{\sqrt{\pi}} \int_0^1 \exp(b^2 u^2) du$$

Note that our filtering integral Eq. (5.18) involves the terms of the form

$$y = \exp(x) \left(1 - \operatorname{erf}(\sqrt{x})\right)$$

where, for example, $x = \frac{\eta^2}{2d}$. An interesting point is that computational difficulties arise if we attempt to evaluate y for large x values. This is because y then involves the product of a large and a very small number. We look into this now.

The function y is definitely not unbounded – in fact as $x \rightarrow \infty$, we have:

$$\lim_{x \rightarrow \infty} y = \lim_{x \rightarrow \infty} \frac{1 - \operatorname{erf}(\sqrt{x})}{\exp(-x)} = \lim_{x \rightarrow \infty} \frac{1}{\sqrt{\pi x}} = 0$$

where at the second equality, l'Hopitals Rule was used. Below we plot the exact function y , and also its approximation (made as in Eq. (5.52)), which is $y = 1/\sqrt{\pi x}$.

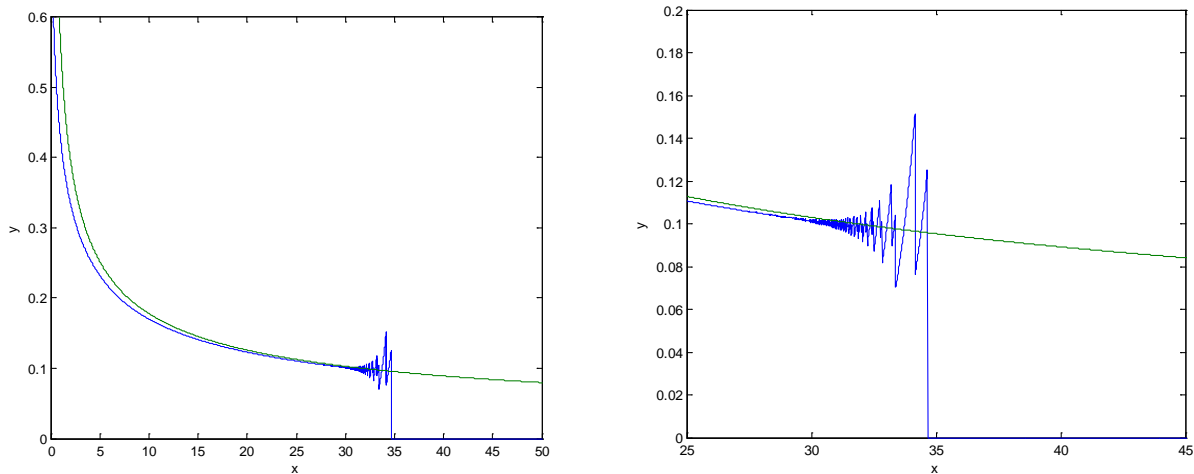


Figure 23: The function $y = \exp(x) \left(1 - \operatorname{erf}(\sqrt{x})\right)$ is in blue. Computationally, it behaves anomalously around $x = 28$ and above. The approximation $y = 1/\sqrt{\pi x}$ to this function is shown in green. A close-up of the anomalous behaviour region is shown on the right.

One can see that for values of x larger than about 28, the computer is no longer able to calculate y accurately. At this point, $\exp(28)$ is of the order 10^{12} , while $1 - \operatorname{erf}(\sqrt{28})$ is of the order 10^{-14} .

This raises some issues when we are using Gaussian filtering, when $\frac{\eta^2}{2d}$ is quite large. It turns out that this is *not* a problem that arises when vacuum spectra are considered – this is because terms of the form $\exp(x) \left(1 - \operatorname{erf}(\sqrt{x})\right)$ just mentioned are imaginary for the vacuum and thus are eliminated when we take the real part – see Eq. (5.36). Difficulties would show up in the imaginary part of that spectrum, however. For the Mollow triplet, the situation is not so simple – here η can be complex, so these terms are not necessarily eliminated when we consider the spectrum. However, the complex η values that would cause any problems turn

out to be much smaller than those in the vacuum, so we again do not have this difficulty. It is something to be aware of, however.

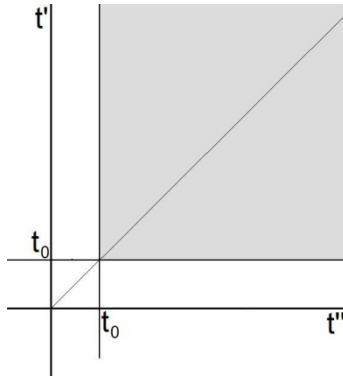
Appendix B

In this appendix we give a full derivation of the filtering integral Eq. (5.18):

$$I = \lim_{t_0 \rightarrow \infty} C^2 \int_{t_0}^{\infty} dt' \int_{t_0}^{\infty} dt'' \exp[-d(t + \tau - t')^2 - d(t - t')^2] \exp[-\eta|t' - t'']]$$

What follows is by no means intended to be the simplest way to perform this integral. We have merely done it directly.

The region of integration is the semi-infinite shaded region below:



Now we have:

$$|t' - t''| = \begin{cases} t' - t'', t' \geq t'' \\ t'' - t', t' < t'' \end{cases}$$

The first line of this applies to the upper triangular part of the region; the second line to the lower part. We split the integral up over precisely these regions; (excluding the limit for now):

$$I = I_{lower} + I_{upper}$$

$$\begin{aligned} &= C^2 \int_{t_0}^{\infty} \int_{t_0}^{t''} \exp[-d(t + \tau - t')^2 - d(t - t')^2 - \eta(t'' - t')] dt' dt'' \\ &+ C^2 \int_{t_0}^{\infty} \int_{t_0}^{t'} \exp[-d(t + \tau - t')^2 - d(t - t')^2 - \eta(t' - t'')] dt'' dt' \end{aligned}$$

Expand the argument of the first exponential: $-d(t + \tau - t')^2 - d(t - t')^2 - \eta(t'' - t')$, and write it as:

$$[-d](t')^2 + [2d(t + \tau) + \eta](t') + [-d(t + \tau)^2 - d(t - t'')^2 - \eta t'']$$

We have written it as a quadratic in t' as that is our first integration variable in the first integral.

Likewise for the argument of the second exponential:

$$-d(t + \tau - t')^2 - d(t - t')^2 - \eta(t' - t'') = [-d](t'')^2 + [2dt + \eta](t'') + [-d(t + \tau - t')^2 - dt^2 - \eta t']$$

Aside 1

The normalized error function is

$$\operatorname{erf}(x) = \frac{2}{\sqrt{\pi}} \int_0^x \exp(-t^2) dt$$

The normalization is such that $\operatorname{erf}(x) \rightarrow 1$ as $x \rightarrow \infty$, and $\operatorname{erf}(x) \rightarrow -1$ as $x \rightarrow -\infty$.

We write:

$$E(m, n) = \int_m^n \exp(-t^2) dt = \frac{\sqrt{\pi}}{2} (\operatorname{erf}(n) - \operatorname{erf}(m))$$

With this notation, we find that, for constants a and b ($a > 0$):

$$\begin{aligned} \int_m^n \exp(-ax^2 + bx) dx &= \int_m^n \exp\left(-a\left(x - \frac{b}{2a}\right)^2 + \frac{b^2}{4a}\right) dx \\ &= \exp\left(\frac{b^2}{4a}\right) \int_m^n \exp\left(-\left(\sqrt{a}x - \frac{b}{2\sqrt{a}}\right)^2\right) dx \end{aligned}$$

Letting $t = \sqrt{a}x - \frac{b}{2\sqrt{a}}$ gives:

$$\int_m^n \exp(-ax^2 + bx) dx = \exp\left(\frac{b^2}{4a}\right) \int_{\sqrt{a}m - \frac{b}{2\sqrt{a}}}^{\sqrt{a}n - \frac{b}{2\sqrt{a}}} \exp(-t^2) \frac{dt}{\sqrt{a}} = \frac{1}{\sqrt{a}} \exp\left(\frac{b^2}{4a}\right) E\left(\sqrt{a}n - \frac{b}{2\sqrt{a}}, \sqrt{a}m - \frac{b}{2\sqrt{a}}\right)$$

We'll use this result now. We get:

$$\begin{aligned} I &= C^2 \int_{t_0}^{\infty} \exp\left(-d(t + \tau)^2 - d(t - t'')^2 - \eta t''\right) \frac{1}{\sqrt{d}} \exp\left(\frac{(2d(t + \tau) + \eta)^2}{4d}\right) E(f(t_0), f(t'')) dt'' \\ &\quad + C^2 \int_{t_0}^{\infty} \exp\left(-d(t + \tau - t')^2 - dt^2 - \eta t'\right) \frac{1}{\sqrt{d}} \exp\left(\frac{(2dt + \eta)^2}{4d}\right) E(g(t_0), g(t')) dt' \end{aligned}$$

The functions f and g transform the arguments as described in *Aside 1* (i.e. dependent on the values a and b). There is one integral remaining; we take out some constants, and rewrite E in terms of the error function:

$$\begin{aligned} I &= \frac{C^2}{2} \frac{\sqrt{\pi}}{\sqrt{d}} \exp\left(\frac{(2d(t + \tau) + \eta)^2}{4d}\right) \int_{t_0}^{\infty} \exp(-d(t + \tau)^2 - d(t - t'')^2 - \eta t'') \left(\operatorname{erf}(f(t'')) - \operatorname{erf}(f(t_0))\right) dt'' \\ &\quad + \frac{C^2}{2} \frac{\sqrt{\pi}}{\sqrt{d}} \exp\left(\frac{(2dt + \eta)^2}{4d}\right) \int_{t_0}^{\infty} \exp(-d(t + \tau - t')^2 - dt^2 - \eta t') \left(\operatorname{erf}(g(t')) - \operatorname{erf}(g(t_0))\right) dt' \end{aligned}$$

Fully, there are four terms in the integral then:

$$\begin{aligned}
I &= \frac{C^2}{2} \sqrt{\frac{\pi}{d}} \exp\left(\frac{(2d(t+\tau)+\eta)^2}{4d}\right) \int_{t_0}^{\infty} \exp(-d(t+\tau)^2 - d(t-t'')^2 - \eta t'') \operatorname{erf}\left(t''\sqrt{d} - \frac{2d(t+\tau)+\eta}{2\sqrt{d}}\right) dt'' \\
&\quad - \operatorname{erf}\left(t_0\sqrt{d} - \frac{2d(t+\tau)+\eta}{2\sqrt{d}}\right) \frac{C^2}{2} \sqrt{\frac{\pi}{d}} \exp\left(\frac{(2d(t+\tau)+\eta)^2}{4d}\right) \int_{t_0}^{\infty} \exp(-d(t+\tau)^2 - d(t-t'')^2 - \eta t'') dt'' \\
&\quad + \frac{C^2}{2} \sqrt{\frac{\pi}{d}} \exp\left(\frac{(2dt+\eta)^2}{4d}\right) \int_{t_0}^{\infty} \exp(-d(t+\tau-t')^2 - dt^2 - \eta t') \operatorname{erf}\left(t'\sqrt{d} - \frac{2dt+\eta}{2\sqrt{d}}\right) dt' \\
&\quad - \operatorname{erf}\left(t_0\sqrt{d} - \frac{2dt+\eta}{2\sqrt{d}}\right) \frac{C^2}{2} \sqrt{\frac{\pi}{d}} \exp\left(\frac{(2dt+\eta)^2}{4d}\right) \int_{t_0}^{\infty} \exp(-d(t+\tau-t')^2 - dt^2 - \eta t') dt'
\end{aligned}$$

Aside 2

For constants a, b, p, q , we have the following integral:

$$\int_{-\infty}^{\infty} \exp(-(ax+b)^2) \operatorname{erf}(px+q) dx = \frac{\sqrt{\pi}}{a} \operatorname{erf}\left(\frac{aq-bp}{\sqrt{a^2+p^2}}\right)$$

See reference [16].

It is here that we take the limit $t_0 \rightarrow -\infty$, in order to use the result of *Aside 2*. Since $\operatorname{erf}(x) \rightarrow -1$ as $x \rightarrow -\infty$, we get:

$$\begin{aligned}
I &= \frac{C^2}{2} \sqrt{\frac{\pi}{d}} \exp\left(\frac{(2d(t+\tau)+\eta)^2}{4d}\right) \int_{-\infty}^{\infty} \exp(-d(t+\tau)^2 - d(t-t'')^2 - \eta t'') \operatorname{erf}\left(t''\sqrt{d} - \frac{2d(t+\tau)+\eta}{2\sqrt{d}}\right) dt'' \\
&\quad + \frac{C^2}{2} \sqrt{\frac{\pi}{d}} \exp\left(\frac{(2d(t+\tau)+\eta)^2}{4d}\right) \int_{-\infty}^{\infty} \exp(-d(t+\tau)^2 - d(t-t'')^2 - \eta t'') dt'' \\
&\quad + \frac{C^2}{2} \sqrt{\frac{\pi}{d}} \exp\left(\frac{(2dt+\eta)^2}{4d}\right) \int_{-\infty}^{\infty} \exp(-d(t+\tau-t')^2 - dt^2 - \eta t') \operatorname{erf}\left(t'\sqrt{d} - \frac{2dt+\eta}{2\sqrt{d}}\right) dt' \\
&\quad + \frac{C^2}{2} \sqrt{\frac{\pi}{d}} \exp\left(\frac{(2dt+\eta)^2}{4d}\right) \int_{-\infty}^{\infty} \exp(-d(t+\tau-t')^2 - dt^2 - \eta t') dt'
\end{aligned}$$

The first and third terms will require the use of *Aside 2*; the second and forth are just Gaussian integrals.

We need to complete the square in the exponential arguments:

$$\begin{aligned}
-d(t+\tau)^2 - d(t-t'')^2 - \eta t'' &= [-d](t'')^2 + [2dt - \eta]t'' + [-dt^2 - d(t+\tau)^2] \\
&= -d\left(t'' - \frac{2dt - \eta}{2d}\right)^2 + \frac{(2dt - \eta)^2}{4d} - dt^2 - d(t+\tau)^2
\end{aligned}$$

This is for the first and second terms. For the third and forth terms:

$$\begin{aligned}
-d(t+\tau-t')^2 - dt^2 - \eta t' &= [-d](t')^2 + [2d(t+\tau) - \eta]t' - dt^2 - d(t+\tau)^2 \\
&= -d\left(t' - \frac{2d(t+\tau) - \eta}{2d}\right)^2 + \frac{(2d(t+\tau) - \eta)^2}{4d} - dt^2 - d(t+\tau)^2
\end{aligned}$$

Hence:

$$\begin{aligned}
I &= \frac{C^2}{2} \sqrt{\frac{\pi}{d}} \exp\left(\frac{(2d(t+\tau)+\eta)^2 + (2dt-\eta)^2}{4d} - dt^2 - d(t+\tau)^2\right) \times \\
&\quad \int_{-\infty}^{\infty} \exp\left(-\left(\sqrt{d}t'' - \frac{2dt-\eta}{2\sqrt{d}}\right)^2\right) \operatorname{erf}\left(t''\sqrt{d} - \frac{2d(t+\tau)+\eta}{2\sqrt{d}}\right) dt'' \\
&\quad + \frac{C^2}{2} \sqrt{\frac{\pi}{d}} \exp\left(\frac{(2d(t+\tau)+\eta)^2 + (2dt-\eta)^2}{4d} - dt^2 - d(t+\tau)^2\right) \int_{-\infty}^{\infty} \exp\left(-\left(\sqrt{d}t'' - \frac{2dt-\eta}{2\sqrt{d}}\right)^2\right) dt'' \\
&\quad + \frac{C^2}{2} \sqrt{\frac{\pi}{d}} \exp\left(\frac{(2d(t+\tau)-\eta)^2 + (2dt+\eta)^2}{4d} - dt^2 - d(t+\tau)^2\right) \times \\
&\quad \int_{-\infty}^{\infty} \exp\left(-\left(\sqrt{d}t' - \frac{2d(t+\tau)-\eta}{2\sqrt{d}}\right)^2\right) \operatorname{erf}\left(t'\sqrt{d} - \frac{2dt+\eta}{2\sqrt{d}}\right) dt' \\
&\quad + \frac{C^2}{2} \sqrt{\frac{\pi}{d}} \exp\left(\frac{(2d(t+\tau)-\eta)^2 + (2dt+\eta)^2}{4d} - dt^2 - d(t+\tau)^2\right) \int_{-\infty}^{\infty} \exp\left(-\left(\sqrt{d}t' - \frac{2d(t+\tau)-\eta}{2\sqrt{d}}\right)^2\right) dt'
\end{aligned}$$

The integrals are now in the form of *Aside 2*; the Gaussian integrals require the result

$$\int_{-\infty}^{\infty} \exp(-(ax+b)^2) dx = \frac{\sqrt{\pi}}{a}$$

for $a > 0$.

We find:

$$\begin{aligned}
I &= \frac{C^2}{2} \sqrt{\frac{\pi}{d}} \exp\left(\frac{\eta^2}{2d} + \eta\tau\right) \frac{\sqrt{\pi}}{\sqrt{d}} \operatorname{erf}\left(\frac{1}{\sqrt{2d}}\left(\frac{-2d(t+\tau)-\eta}{2} + \frac{2dt-\eta}{2}\right)\right) \\
&\quad + \frac{C^2}{2} \sqrt{\frac{\pi}{d}} \exp\left(\frac{\eta^2}{2d} + \eta\tau\right) \frac{\sqrt{\pi}}{\sqrt{d}} \\
&\quad + \frac{C^2}{2} \sqrt{\frac{\pi}{d}} \exp\left(\frac{\eta^2}{2d} - \eta\tau\right) \frac{\sqrt{\pi}}{\sqrt{d}} \operatorname{erf}\left(\frac{1}{\sqrt{2d}}\left(\frac{-2dt-\eta}{2} + \frac{2d(t+\tau)-\eta}{2}\right)\right) \\
&\quad + \frac{C^2}{2} \sqrt{\frac{\pi}{d}} \exp\left(\frac{\eta^2}{2d} - \eta\tau\right) \frac{\sqrt{\pi}}{\sqrt{d}}
\end{aligned}$$

Final simplification of the 'erf' arguments gives:

$$I = \frac{C^2\pi}{2d} \exp\left(\frac{\eta^2}{2d} + \eta\tau\right) \left[\operatorname{erf}\left(\frac{-d\tau - \eta}{\sqrt{2d}}\right) + 1\right] + \frac{C^2\pi}{2d} \exp\left(\frac{\eta^2}{2d} - \eta\tau\right) \left[\operatorname{erf}\left(\frac{d\tau - \eta}{\sqrt{2d}}\right) + 1\right]$$

Slight rearrangements may be made using the fact that the error function is odd: $\operatorname{erf}(-x) = -\operatorname{erf}(x)$.

Appendix C

We here give the full solutions to Eqs. (5.61)-(5.64). These are also evaluated in [7], where Laplace Transforms were used instead to acquire exactly the same solutions. We follow the notational convention outlined there. Define the following vectors, each having length 4:

A vector of time-dependent exponentials:

$$E = \begin{bmatrix} 1 & \exp\left(-\frac{\gamma t}{2}\right) & \exp\left(\left(-\frac{3\gamma}{4} + \delta\right)t\right) & \exp\left(\left(-\frac{3\gamma}{4} - \delta\right)t\right) \end{bmatrix}$$

Assorted vectors of constants:

$$F^- = \begin{bmatrix} \frac{-iY}{\sqrt{2}(1+Y^2)} & 0 & \frac{-iY}{2\sqrt{2}\delta(1+Y^2)}\left(\frac{1}{2}\gamma\left(Y^2 - \frac{1}{2}\right) - \delta\right) & \frac{-iY}{2\sqrt{2}\delta(1+Y^2)}\left(-\frac{1}{2}\gamma\left(Y^2 - \frac{1}{2}\right) - \delta\right) \end{bmatrix}$$

$$F^+ = \begin{bmatrix} \frac{-iY}{\sqrt{2}(1+Y^2)} & 0 & \frac{-iY}{2\sqrt{2}\delta(1+Y^2)}\left(\frac{1}{2}\gamma\left(-Y^2 - \frac{5}{2}\right) - \delta\right) & \frac{-iY}{2\sqrt{2}\delta(1+Y^2)}\left(\frac{1}{2}\gamma\left(Y^2 + \frac{1}{2}\right) - \delta\right) \end{bmatrix}$$

$$G^- = \begin{bmatrix} 0 & \frac{1}{2} & -\frac{1}{2}\left(\frac{1}{2} + \frac{\gamma}{8\delta}\right) & -\frac{1}{2}\left(\frac{1}{2} - \frac{\gamma}{8\delta}\right) \end{bmatrix}$$

$$G^+ = \begin{bmatrix} 0 & \frac{1}{2} & \frac{1}{2}\left(\frac{1}{2} + \frac{\gamma}{8\delta}\right) & \frac{1}{2}\left(\frac{1}{2} - \frac{\gamma}{8\delta}\right) \end{bmatrix}$$

$$H = \begin{bmatrix} \frac{-1}{1+Y^2} & 0 & \frac{1}{\delta\gamma(1+Y^2)}\left(\frac{\gamma}{4} - \delta\right)\left(\frac{1}{2}\gamma\left(Y^2 - \frac{1}{2}\right) - \delta\right) & \frac{1}{\delta\gamma(1+Y^2)}\left(\frac{\gamma}{4} + \delta\right)\left(-\frac{1}{2}\gamma\left(Y^2 - \frac{1}{2}\right) - \delta\right) \end{bmatrix}$$

$$I = \begin{bmatrix} 0 & 0 & \frac{i\sqrt{2}}{Y\gamma}\left(\frac{\gamma}{4} - \delta\right)\left(\frac{1}{2} + \frac{\gamma}{8\delta}\right) & \frac{i\sqrt{2}}{Y\gamma}\left(\frac{\gamma}{4} + \delta\right)\left(\frac{1}{2} - \frac{\gamma}{8\delta}\right) \end{bmatrix}$$

$$J = \begin{bmatrix} \frac{-1}{1+Y^2} & 0 & \frac{1}{\delta\gamma(1+Y^2)}\left(\frac{\gamma}{4} - \delta\right)\left(\frac{1}{2}\gamma\left(-Y^2 - \frac{5}{2}\right) - \delta\right) & \frac{1}{\delta\gamma(1+Y^2)}\left(\frac{\gamma}{4} + \delta\right)\left(\frac{1}{2}\gamma\left(Y^2 + \frac{1}{2}\right) - \delta\right) \end{bmatrix}$$

By forming the inner product (without taking complex conjugates) of each of these with the vector of exponentials E , we define 7 functions:

$$f_-(t) = \sum_{n=1}^4 F_n^- E_n, \quad f_+(t) = \sum_{n=1}^4 F_n^+ E_n$$

$$g_-(t) = \sum_{n=1}^4 G_n^- E_n, \quad g_+(t) = \sum_{n=1}^4 G_n^+ E_n$$

$$h(t) = \sum_{n=1}^4 H_n E_n, \quad i(t) = \sum_{n=1}^4 I_n E_n, \quad j(t) = \sum_{n=1}^4 J_n E_n$$

Finally, we get solutions:

$$X_{21}(t) = [-f_-(t)]X_{11}(0) + [-f_+(t)]X_{22}(0) + [g_-(t)]X_{12}(0) + [g_+(t)]X_{21}(0)$$

$$X_{12}(t) = [f_-(t)]X_{11}(0) + [f_+(t)]X_{22}(0) + [g_+(t)]X_{12}(0) + [g_-(t)]X_{21}(0)$$

Of course, we see that $[X_{12}(t)]^\dagger = X_{21}(t)$ as expected. Additionally,

$$X_{22}(t) - X_{11}(t) = [h(t)]X_{11}(0) + [j(t)]X_{22}(0) + [i(t)]X_{12}(0) + [-i(t)]X_{21}(0)$$

and

$$X_{22}(t) + X_{11}(t) = X_{22}(0) + X_{11}(0)$$

These provide us with full solutions to Eqs. (5.61)-(5.64).

Appendix D

Here we give the coefficients $P_{ijk}^{(1)}$, $P_{ijk}^{(2)}$ and $P_{ijk}^{(3)}$ given in Eqs. (5.71), (5.78) and (5.83). See [7]. We have:

$$P_{ijk}^{(1)} = \left(\frac{1}{2} F_i^- G_j^+ - \frac{1}{4} G_i^+ I_j \right) \left(\frac{i}{\sqrt{2}} \frac{Y}{1+Y^2} (1+H_k) + \frac{1}{2} \frac{Y^2}{1+Y^2} I_k \right) \\ + \left(\frac{1}{2} G_i^+ (1+H_j) - F_i^- F_j^- \right) \left(\frac{i}{\sqrt{2}} \frac{Y}{1+Y^2} F_k^- + \frac{1}{2} \frac{Y^2}{1+Y^2} G_k^+ \right)$$

$$P_{ijk}^{(2)} = - \left(\frac{1}{2} F_i^- G_j^- + \frac{1}{4} G_i^+ I_j \right) \left(\frac{i}{\sqrt{2}} \frac{Y}{1+Y^2} (1+H_k) + \frac{1}{2} \frac{Y^2}{1+Y^2} I_k \right) \\ + \left(\frac{1}{2} G_i^+ (1+H_j) - F_i^- F_j^- \right) \left(\frac{i}{\sqrt{2}} \frac{Y}{1+Y^2} F_k^- + \frac{1}{2} \frac{Y^2}{1+Y^2} G_k^+ \right)$$

$$P_{ijk}^{(3)} = \left(\frac{1}{2} F_i^- G_j^+ + \frac{1}{4} G_i^- I_j \right) \left(\frac{i}{\sqrt{2}} \frac{Y}{1+Y^2} (1+H_k) + \frac{1}{2} \frac{Y^2}{1+Y^2} I_k \right) \\ + \left(\frac{1}{2} G_i^+ (1+H_j) + F_i^- F_j^- \right) \left(-\frac{i}{\sqrt{2}} \frac{Y}{1+Y^2} F_k^- + \frac{1}{2} \frac{Y^2}{1+Y^2} G_k^- \right)$$

References

Papers

- [1] Bennett, C.H., Brassard, G., Crépeau, C., Jozsa, R., Peres, A., Wootters, W.K. *Teleporting an Unknown Quantum State via Dual Classical and Einstein-Podolsky-Rosen Channels*. In the Physical Review Letters, **70** 1895-1899 (1993).
- [2] Braunstein, S.L., Furusawa, A., Fuchs, C.A., Kimble, H.J., Polzik, E.S., Sorensen, J.L. *Unconditional Quantum Teleportation*. In Science **282** 706-709 (1998).
- [3] Braunstein, S.L., Kimble, H.J. *Teleportation of Continuous Quantum Variables*. In the Physical Review Letters, **80** 869-872 (1998).
- [4] Erez, N., Vaidman, L., Retzker, A. *Another look at Quantum Teleportation*. In the International Journal of Quantum Information **4** 197-208 (2006).
- [5] Noh, C., Chia, A., Nha, H., Collett, M.J., Carmichael, H.J. *Quantum Teleportation of the Temporal Fluctuations of Light*. In the Physical Review Letters, **102** 230501-1,4 (2009).
- [6] Vaidman, L. *Teleportation of quantum states*. In Physical Review A, **49** 1473-1476 (1994).

Theses

- [7] Noh, C. *Broadband Teleportation and Entanglement in Cascaded Open Quantum Systems*. Doctoral Thesis at the University of Auckland (December 2008).

Textbooks

- [8] Carmichael, H.J. *Statistical Methods in Quantum Optics Volume 1*. Springer-Verlag Berlin Heidelberg (1999).
- [9] Erdélyi, A. *Tables of Integral Transforms, Volume I*. USA: McGraw-Hill (1954).
- [10] Fox, M. *Quantum Optics – An introduction*. Oxford University Press (2006).
- [11] Gardiner, C.W. *Handbook of Stochastic Methods for Physics, Chemistry and the Natural Sciences*. Springer-Verlag Berlin Heidelberg (1983).
- [12] J.C. Garrison and R.Y. Chiao. *Quantum Optics*. Oxford University Press (2008).
- [13] Loudon, R. *The Quantum Theory of Light*. 3rd Edition, Oxford University Press (2000).
- [14] Milburn, G.J. and Walls, D.F. *Quantum Optics, 2nd Edition*. Springer (2007).
- [15] Sakurai, J.J. *Modern Quantum Mechanics, Revised Edition*. Addison Wesley Longman (1994).

Internet

- [16] Briggs, K. *Integrals involving erf*. <http://keithbriggs.info/documents/erf-integrals.pdf> (2003, December 29).
- [17] Weisstein, Eric W. "Erf." From *Mathworld* – A Wolfram Web Resource. <http://mathworld.wolfram.com/Erf.html>.
- [18] Weisstein, Eric W. "Delta Function." From *MathWorld*--A Wolfram Web Resource. <http://mathworld.wolfram.com/DeltaFunction.html>.